

DUKE POWER COMPANY

P.O. BOX 33189
CHARLOTTE, N.C. 28242

HAL B. TUCKER
VICE PRESIDENT
NUCLEAR PRODUCTION

TELEPHONE
(704) 373-4531

November 5, 1982

Mr. Harold R. Denton, Director
Office of Nuclear Reactor Regulation
U. S. Nuclear Regulatory Commission
Washington, D. C. 20555

Attention: Ms. E. G. Adensam, Chief
Licensing Branch No. 4

Re: McGuire Nuclear Station
Docket Nos. 50-369, 50-370

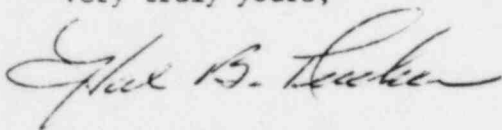
Dear Mr. Denton:

Attached herewith are 20 copies of Revision 5 to Duke Power Company's report "An Analysis of Hydrogen Control Measures at McGuire Nuclear Station". This revision contains the following:

- 1) Response to Mr. R. L. Tedesco's letter of April 1', 1982 requesting a summary report. Section 6.2 has been revised in its entirety to serve as a summary report.
- 2) Responses to Mr. T. M. Novak's letter of August 9, 1982 requesting information on CLASIX computer program.
- 3) Responses to Mr. T. M. Novak's letter of September 17, 1982 requesting information on the research program, equipment survivability and CLASIX analyses.
- 4) Interim report on the final testing at Whiteshell on combustion phenomena (the three reports in Appendix 2J fully describe the results of the Whiteshell test program).
- 5) Minor revisions to reflect the fact that the research program is complete.

Please advise if there are further questions regarding this matter.

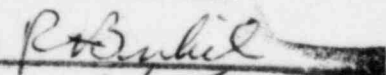
Very truly yours,



Hal B. Tucker

GAC/php
Attachment

DESIGNATED ORIGINAL

Certified By 

11/15/82

B021
1/20

8211160363 821105
PDR ADOCK 05000369
P PDR

Mr. Harold R. Denton, Director
November 5, 1982
Page 2

cc: Mr. James P. O'Reilly, Regional Administrator
U. S. Nuclear Regulatory Commission
Region II
101 Marietta Street, Suite 3100
Atlanta, Georgia 30303

Senior Resident Inspector
McGuire Nuclear Station

AN ANALYSIS OF HYDROGEN CONTROL MEASURES AT
McGUIRE NUCLEAR STATION

Insertion Sheet
Revision 5
November 5, 1982

Remove these pages:

Insert these pages:

Volume I - Section 1

| | |
|-------|-------|
| 1.1-1 | 1.1-1 |
| 1.2-1 | 1.2-1 |
| 1.3-1 | 1.3-1 |
| 1.4-1 | 1.4-1 |
| 1.5-1 | 1.5-1 |

Volume I - Section 2

| | |
|-------|-------|
| 2.6-1 | 2.6-1 |
| 2.6-2 | 2.6-2 |
| | 2.6-3 |
| | 2.6-4 |
| 2.7-1 | 2.7-1 |
| 2.7-2 | 2.7-2 |
| 2.8-1 | 2.8-1 |
| 2.8-2 | 2.8-2 |
| | 2.8-3 |
| 2.9-1 | 2.9-1 |
| 2.9-2 | 2.9-2 |

Volume III - Section 2

Replace Appendix 2J Cover Page with revised Cover Page.
Insert Interim Project Report, July 1982 into Appendix 2J with other reports.

Volume III - Section 4

| | |
|-------------|-------------|
| Table 4.3-7 | Table 4.3-7 |
|-------------|-------------|

Volume III - Section 6

| | |
|---------------------|---------------------|
| 6.2-1 through 6.2-4 | 6.2-1 through 6.2-6 |
|---------------------|---------------------|

Volume III - Section 7

| | |
|----|-----------------------|
| -- | 7.0-43 through 7.0-97 |
|----|-----------------------|

1.1 IMPROVEMENTS IN SYSTEM DESIGN

A complete description of the permanent Hydrogen Mitigation System for McGuire is given in Section 3.0. This section presents the rationale for the selection of this system, lists and justifies the design criteria for the system, and discusses system operation and testing. Improvements made in the system since 1981 include additional igniters in the upper plenum area of the ice condenser, electrical separation of igniters in the lower containment to improve reliability in the event of flooding, and establishment and verification of correct system operating parameters.

| 5

1.2 IMPROVEMENT IN CONTAINMENT RESPONSE ANALYSIS

One area which received much attention was the analysis of the response of the containment to a loss of coolant accident with hydrogen release and deliberate hydrogen ignition. The computer code CLASIX, which was described in previous submittals by Duke and used extensively for analysis, was improved and updated in order to remove unnecessary conservatism and increase its accuracy and predictive capability. One significant improvement in CLASIX was the incorporation of heat sink models so that the code may realistically account for energy deposition in the containment walls and structure. CLASIX can also be used for the prediction of the complete transient and is no longer dependent on LOTIC to predict pre-hydrogen burn conditions. Many minor improvements to the code were made to decrease running time. A topical report containing the complete description of CLASIX and its verification has been previously submitted by TVA. Section 4.0 of this report describes the results of analyses of the response of the McGuire containment to hydrogen burning.

1.3 IMPROVEMENTS IN EQUIPMENT SURVIVABILITY ANALYSES

A significant effort was expended to improve the calculational models used | 5
to establish that essential equipment in the containment will remain functional
during and after deliberate hydrogen burning. The models now include, where
appropriate, multi-dimensional analysis of heat transfer, explicit treatment of
radiation and convection associated with moving flames, more realistic assump-
tions concerning geometric arrangements of equipment, and more mechanistic
views of the nature of hydrogen flames. Attempts have been made to eliminate
mutually exclusive assumptions and thus make the calculational results more
representative of actual equipment response. Analyses of equipment surviva-
bility are discussed in Section 5.0.

1.4 ADVANCES IN RESEARCH

An extensive research effort was sponsored by the ice condenser owners and EPRI. Significant success was achieved in establishing the effectiveness of igniters at low hydrogen concentrations, the effects of steam and fogging on hydrogen ignition and burning, the transport of hydrogen through the containment atmosphere, the effects of turbulence on hydrogen combustion and equipment survivability. Additional research sponsored by the ice condenser owners investigated alternate hydrogen control concepts in addition to the distributed ignition concept. The overall effect of the results of this research has been to increase the confidence that the hydrogen ignition system will perform its design function to mitigate the effects of hydrogen release to the containment during a loss of coolant accident. (The research program and results are discussed in Section 2.0.)

5

5

1.5 RESPONSE TO NRC QUESTIONS AND COMMENTS

Duke has received from NRC several formal transmittals of questions and requests for information concerning hydrogen ignition and the response of the McGuire containment. Section 7.0 contains Duke's reply to these questions or references those sections of the main body of the submittal where the information may be found. 5

2.6 COMBUSTION CONTROL STUDIES

2.6.1 Purpose

Two physical mechanisms that could affect the characteristics of a deflagration are igniter location and the presence of water spray or fog. To address these two mechanisms a series of tests was conducted by Acurex Corporation at the Stanford Research Institute. Phase 1 of the project investigated the effect of igniter location on hydrogen deflagrations within a compartment. Tests were similar in nature to those conducted at Fenwal (see Section 2.1) with the variable of igniter location added. Phase 2 of the project investigated the effects of a water fog on the pressure rise that accompanies a deflagration. Tests were based on studies conducted at Factory Mutual Research (see Section 2.5).

5

2.6.2 Summary

The test vessel used for both phases of this project has a volume of approximately 630 ft³. The vessel is approximately 17 feet high with a 7 foot inside diameter. An igniter assembly supplied by Duke Power Company was the ignition source for all tests. Flame front location and vessel atmosphere temperature were measured by Type K thermocouples. Pressure rises were measured with strain gauge and piezoelectric pressure transducers. Figure 2.6-1 provides a flow diagram of the test apparatus. Instrumentation locations are shown in Figure 2.6-2.

All Phase 1 tests were transient tests with the ignitor pre-energized. Igniter assemblies were located near the top, at the center, and near the bottom of the test vessel. Tests were conducted with hydrogen injection, hydrogen/steam injection, and hydrogen/steam injection with water spray present. A gas

chromatograph was used to determine the vessel atmosphere constituents at the conclusion of each test. Test results are presented in Appendix 2H.

Static and transient tests were conducted in Phase 2. The igniter assembly was located near the bottom of vessel for all tests. Static tests were conducted without water fog and with water fog at two different droplet sizes and concentrations. Transient tests were conducted with hydrogen injection and with hydrogen/steam injection. Comparisons were made with similar tests in Phase 1, both with and without sprays. Vessel atmosphere constituents were determined with a gas chromatograph after each test. Results of the Acurex tests are presented in Appendix 2H.

Results of the Phase 1 tests indicated that igniter location has some effect on combustion characteristics. This effect was shown to depend on: (1) whether the test was quiescent or transient, (2) the location of the igniter relative to the hydrogen source, and (3) the amount of turbulence present. The tests showed that, during transient injection periods, the pressure rise was less when the igniter was located near the region where the entering hydrogen mixed and first became flammable. The location of this region within containment would be determined by the geometry of each plant compartment, the hydrogen entry location and velocity, and the presence of turbulence within the compartment. The Phase 1 tests also indicated that the potential for a larger pressure rise existed when the hydrogen source jet continued to bypass the igniter until the bulk of the vessel had reached a flammable concentration. It is noteworthy that the Hanford tests (see Section 2.9) demonstrated that an ice condenser's lower compartment region would be well-mixed, which, according to the Acurex tests, tends to reduce the significance of igniter

location relative to the inlet mixing region. Thus it was concluded that additional ignitor location effects testing was not necessary. The Phase 1 tests also confirmed previous findings on the pressure mitigative effects of steam and water sprays due to turbulence-induced mixing.

Results of the Phase 2 tests showed that a water micro-fog had no pressure mitigative effect during hydrogen combustion in quiescent mixtures. This indicated that the dominant effect of the fog droplets was not as a heat sink. The pressure mitigative effect of micro-fogs in the transient tests seemed to be due to induced turbulence similar to the effect of sprays in some of the Phase 1 tests. This induced turbulence promoted mixing which enhanced the potential for near-limit combustion of the entering hydrogen.

Since an ice condenser containment would be sufficiently turbulent to ensure good mixing during a degraded core accident (see Section 2.9), it was concluded that inducing additional turbulence with micro-fogging would be unnecessary.

In addition to the above conclusions based on the test objectives, an evaluation of the tests revealed additional information from which conclusions were drawn. The GM igniter assemblies, identical to those in Duke Power's McGuire Nuclear Station survived over five cumulative hours of exposure to combustion test environments. The assembly and power cable continued to operate without failure. The second additional conclusion dealt with estimated flame speeds. Although the test was not specifically instrumented to obtain flame speeds, it was possible to calculate "average" flame speeds from the pressure rise data of several transient and quiescent tests. The calculated flame speeds in the transient tests varied from 1-2 ft/sec with steam present and either top or bottom ignition to 4 ft/sec with no steam present and bottom

ignition. Flame speeds from the quiescent tests varied from 3-8 ft/sec as the hydrogen concentration was increased from 5 to 11 volume percent. Thus, we conclude that these data support the flame speed ranges used in the CLASIX analyses (see Section 4.0). Another important result of the transient test series was that the nature of combustion was always deflagrative instead of detonative even when a hydrogen-rich mixture was entering the vessel. Perhaps the most significant observation was the extreme contrast in pressure rise between quiescent and transient combustion tests. The pressure rises during all of the transient tests in both Phase 1 and 2 was dramatically less than during the quiescent tests (with the exception of one very lean mixture quiescent test). From this contrast, we conclude that caution must be used in the direct application of data from quiescent tests to the investigation of transient conditions. A final conclusion is that since the expected containment postaccident environment would more closely resemble the transient test conditions, it follows that the pressure rises from sequential combustion should be relatively benign.

2.7 IGNITER PERFORMANCE

2.7.1 Purpose

The project described in Section 2.1 demonstrated the capabilities of a GM AC-7G glow plug as a hydrogen ignition source. However, very little data was obtained on the effect of reduced voltage or on response of the glow plug during and after combustion. Tests were conducted at the Whiteshell Nuclear Research Establishment to gain this additional knowledge of the glow plug as an igniter. In addition, a survey was conducted on the suitability of other igniter designs. If a promising igniter design was identified, ignition tests would also be conducted by Whiteshell.

2.7.2 Summary

The test vessel had a volume of approximately 0.6 cubic feet and was equipped with a pair of 4 inch viewports for observing and/or photographing tests. A schematic of the vessel is shown in Figure 2.7-1. Pipes shown entering the vessel were used for gas injection and sampling. One pipe was connected to a strain gauge pressure transducer. Fast response Type K thermocouples were used to measure atmosphere temperature as well as glow plug temperature.

The test program consisted of three phases. Additional data on the lower flammability limit of hydrogen-steam-air mixtures was obtained from Phase 1. Both static and turbulent tests were conducted. A temperature history of the glow plug was obtained with each test. The glow plug was operated at 14 volts. Phase 2 consisted of test similar to Phase 1. However, in this phase, the glow plug was operated at reduced voltages. At the present, Phase 3 was reserved for conducting ignition tests with an alternative igniter design.

Data was obtained on glow plug performance in various hydrogen-steam-air mixtures. The glow plug was operated at 12 and 14 volts in quiescent and turbulent conditions. Numerous tests were conducted to determine the lower ignition limits and corresponding igniter surface temperatures in various premixed hydrogen-air-steam mixtures. Hydrogen concentrations were varied between 4-15 volume percent and steam concentrations varied between 0-60 volume percent. The measurement of igniter surface temperature required for ignition showed that the igniter at its normal operating temperature has considerable margin even for high steam concentrations. An interim report is included in Appendix 2I.

2.8 COMBUSTION PHENOMENA

2.8.1 Purpose

The effects of turbulence on combustion is a phenomena that is not easily predicted. Most knowledge of this phenomena is based on experimental work with detonable mixtures. Analyses of ice condenser containments have shown that given the hydrogen concentrations present, the level of turbulence in containment should not have a significant effect on the combustion of hydrogen.

To verify this, tests were conducted at the Whiteshell Nuclear Research Establishment to study the effects of turbulence on the combustion of lean hydrogen concentrations. In addition, tests were conducted to verify the completeness of combustion and the reaction rates for various steam-air-hydrogen mixtures. | 5

2.8.2 Summary

The test vessel was an eight foot diameter sphere with a volume of approximately 220 cubic feet. Instrumentation included, fast response thermocouples, pressure transducers, and ion probes. Gas chromatography was used to determine atmosphere constituents. A schematic of the test apparatus is shown in Figure 2.8-1. | 5

The test program was divided into four phases. Phase 1 investigated the extent of reaction for various steam-air-hydrogen mixtures. The hydrogen concentration was varied from approximately 5 to 10% and steam from 0 to 30%. Hydrogen concentrations from 10 to 42% were studied in Phase 2. Data from these tests were used to validate pressure transient correlations developed by Whiteshell. As in Phase 1, the steam concentration was varied from 0 to 30%. Turbulence effects were studied in Phase 3. Turbulence was created with fans and grating. | 5

Tests were conducted with both items individually and jointly. Fan flow was varied from zero to a combined maximum of approximately 3000 cfm. The grating consisted of a 1/4 inch plate perforated with 1 inch diameter holes, resulting in a blockage of 50%. Plates were located one third and two thirds the vessel height. Hydrogen concentrations were varied from 6 to 20 v/o. In Phase 4, a pipe approximately one foot in diameter and 20 feet long was attached to the sphere. Tests were conducted with uniform and non-uniform hydrogen concentrations varying from 6 to 20%. Ignition was in the pipe and in the sphere. These tests provided data on the effects of flame propagation from one geometry into another, as well as the effects of propagation from one concentration to another.

Test results obtained appear to confirmed that steam and turbulence have competing effects on hydrogen combustion. Steam tended to reduce the rate and degree of combustion, while turbulence promoted rapid and more complete combustion. However, as the hydrogen concentration approached stoichiometric, the effect of turbulence became marginal. The effect of gratings was dependent on the hydrogen concentration. Gratings appeared to enhance the combustion rate of lean mixtures due to splitting of the fire ball. However, the heat sink effect of the gratings appeared to dominate for relatively rich concentrations; thus reducing the peak pressure. Varying the ignition location from the pipe end to the sphere's center confirmed that lean mixtures propagate more readily in the upward than horizontal direction when turbulence is not present. Although the burst disc separating the pipe and sphere induced local turbulence, no significant effects of propagating flames between unequal concentrations were observed.

Based on these tests, it was concluded that the observed effects of steam, induced turbulence, connected geometrics, and unequal hydrogen concentrations were consistent with our understanding of hydrogen combustion phenomena. The results of these tests are located in three interim reports provided in Appendix 2J. These reports are dated December, 1981, April, 1982, and July, 1982.

2.9 HYDROGEN MIXING AND DISTRIBUTION

2.9.1 Purpose

Concerns have been expressed regarding the potential for localized accumulation of hydrogen at detonable concentrations. Previous analyses have shown that as a result of the mixing induced by the air return fans and the steam-hydrogen jet itself, the formation of detonable concentrations is precluded.

Additionally, the design of the hydrogen mitigation system assures that the released hydrogen starts burning once a flammable concentration is reached.

However, to provide additional assurances that localized hydrogen accumulation will not occur, tests were conducted by the Hanford Engineering Development Laboratory (HEDL) to verify the mixing characteristics of the air return fans and the steam-hydrogen jet.

2.9.2 Summary

Tests were conducted at HEDL's Containment Systems Test Facility (CSTF). This facility has a height of 67 feet and a diameter of 25 feet. Volume of the facility is approximately 3×10^4 cubic feet. The CSTF was modified to resemble a simplified ice condenser containment. A schematic of the modified CSTF is shown in Figures 2.9-1 and 2.9-2. Atmospheric temperature and hydrogen concentration was measured as a function of time at various locations. Additional measurements included flow velocity and water vapor concentration.

The test program included tests with and without the air return fans. In addition, the injection rate of the jet was varied. Although a majority of the tests were conducted with helium, one test was conducted with hydrogen to assure applicability of the helium tests.

Results indicated that the lower compartment was well mixed; thus precluding the formation of pockets containing significantly higher concentrations of hydrogen. More specifically, the data indicated that:

5

- 1) The air return fans minimize the peak concentration and the maximum concentration difference within the test compartment.
- 2) Test compartment mixing is not strongly dependent on the orientation of the source jet.
- 3) Mixing was very good even without forced circulation by the air return fans.

Based on these tests it was concluded that there is no potential for pocketing of rich hydrogen mixtures and that the containment analysis mixing assumptions are valid. A preliminary project report is provided in Appendix 2K.

5

APPENDIX 2J
COMBUSTION PHENOMENA
INTERIM PROJECT REPORTS

1. STUDY OF HYDROGEN COMBUSTION NEAR LOWER
FLAMMABILITY LIMITS
December, 1981
2. COMBUSTION STUDIES AT HIGH HYDROGEN CONCENTRATIONS
AND THE EFFECT OF OBSTACLES ON COMBUSTION
April, 1982
3. THE EFFECT OF VOLUME GEOMETRY ON THE COMBUSTION
OF UNIFORM AND NON-UNIFORM HYDROGEN CONCENTRATIONS
July, 1982

The Effect of Volume Geometry on the Combustion of
Uniform and Non-uniform Hydrogen Concentrations

Interim Project Report
July, 1982

Prepared by:

K. J. Vehstedt, American Electric Power
F. G. Hudson, Duke Power Company
D. G. Renfro, Tennessee Valley Authority

Project Conducted at:

Whiteshell Nuclear Research Establishment

Project Sponsors:

American Electric Power Service Corporation
Atomic Energy of Canada Limited
Duke Power Company
Electric Power Research Institute
Ontario Hydro
Tennessee Valley Authority

1.0 INTRODUCTION

Phase 4 of the Whiteshell Nuclear Research Establishment (WNRE) hydrogen combustion test program consisted of experiments carried out in the pipe-sphere vessel geometry of the Containment Test Facility (CTF). The effects of varying H_2 concentration, igniter location, and fan-induced turbulence were investigated. H_2 concentrations ranged from just-flammable to near-stoichiometric. In addition, the effects of non-uniform H_2 concentrations were investigated. The test matrix is provided in Tables 1 and 2.

2.0 TEST

The facility used for the present series of experiments consists of a 20-foot long, 12-inch diameter pipe closed at one end and connected to the 8-foot diameter sphere (Figure 1). Two igniter locations, the sphere center and the pipe end, are available. Only the pipe end location was used for the non-uniform concentration tests. The pressure in the pipe and the sphere are measured by several piezo-electric transducers. The flame travel in the pipe is detected by six 0.003" diameter platinum/platinum-10% rhodium thermocouples placed along the length of the pipe. The thermocouples are all equispaced with the spacing of 33.75 inches and oriented horizontally at about the pipe centerline. A schematic of the instrumentation is shown in Figure 1.

The gases were introduced into the system through penetrations in the pipe and the sphere separately, but simultaneously. To ensure uniform mixtures in the pipe-sphere combination, the fan was kept operating during charging, as well as 5 to 10 minutes before the gases were sampled for analysis. The fan is located horizontally about the elevation of the sphere centerline oriented perpendicularly to the pipe.

It was found that at low concentrations, between 6 to 10%, a maximum difference in the concentrations of hydrogen between the pipe and the sphere was about 0.5%. At high concentrations, around 25% hydrogen, the difference was of the order of 2%. Only one fan was used for these experiments.

3.0 PROJECT RESULTS

3.1 UNIFORM CONCENTRATION: PIPE END IGNITION

Figure 2 shows the pressure-time histories at 6.5% hydrogen using end ignition, with and without fan turbulence. In the absence of turbulence, a small increase in the pressure of about 0.3 psi was observed. From the pressure trace, it may be observed that it took nearly 20 seconds for the flame to travel a distance of 22 feet, into the sphere. Since the horizontally mounted thermocouples did not detect the flame front, it was surmised that the flame traveled along the top of the pipe. Gas analysis after the burn showed virtually no change in the hydrogen concentration. In order to verify that the flame indeed traveled along the top of the pipe into the sphere, the fan was turned on (1500 rpm) and the mixture was reignited. The "Fan On" curve in Figure 2 shows the pressure trace for this case. It is obvious from the trace that the flame has traveled along the top of the pipe and reached the sphere in approximately 20 seconds

There is no increase in the pressure in the system until the flame kernel has arrived in the sphere. The combustion in the sphere is very rapid. Gas analysis showed nearly 80% of the hydrogen burnt.

Figures 3 and 4 show the results for a hydrogen concentration of 8%. Here also, without turbulence, the pressure rise is small. Since 8% is below the 8.5% limit for upward followed by downward flame propagation, once the fireball reaches the top of the sphere it gets quenched. However, in the presence of turbulence, the combustion in the sphere is rapid. It can be seen that the flame has arrived at the sphere at approximately 13 seconds. There it develops into a much bigger flame and a backward propagation into the pipe takes place. This is clearly evident from the thermocouple traces in Figure 4. The temperatures measured are quite low. This may be due to delayed thermocouple response, as well as heat losses from the thermocouple. The backward flame propagation speed is reduced in the last portion of flame travel as seen from the traces of T5 and T6. This is due mainly to cooling of the burnt gases in the sphere.

Figures 5, 6, and 7 show combustion experiments for 20% hydrogen. In this case, a fully developed flame propagates along the pipe into the sphere as can be seen from Figure 6. The flame travels in the pipe at an average speed of 200 fps. The flame speed between thermocouples T1 and T2 is approximately 300 fps. At these high hydrogen concentrations, large pressure oscillations were detected by the piezo-electric transducer in the pipe. The oscillations nearly coincided with the instant of complete combustion and had an amplitude of ± 10 psi. The oscillations were nearly completely attenuated in the sphere. The frequency of oscillations is roughly 30 Hz. The calculated frequency of acoustic oscillations in the pipe is 31 Hz which agrees with the observed frequency.

3.2 UNIFORM CONCENTRATION: SPHERE IGNITION

Figures 8 and 9 show combustion at 8.5% hydrogen with central ignition. From the shape of the graph, it is obvious that this corresponds to upward, followed by downward, propagation. It appears that the flame propagates into the pipe at around 10 to 11 seconds (Figure 9), which is during the downward propagation. The combustion is complete at about 14 seconds. The flame speed in the pipe is reduced once the gases in the sphere cool off. This can be seen from flame arrival times at T4, T6, and T6 in Figure 9.

Figures 10 and 11 show experimental results at 10% hydrogen. In this case, the flame front theoretically should be spherical, and one would expect the flame to propagate into the pipe at around 2 seconds, the instant at which the combustion is complete in the sphere. However, Figure 11 shows that the flame has already arrived at the first thermocouple at 1.3 seconds. This asymmetric propagation is likely caused by the perturbation of the connected pipe.

Figures 12, 13, and 14 show pressure and temperature traces for a 20% hydrogen burn. Figure 12 is the pressure trace of the transducer mounted in the sphere (pz4) which shows no detectable oscillations. However, all the transducers in the pipe depicted large pressure oscillations. Here again, pressure oscillations appear soon after the combustion is complete.

Finally, Figures 15, 16, and 17 show combustion at 25% hydrogen. All pressure transducers show large oscillations except those in the sphere. The flame

speed calculated from the thermocouples is approximately 1650 fps between T1 and T2 and 2200 fps between T2 and T3. However, this speed quickly decelerates as it reaches thermocouples T4, T5, and T6. Between T4 and T6, the flame speed has dropped to 400 fps. Figure 17 compares the traces of pz5 and pz6. The amplitude of pressure oscillations is reduced away from the closed end of the pipe. The highest amplitude was observed by the transducer mounted on the pipe flange (pz7, Figure 16) and is greater than the adiabatic pressure by 60 to 70 psi.

3.3 NON-UNIFORM CONCENTRATION

In order to evaluate the effects of constriction by the burst disc holder, a plate with a 6-inch diameter opening, some experiments were done without installing the diaphragms. Figure 18 shows the time of arrival of the flame plotted against distance along the pipe for a hydrogen concentration of 10%. As can be seen, the presence of the constriction has slowed down the flame. In both constricted and unconstricted cases, after a short distance from the igniter, the flame propagated at a nearly constant velocity. Figure 19 shows the pressure-time history as seen by the transducers mounted in the sphere and the pipe-end flange. There is no appreciable pressure rise indicated by either transducer until the flame arrives in the sphere. Once the flame arrives in the sphere, the pressure rise is rapid in the sphere. Due to the presence of the constriction, the pressure in the pipe lags behind the pressure in the sphere. Further, the peak pressure in the pipe is lower. The peak pressure attained in the sphere is about 37.4 psi, nearly 2.3 psi less than for combustion without constriction (for a pipe-sphere geometry).

Figures 20 and 21 compare the flame travel and pressure-time histories for combustion with and without constriction for 20% hydrogen. As before, the flame speeds are higher in the unconstricted case. Without constriction, the flame has accelerated in the final phase of flame travel in the pipe. Though in the unconstricted case the flame has arrived in the sphere somewhat earlier than in the constricted case, the pressure rise in the constricted case is faster, as can be seen from Figure 20. It is possible that the faster burning in the constricted case may be due to turbulence produced in the sphere due to flow effects produced by the constriction.

Figures 22 and 25 show the results of experiments with the burst disc installed. Below 12% hydrogen, the pressure rise in the pipe was not sufficient to rupture the disc. With 12% hydrogen in the pipe and 6% hydrogen in the sphere, there was no appreciable combustion in the sphere. The pressure rise in the sphere was small, about 1.7 psi. As can be seen from the pz7 trace in the pipe, the diaphragm ruptured at about 15 psi. After the rupture, the pressure in the pipe has dropped, and pressure oscillation has set in. However, this time the turbulent flame from the pipe caused rapid burning in the sphere. Under quiescent conditions, combustion at 6% hydrogen is slow and less than 50% of the hydrogen is burnt. But for the case investigated, as seen from the figure, combustion is very rapid. GC measurements indicated nearly 80% burnt.

Figures 24 and 25 show combustion with 10% hydrogen in the sphere and 15% in the pipe. Here again, the burst disc has ruptured close to 16 psi around 0.28 seconds from the instant of ignition. After the disc rupture, the flame has accelerated in the pipe. Both pz7 and pz4 show pressure oscillations in the pipe and the sphere, as can be seen in Figure 25.

Figure 26 shows the pressure-time history at 15% hydrogen in the pipe and 20% in the sphere as measured by pz7. Here also, pressure oscillations set in after the disc ruptures.

4.0 CONCLUSIONS

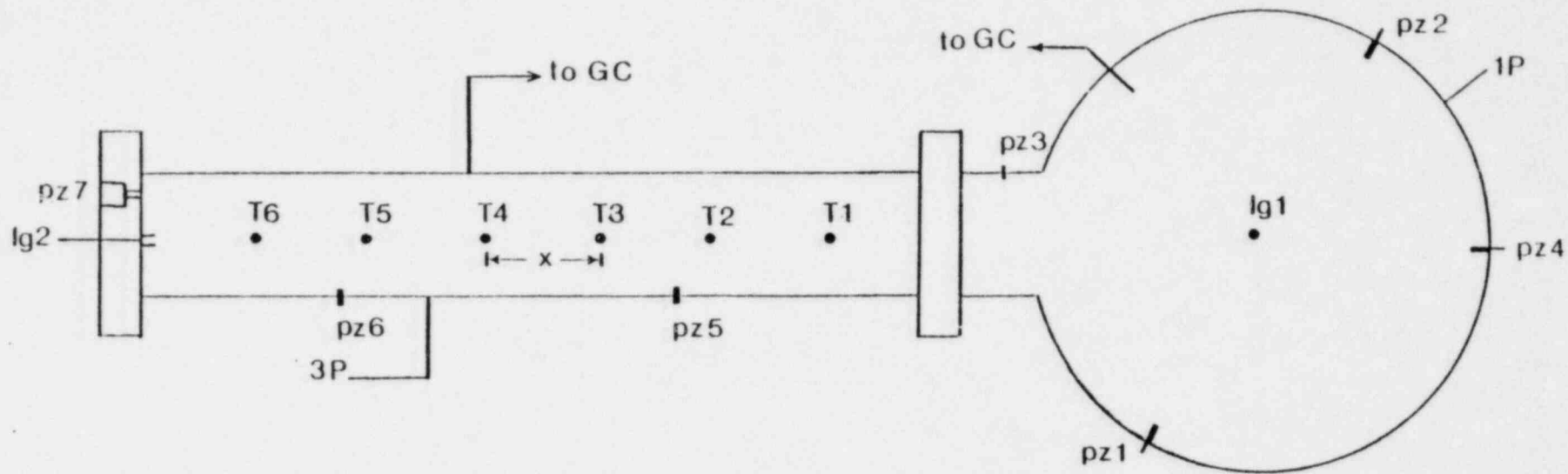
1. For pipe-end ignition, at concentrations between the horizontal and downward limits, the flame propagates only along the top of the pipe into the sphere and eventually gets quenched.
2. For pipe-end ignition, with fan-induced turbulence in the sphere, a fully developed flame flashes back into the pipe.
3. Observed flame speeds are higher with sphere-central ignition than for pipe-end ignition but decrease as the flame propagates away from the sphere.
4. At high hydrogen concentrations (above 20%), large acoustic oscillations are observed in the pipe. They follow the pressure peak, decay slowly, and occur at the same frequency as the calculated natural frequency of the pipe. Oscillations are almost completely attenuated in the sphere.
5. For sphere-central ignition, some observed peak pressures in the pipe are higher than the calculated adiabatic value at very high concentrations. Peak pressures in the sphere are less than adiabatic.
6. The presence of a constriction in the pipe slows down the rate of flame propagation in the pipe.
7. Due to induced turbulence, combustion is more rapid in the sphere when a constriction is present.
8. At high hydrogen concentrations in the pipe, sudden rupture of the disc causes turbulence and increases the extent of burn and the rate of pressure rise even in near limit mixtures.
9. Rupture of the disc sets up pressure oscillations during combustion in the sphere.

TABLE 1
Test Matrix

| <u>Initial H₂ Concentration</u> | <u>Igniter Location</u> | <u>Fan</u> | <u>Figure Number</u> |
|--|-------------------------|------------|----------------------|
| 6.5 | pipe end | off | 2 |
| 6.5 | pipe end | on | 2 |
| 8 | pipe end | off | 3 |
| 8 | pipe end | on | 3, 4 |
| 20 | pipe end | off | 5-7 |
| 8.5 | sphere center | off | 8, 9 |
| 10 | sphere center | off | 10, 11 |
| 20 | sphere center | off | 12-14 |
| 25 | sphere center | off | 15-17 |

TABLE 2
Test Matrix

| <u>Initial H₂ Concentration</u> <u>Pipe</u> | <u>Concentration</u> <u>Sphere</u> | <u>Rupture Disc</u> | <u>Figure Number</u> |
|---|---------------------------------------|---------------------|----------------------|
| 10 | 10 | No | 18, 19 |
| 20 | 20 | No | 20, 21 |
| 12 | 6 | Yes | 22 |
| 15 | 6 | Yes | 23 |
| 15 | 10 | Yes | 24, 25 |
| 15 | 20 | Yes | 26 |



- pz1 to 7 pressure transducers
- T1 to T6 thermocouples
- 1P, 3P Rosemount transmitters
- lg1, lg2 igniters
- x 33.75 inches spacing

SCHEMATIC OF THE INSTRUMENTED PIPE & SPHERE

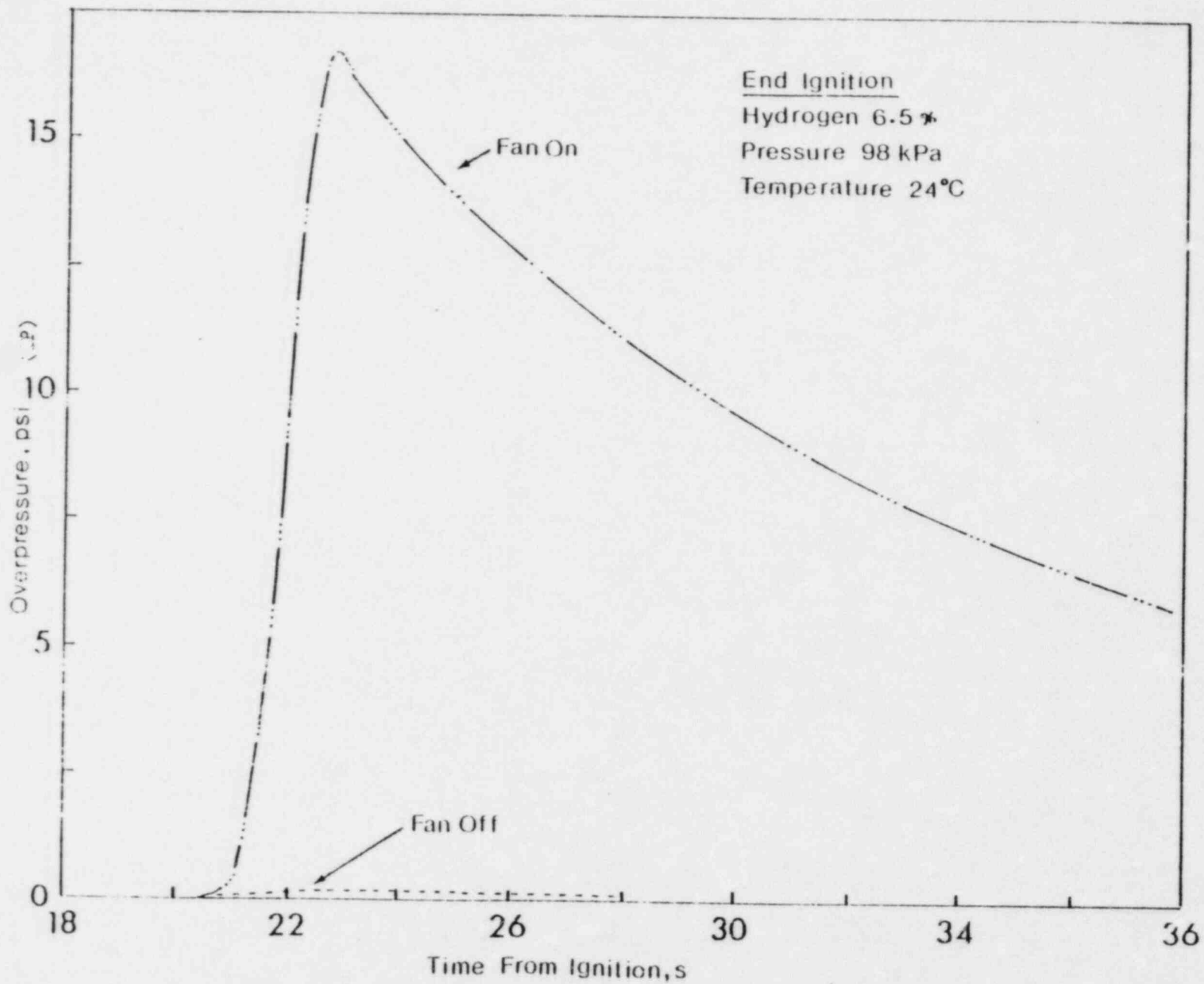


FIGURE 2

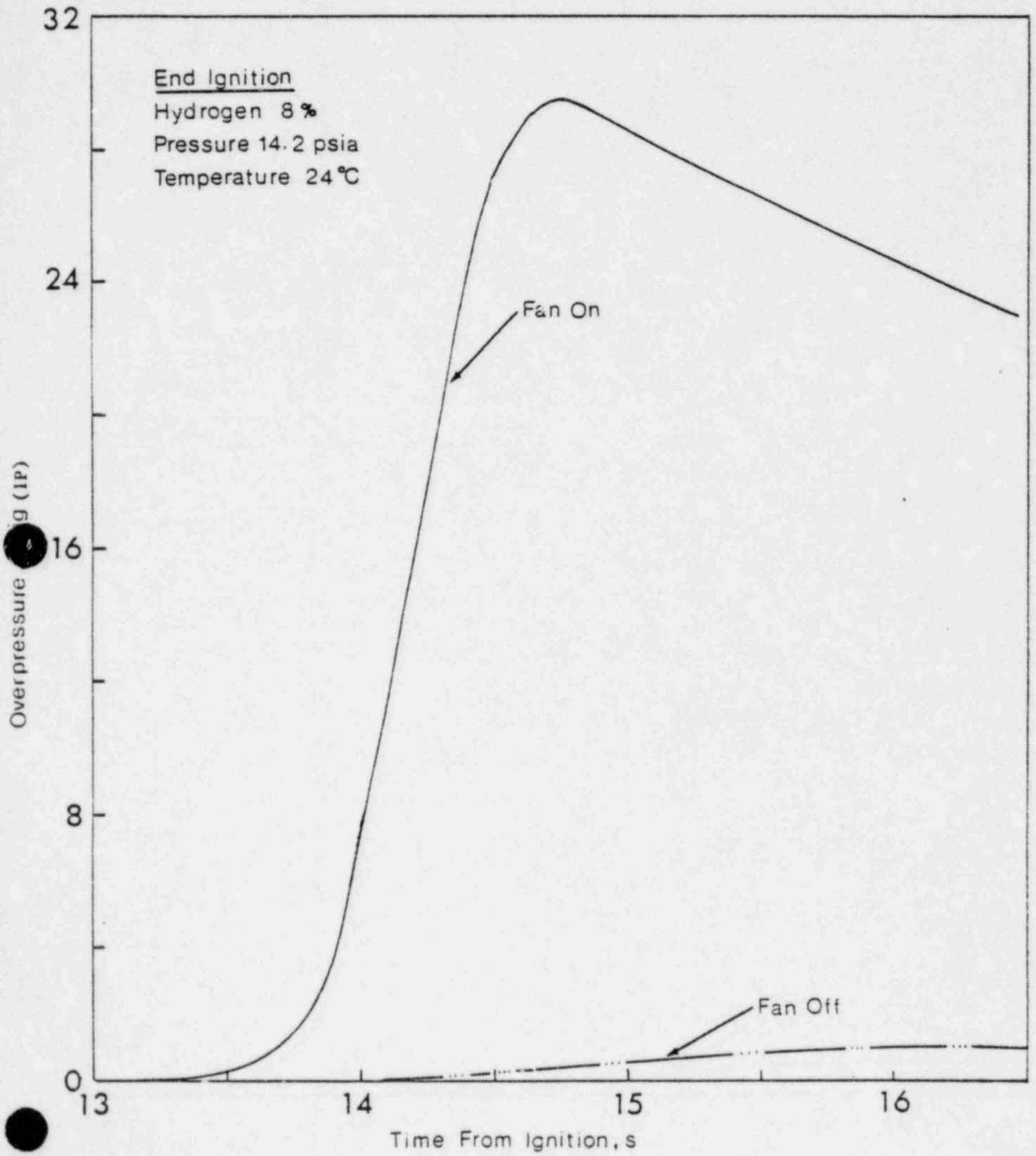


FIGURE 3

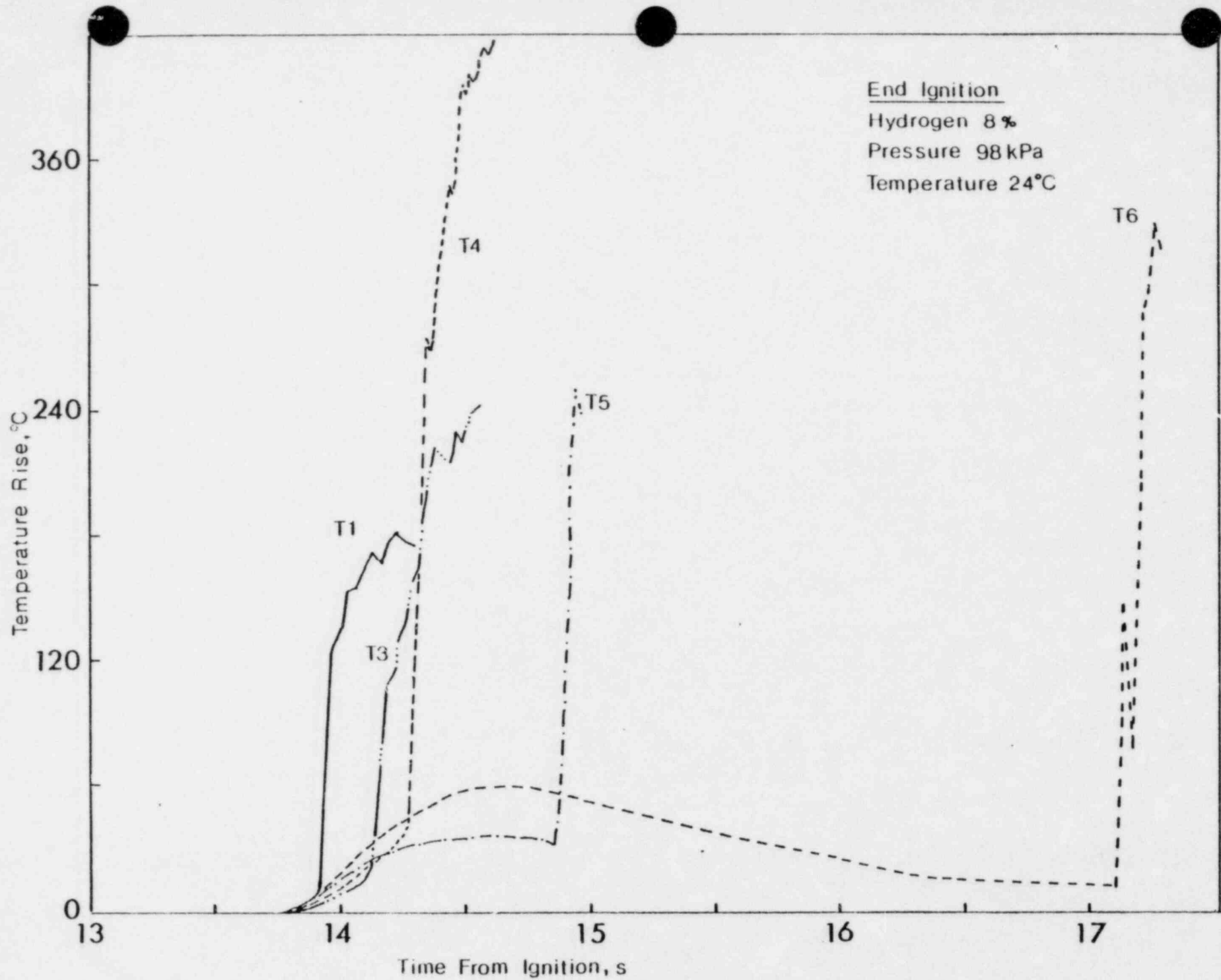


FIGURE 4

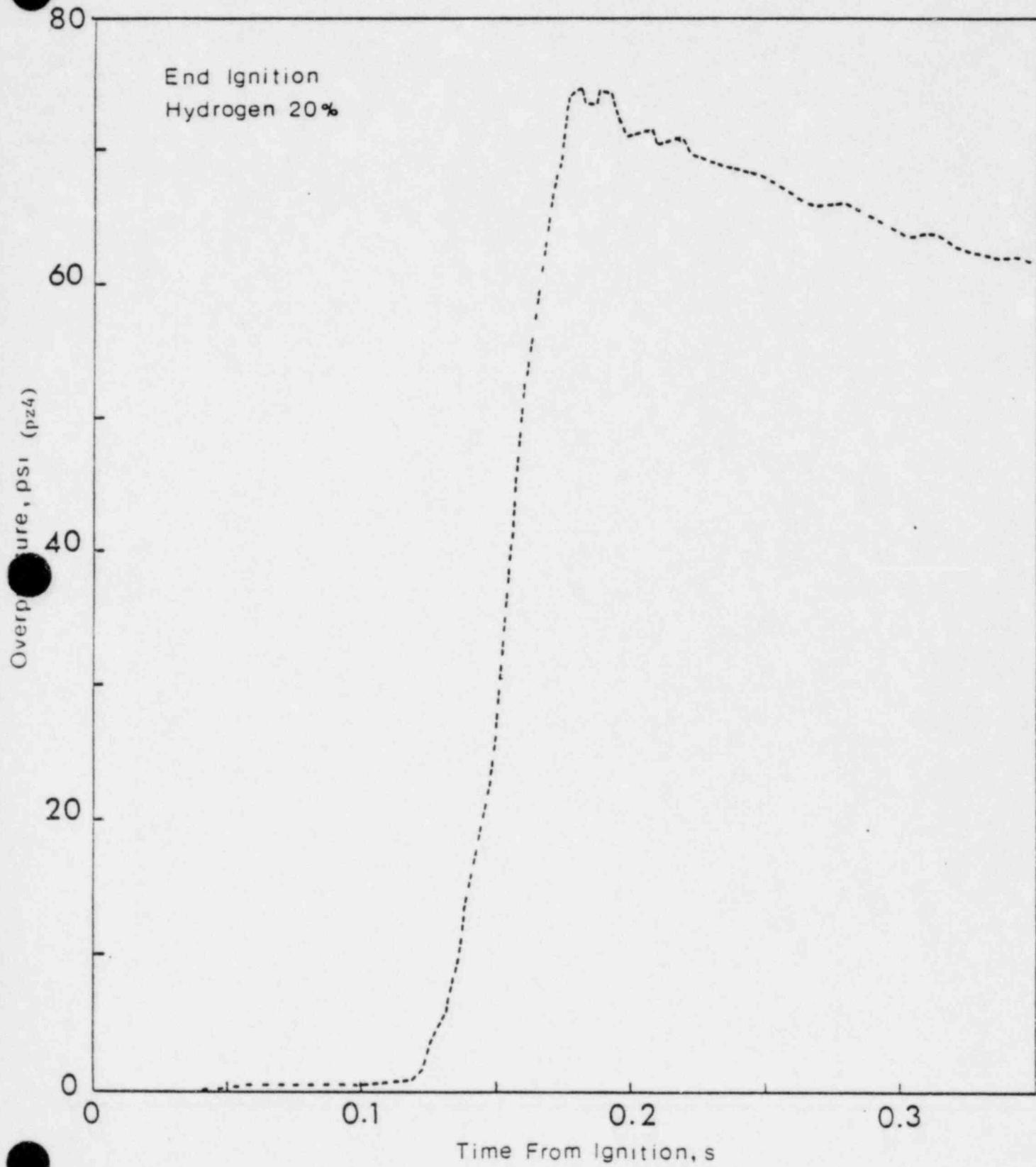


FIGURE 5

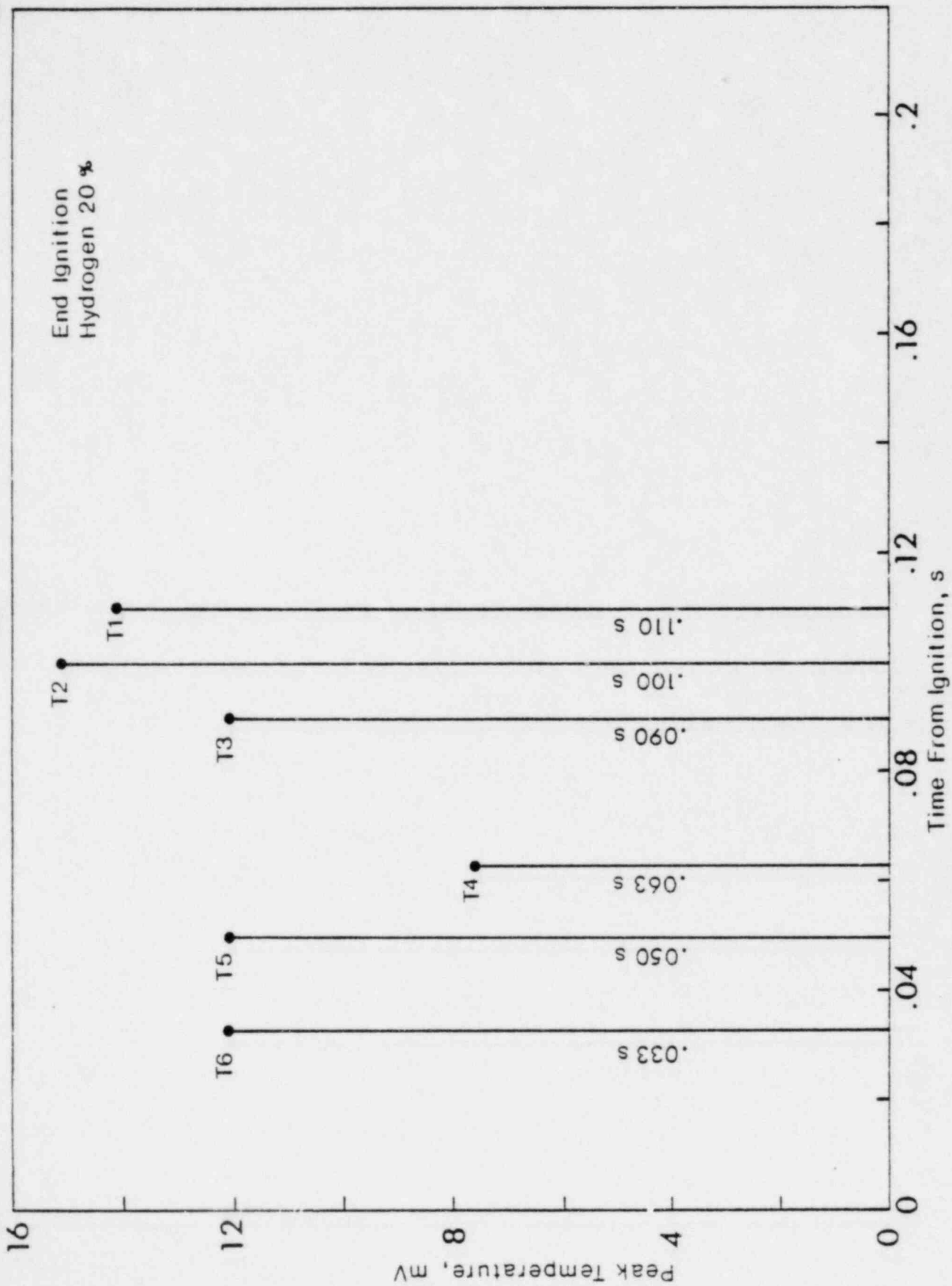


FIGURE 6

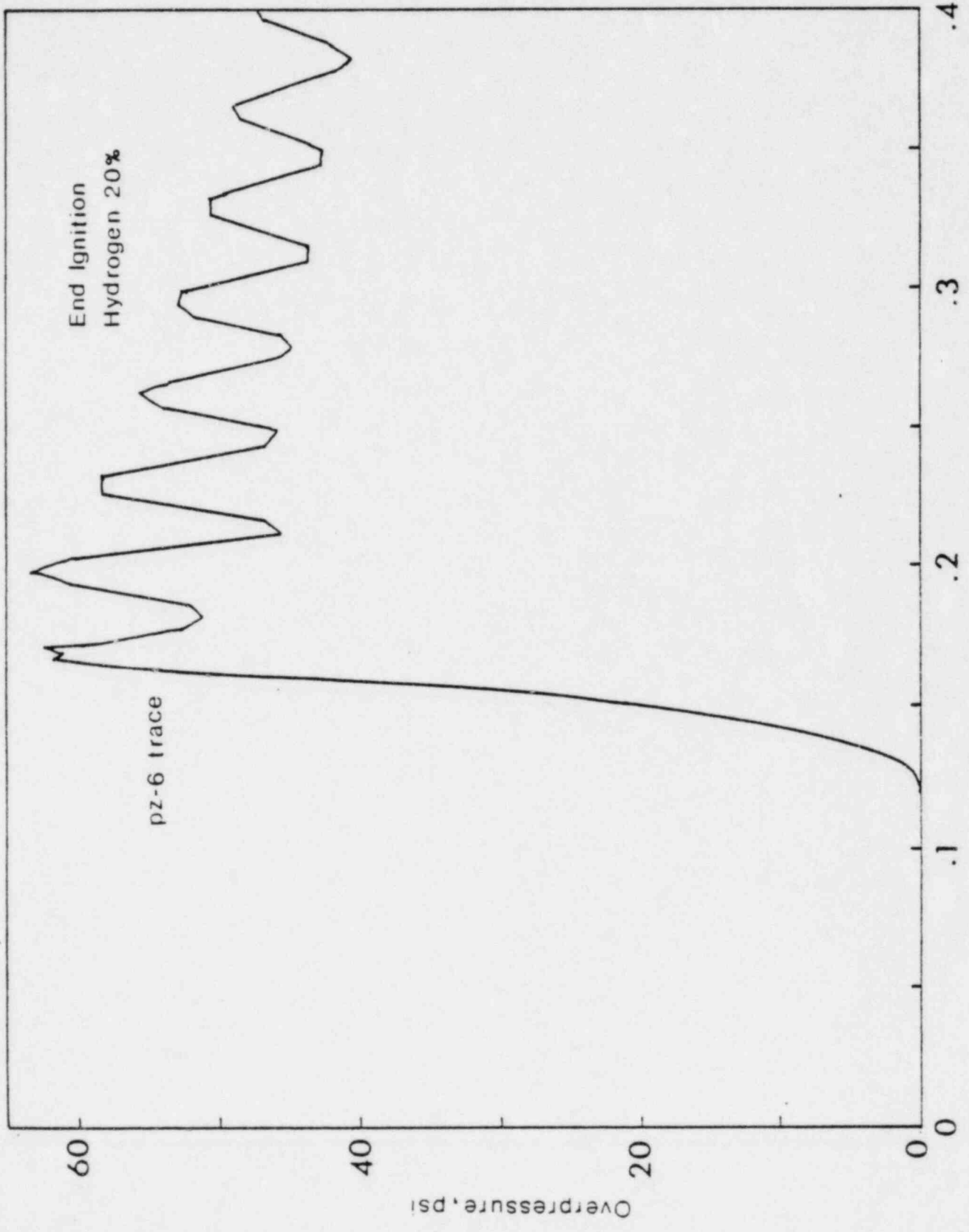


FIGURE 7
Time From Ignition, s

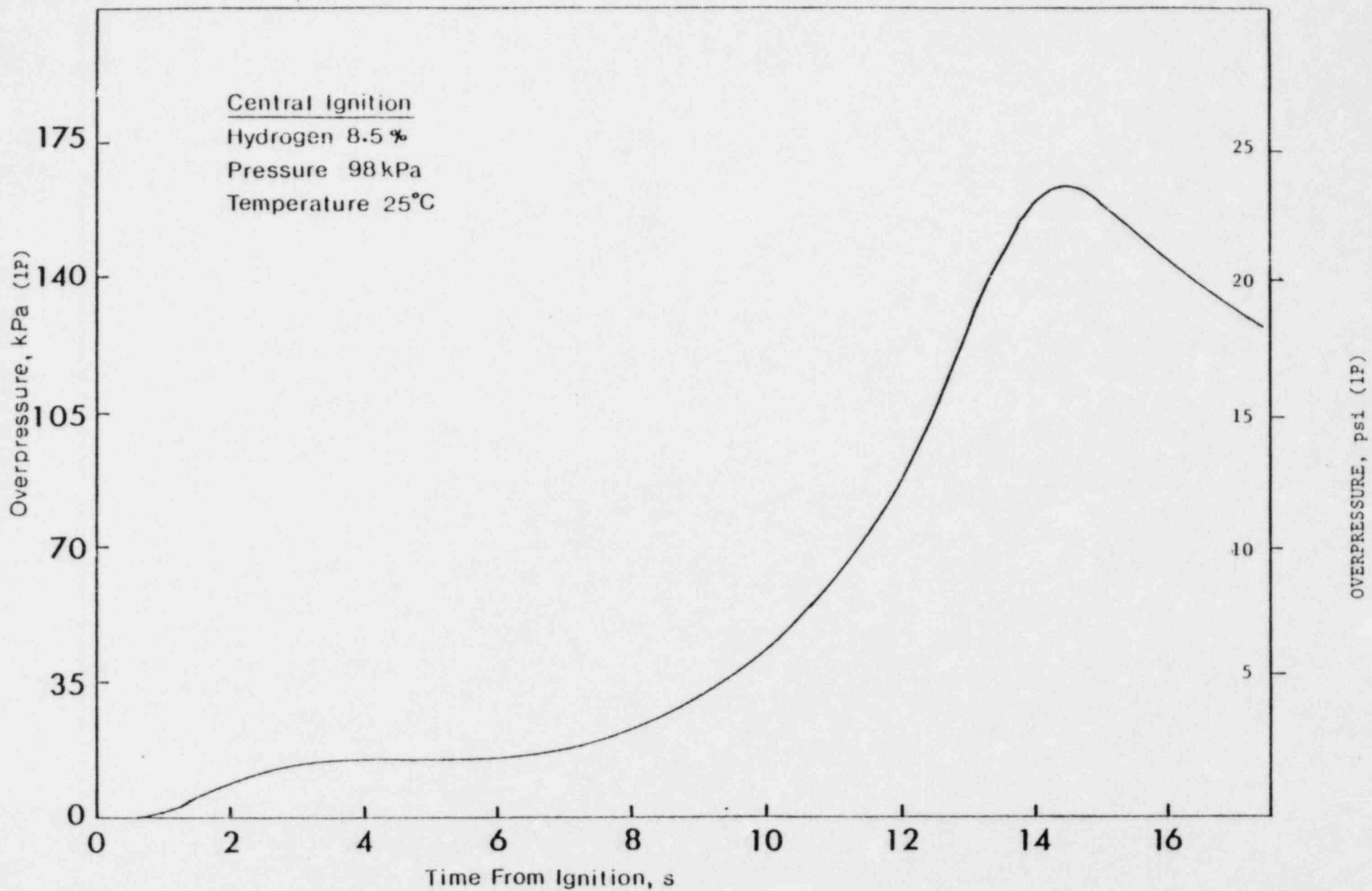
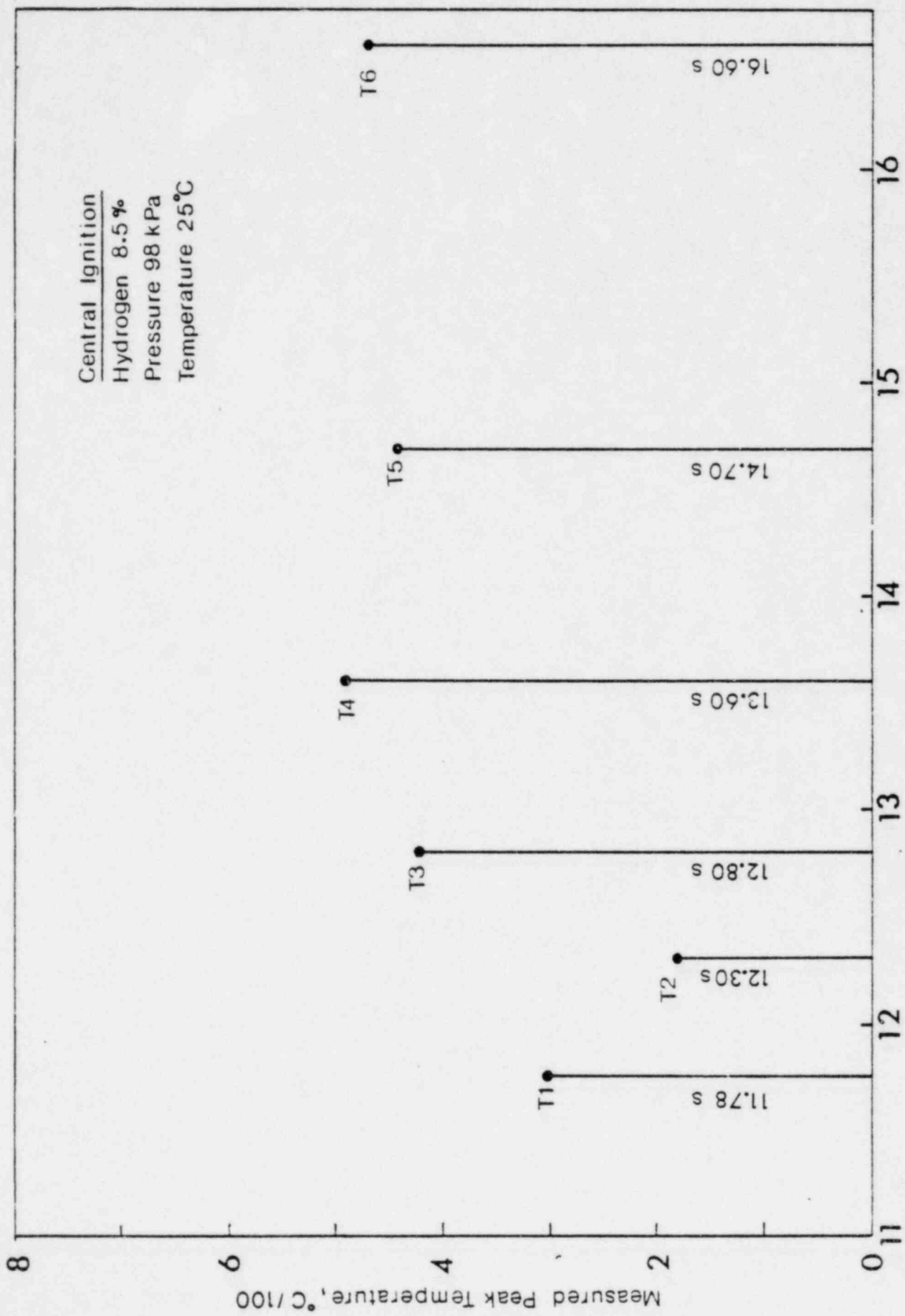


FIGURE 8



Flame Arrival Time, s

FIGURE 9

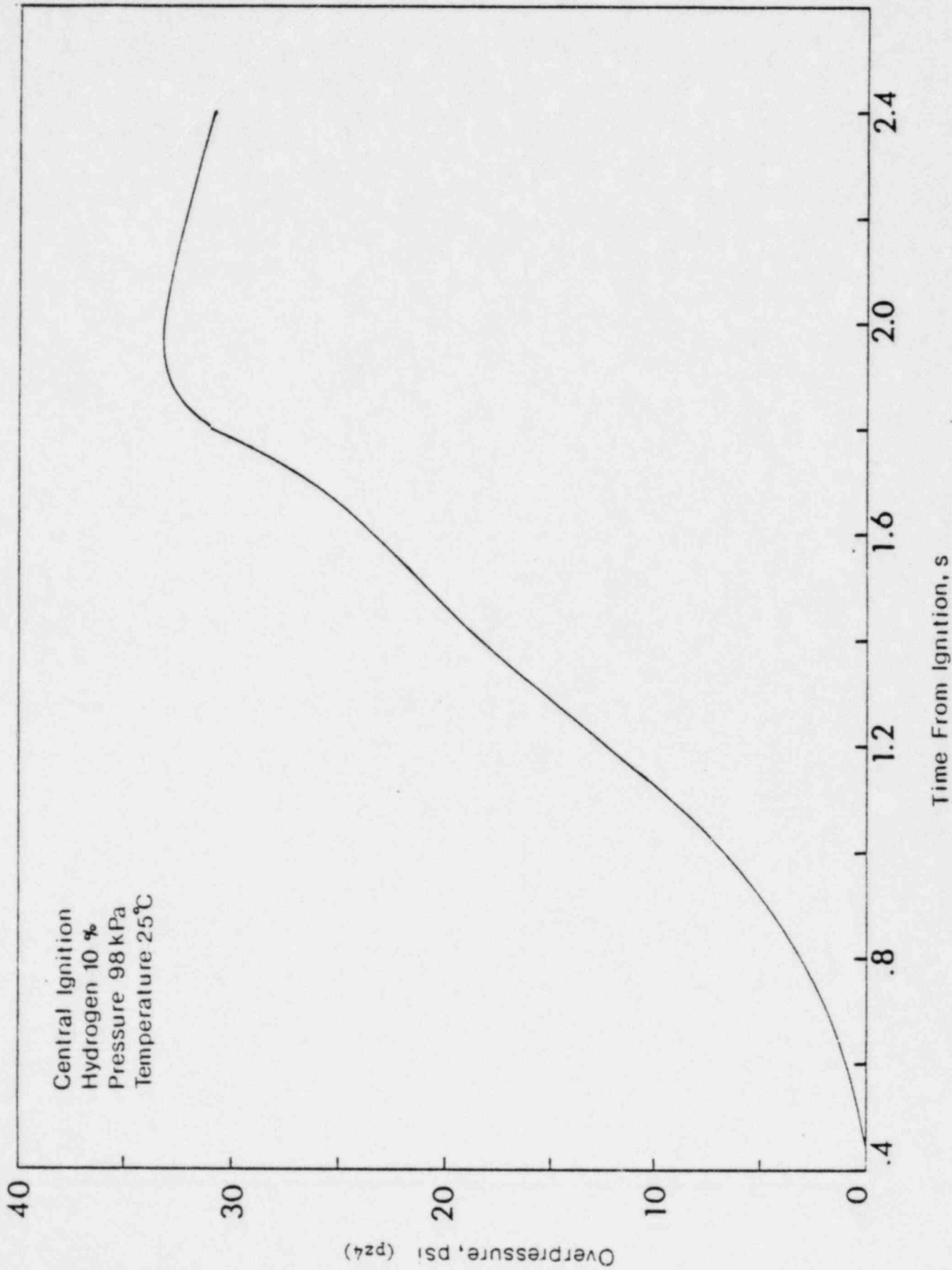


FIGURE 10

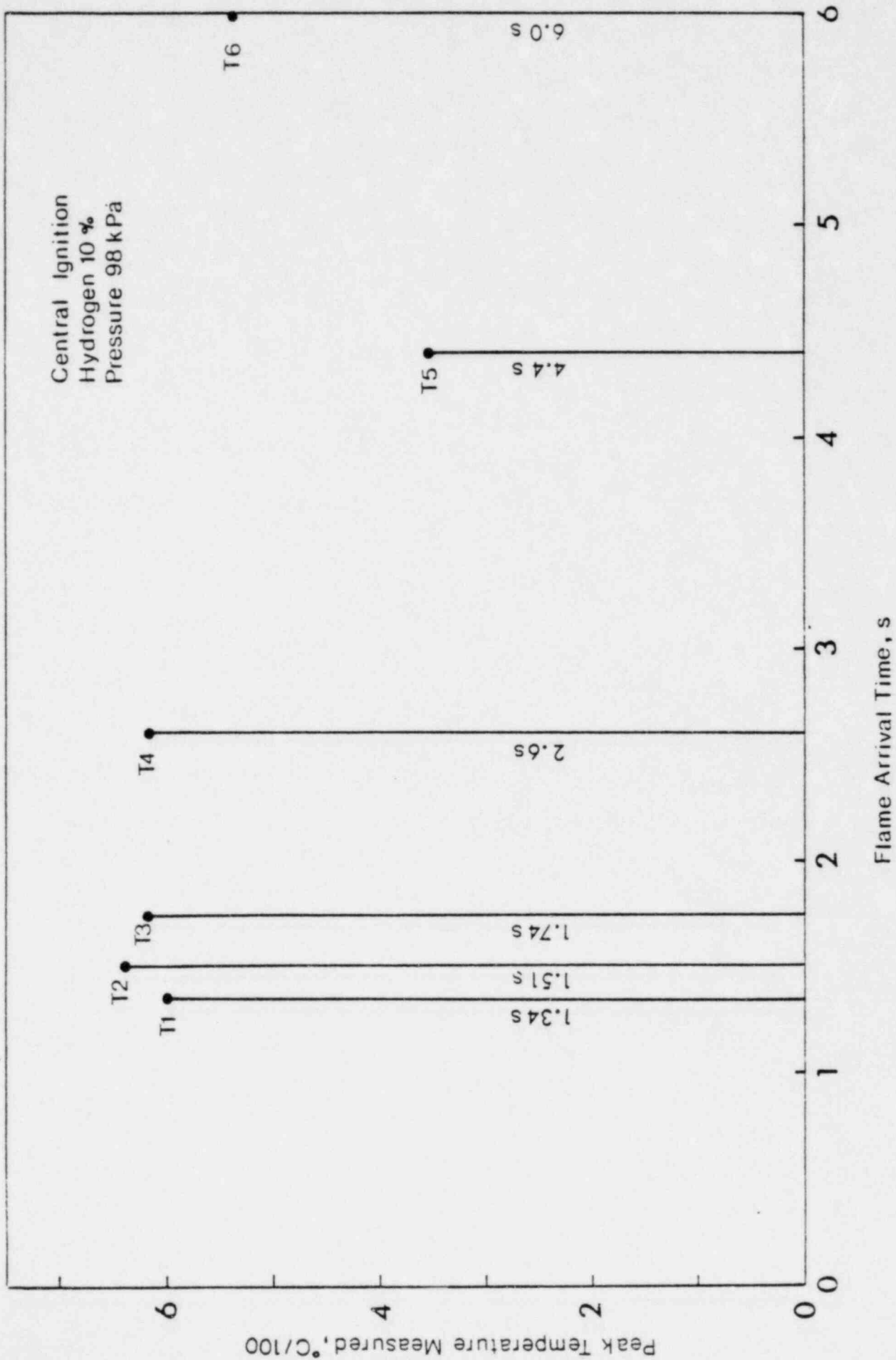


FIGURE 11

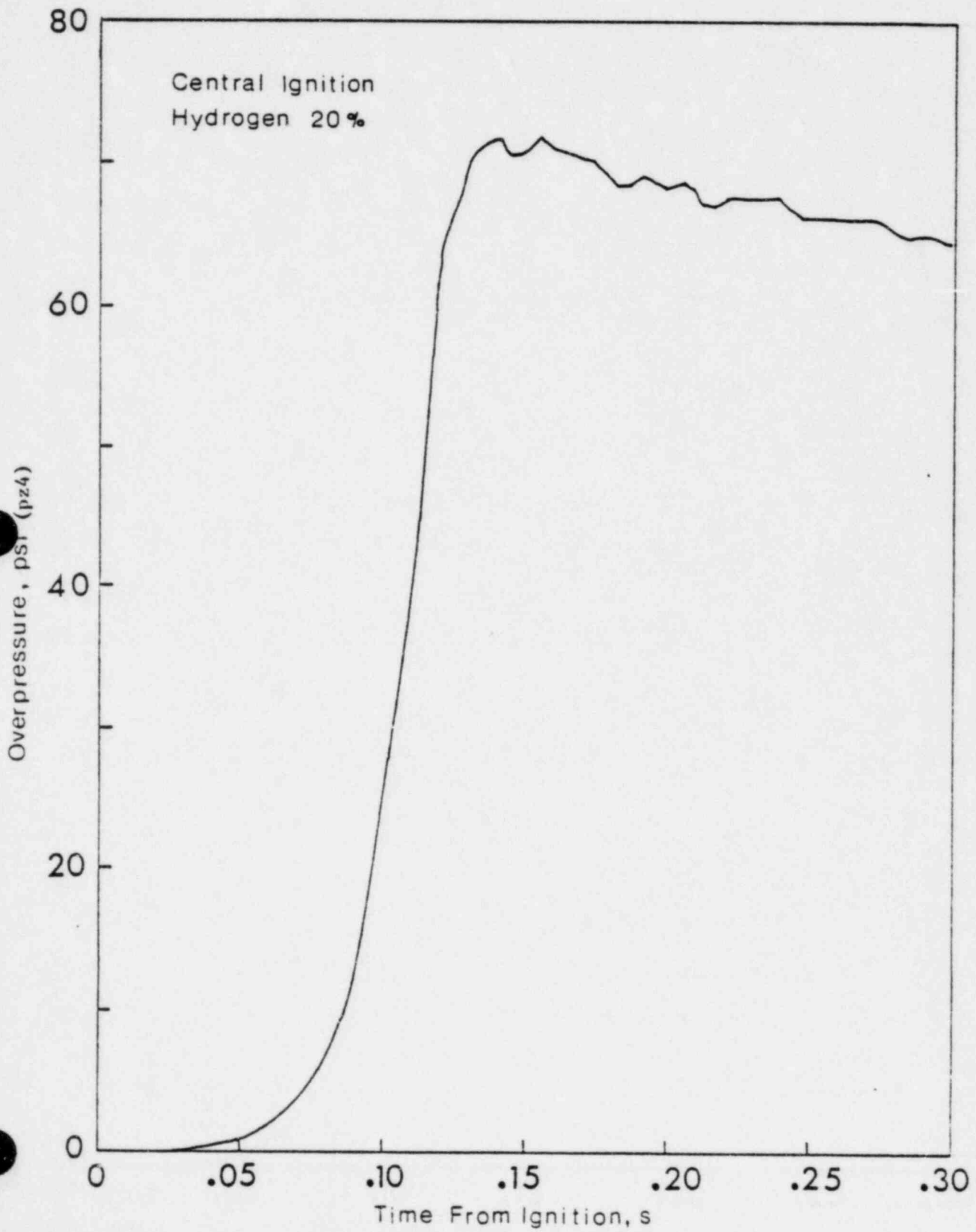


FIGURE 12

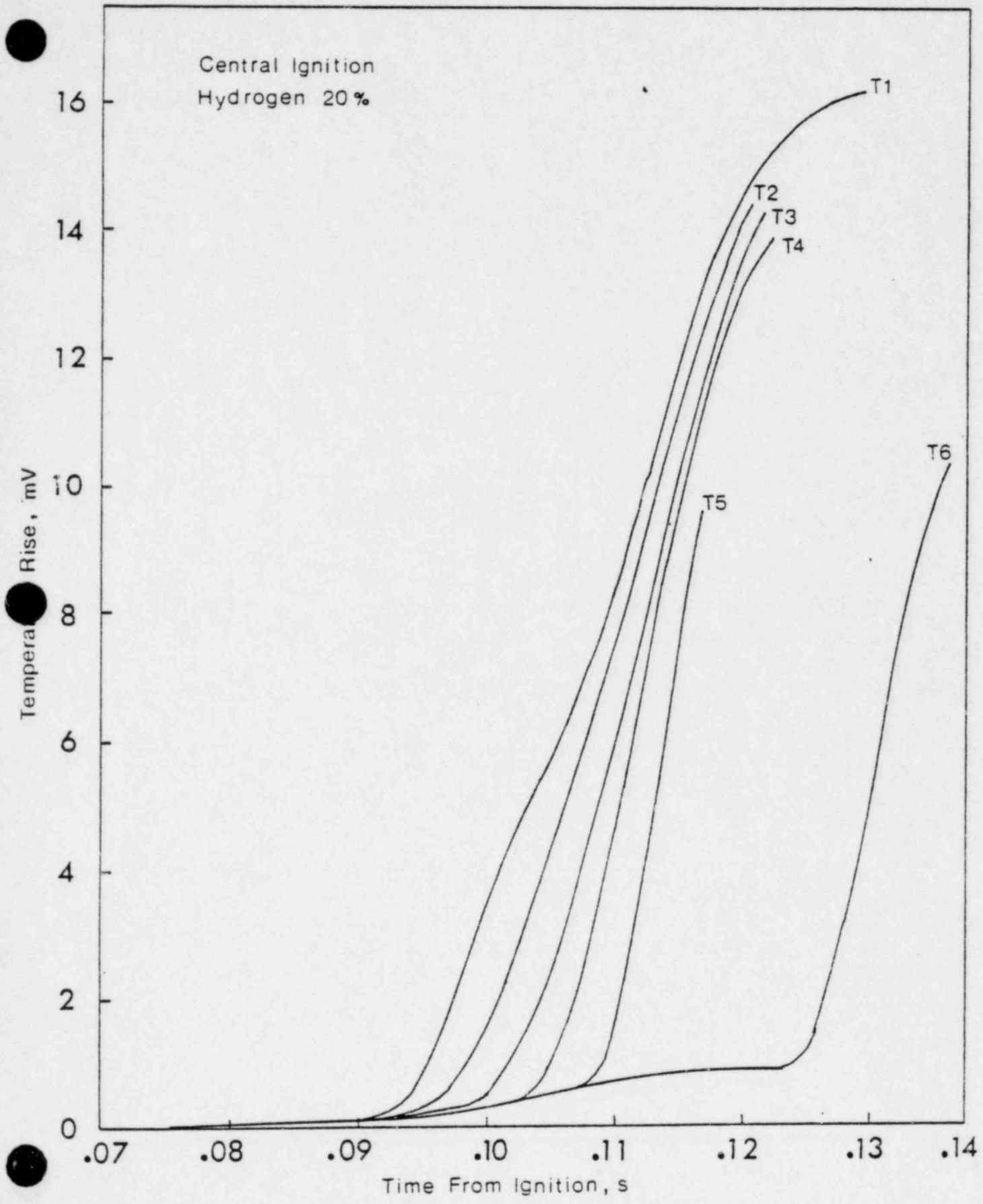


FIGURE 13

Central Ignition
Hydrogen 20%

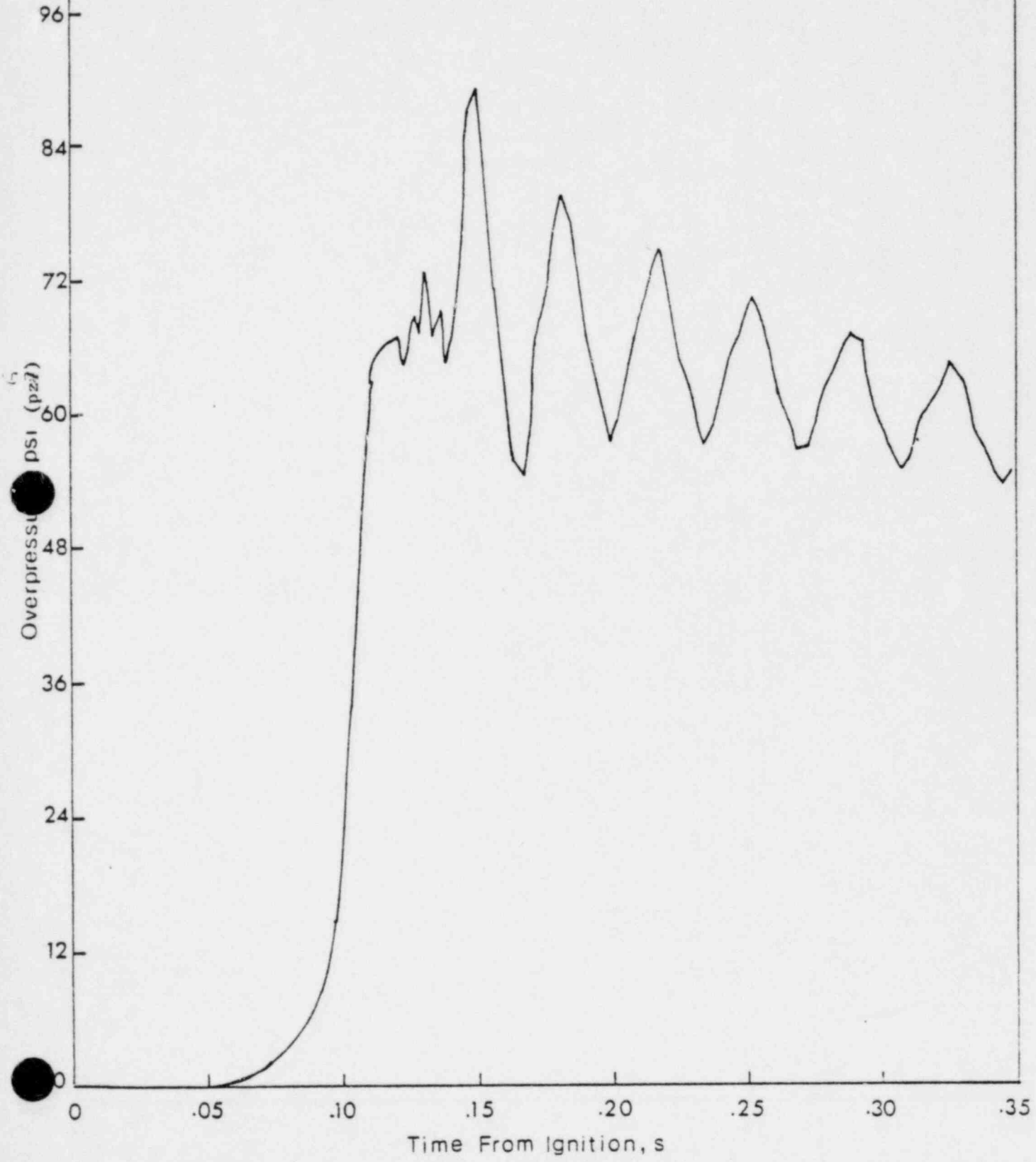


FIGURE 14

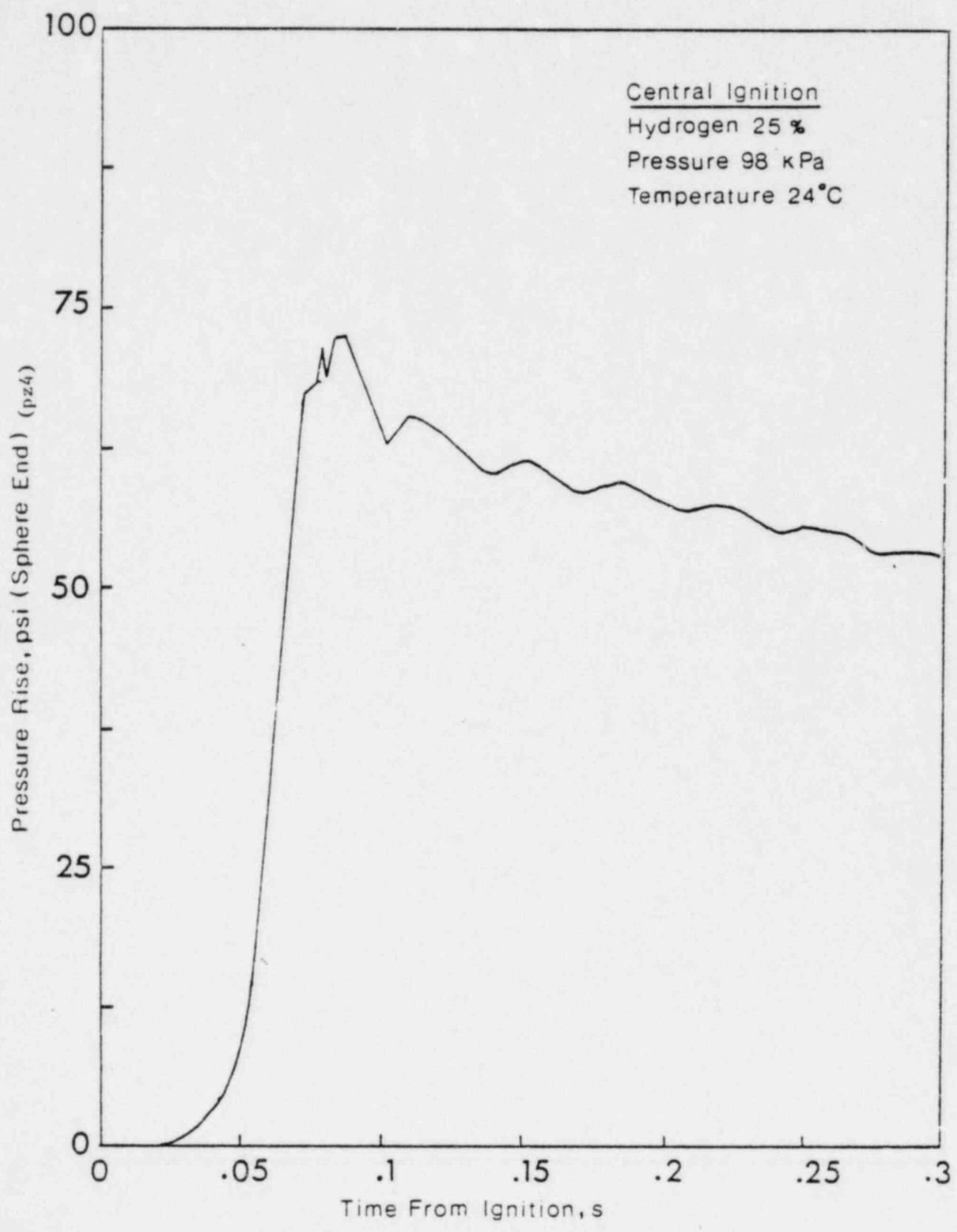


FIGURE 15

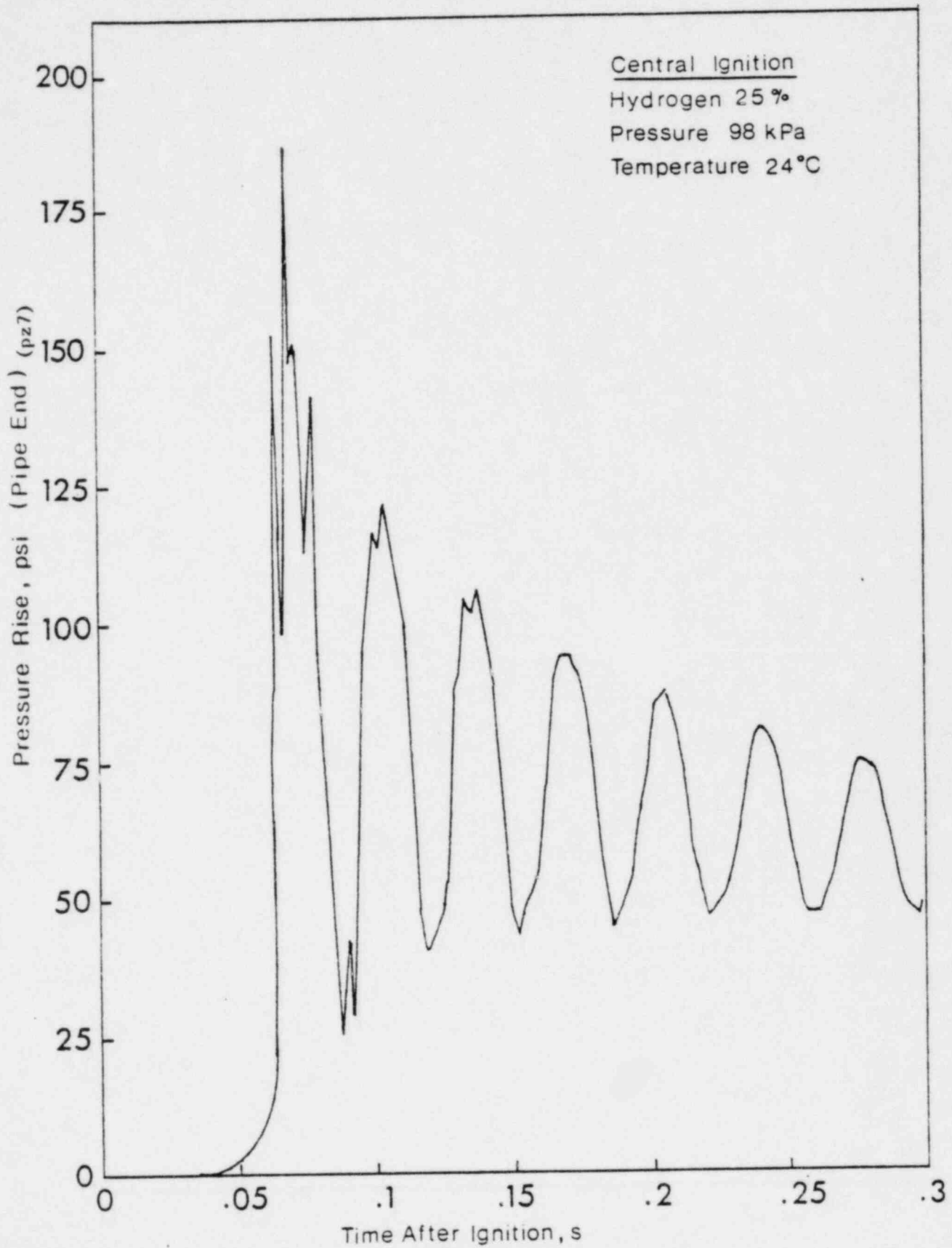


FIGURE 16

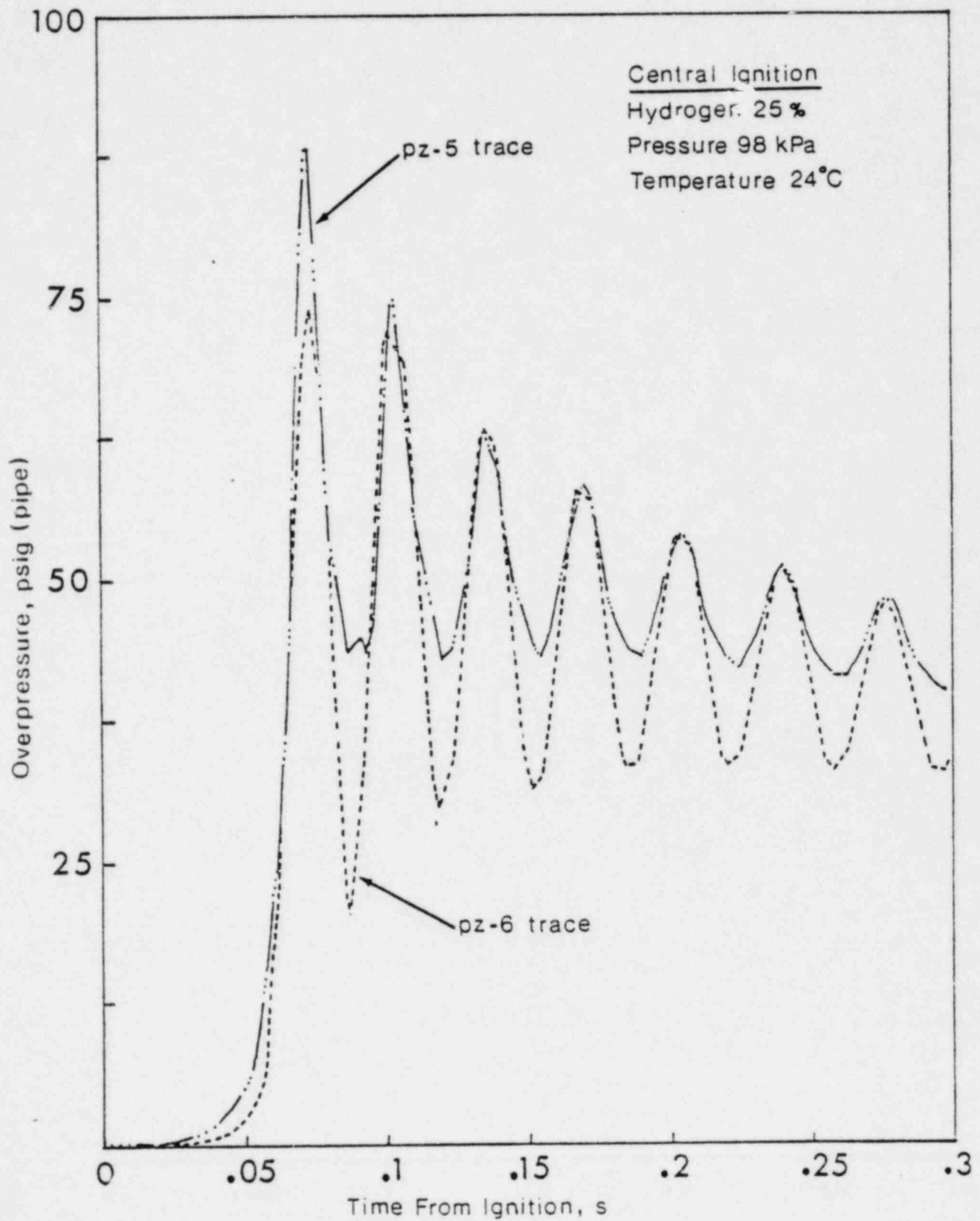


FIGURE 17

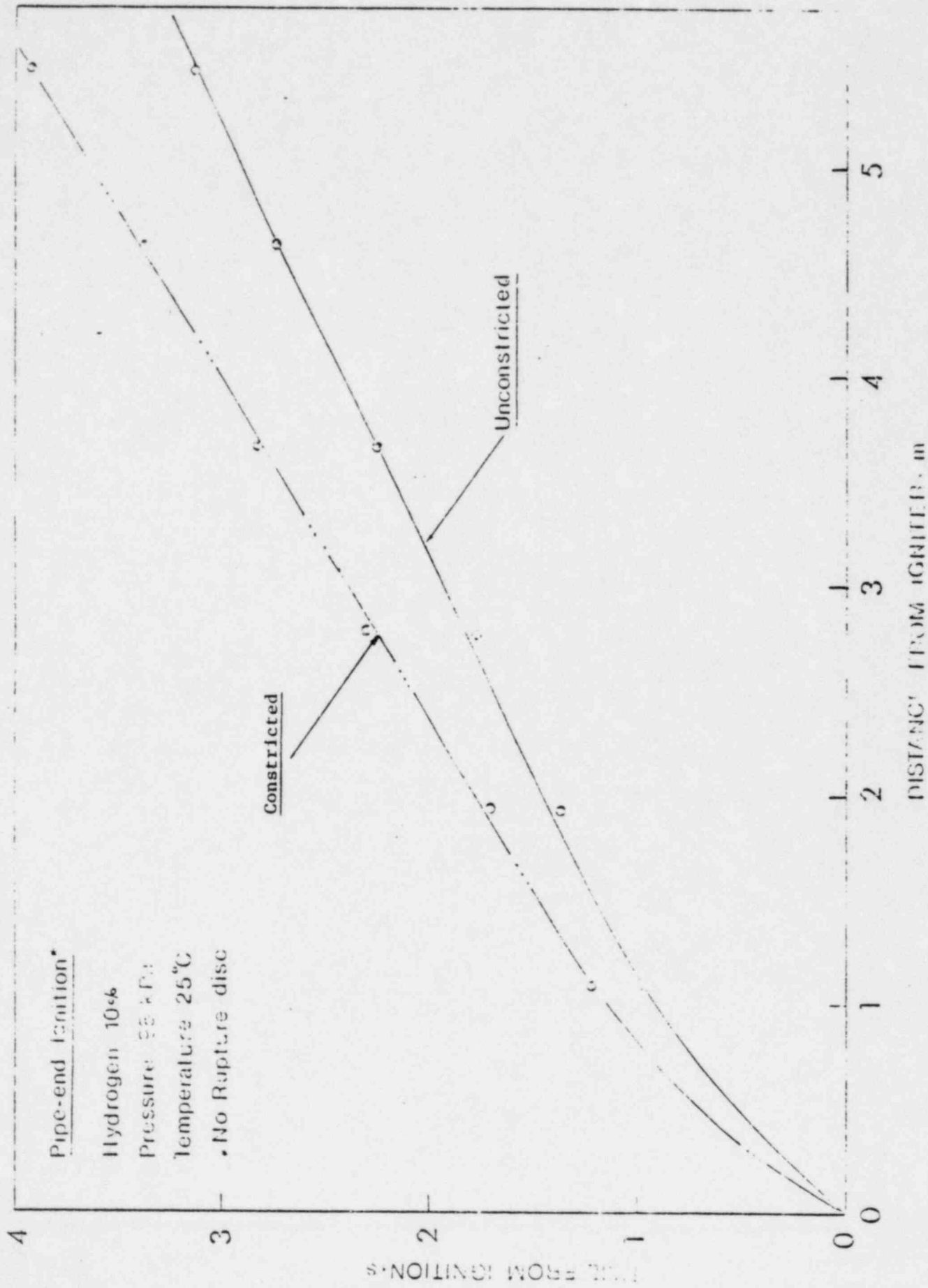


FIGURE 18

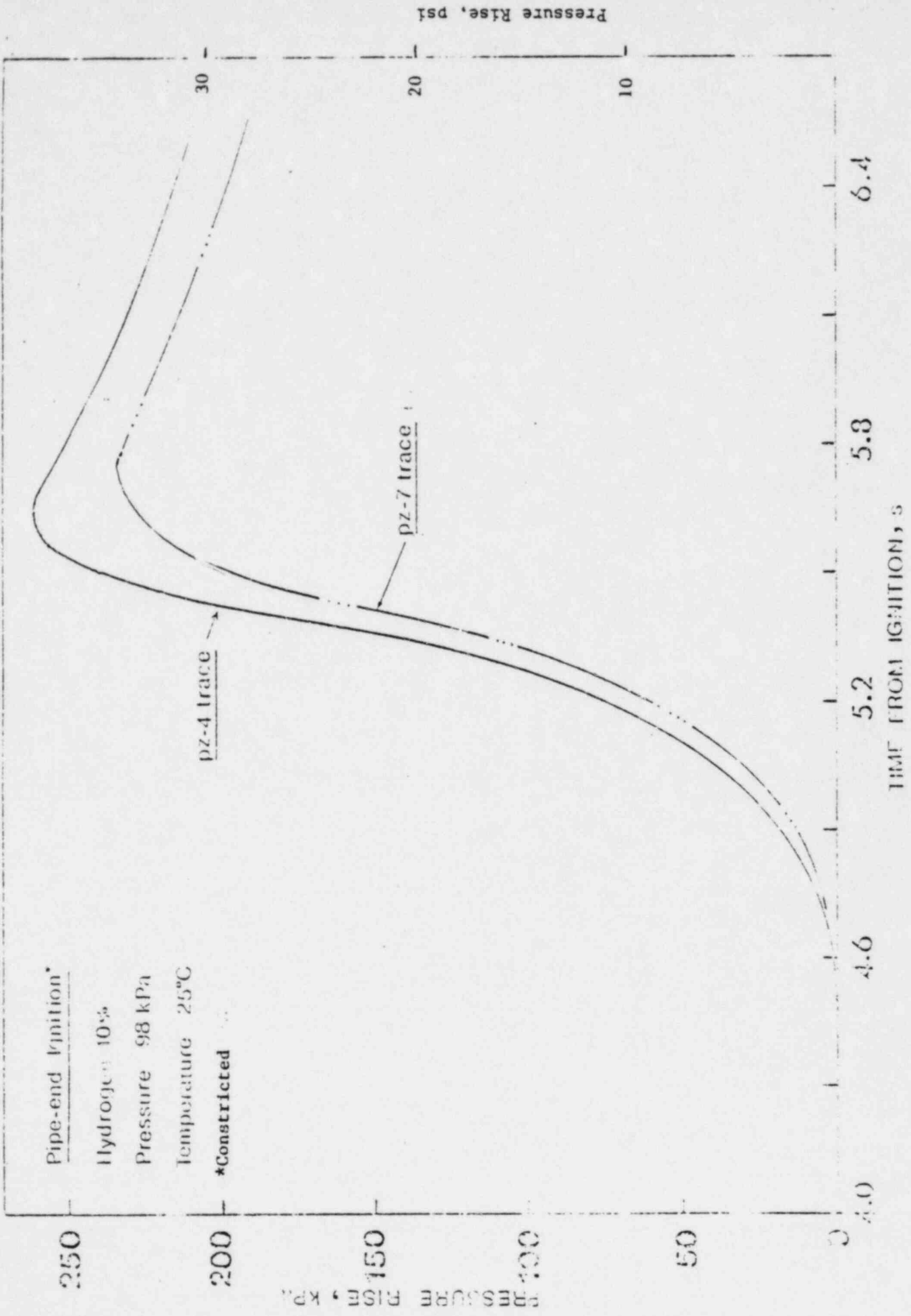
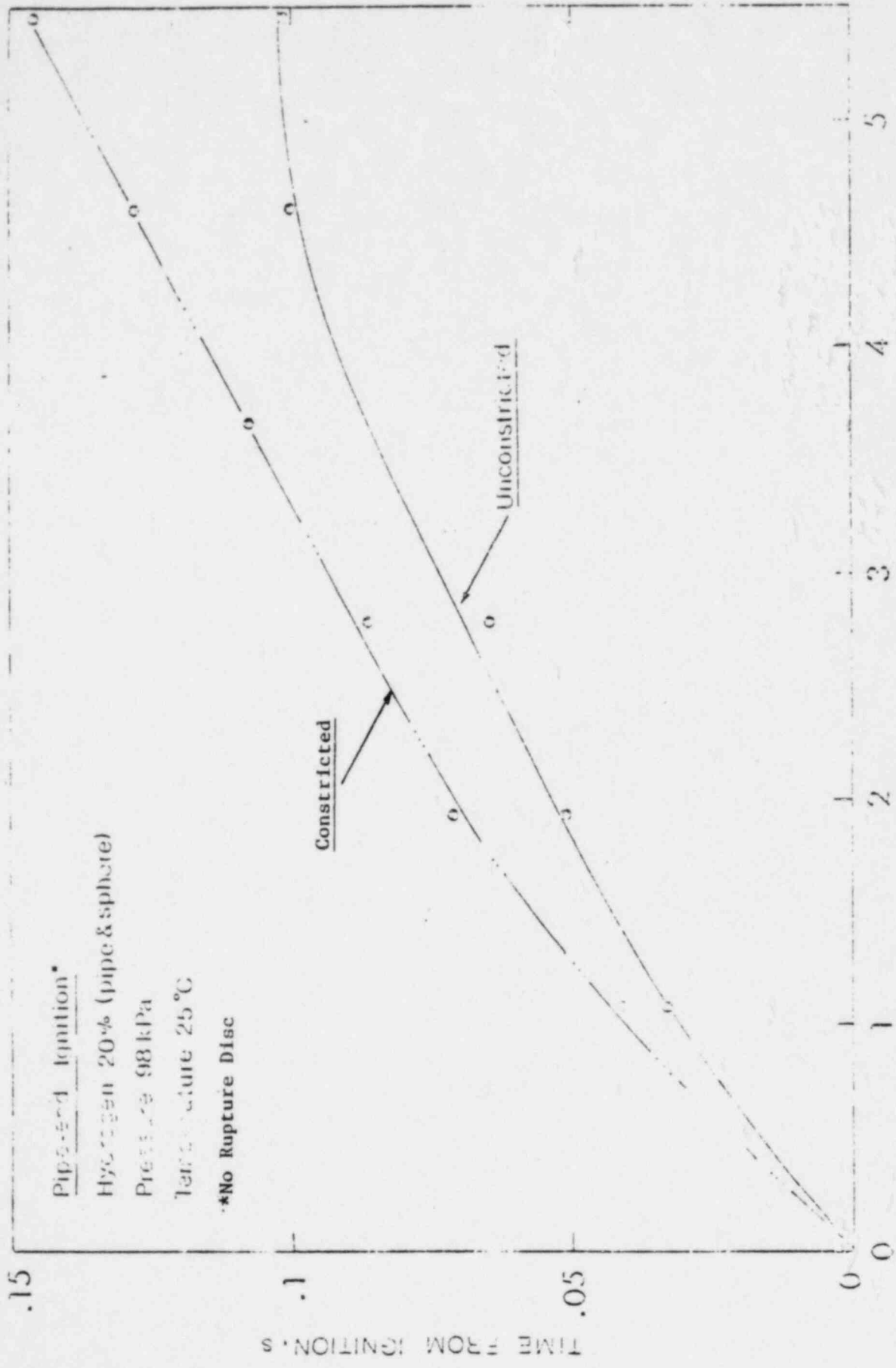


FIGURE 19



DATA FROM ICHTET-30

FIGURE 20

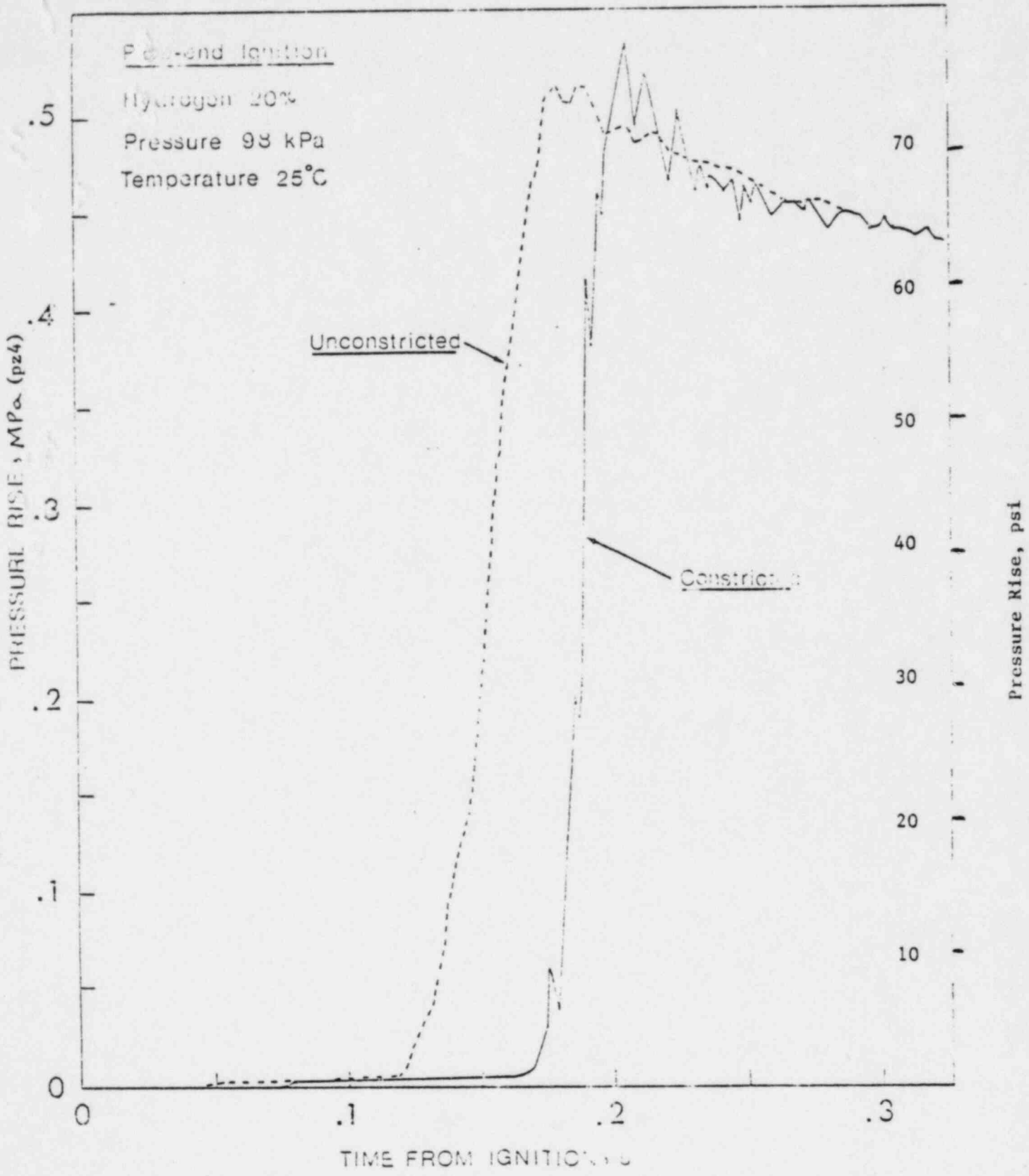


FIGURE 21

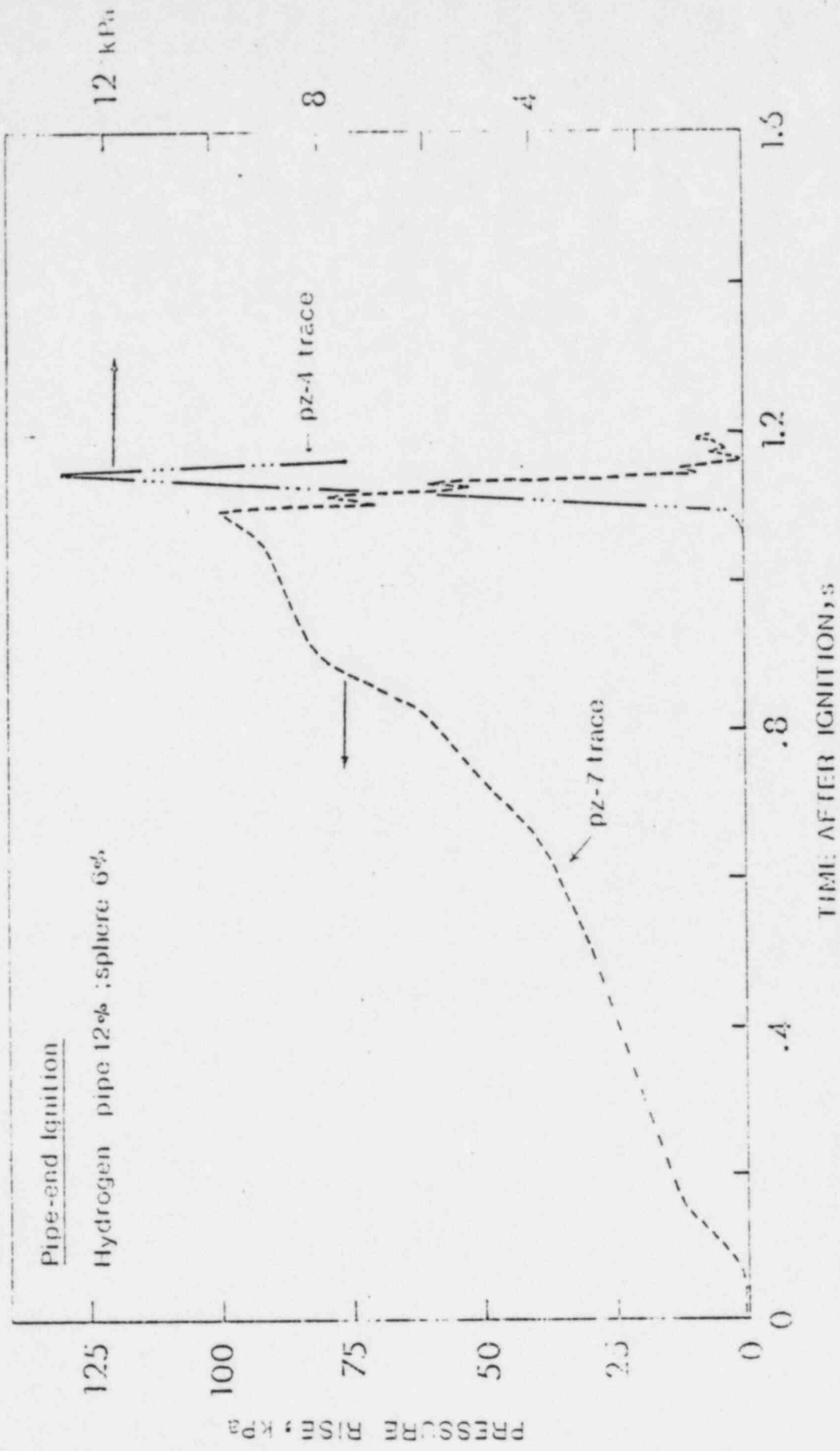


FIGURE 22

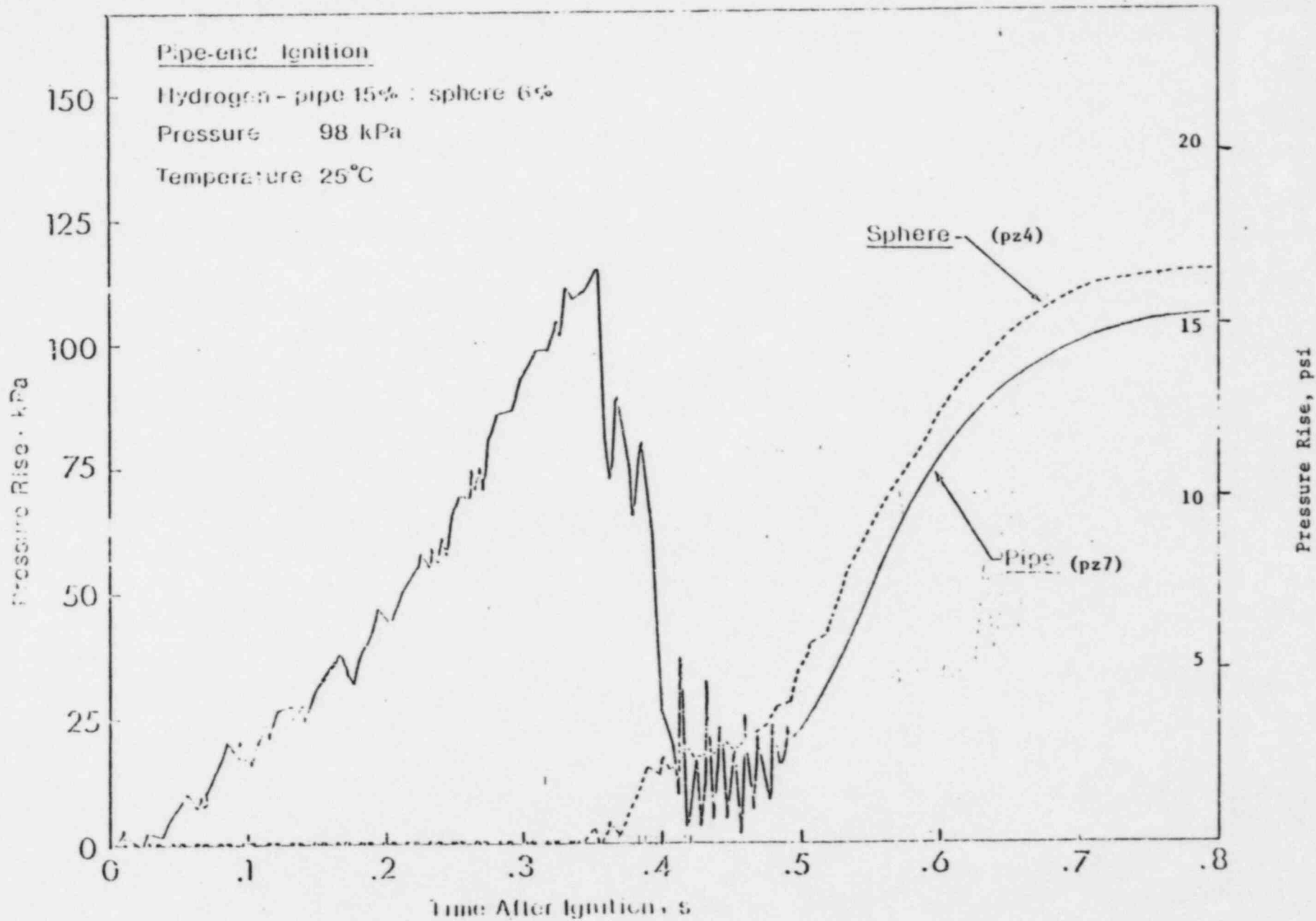
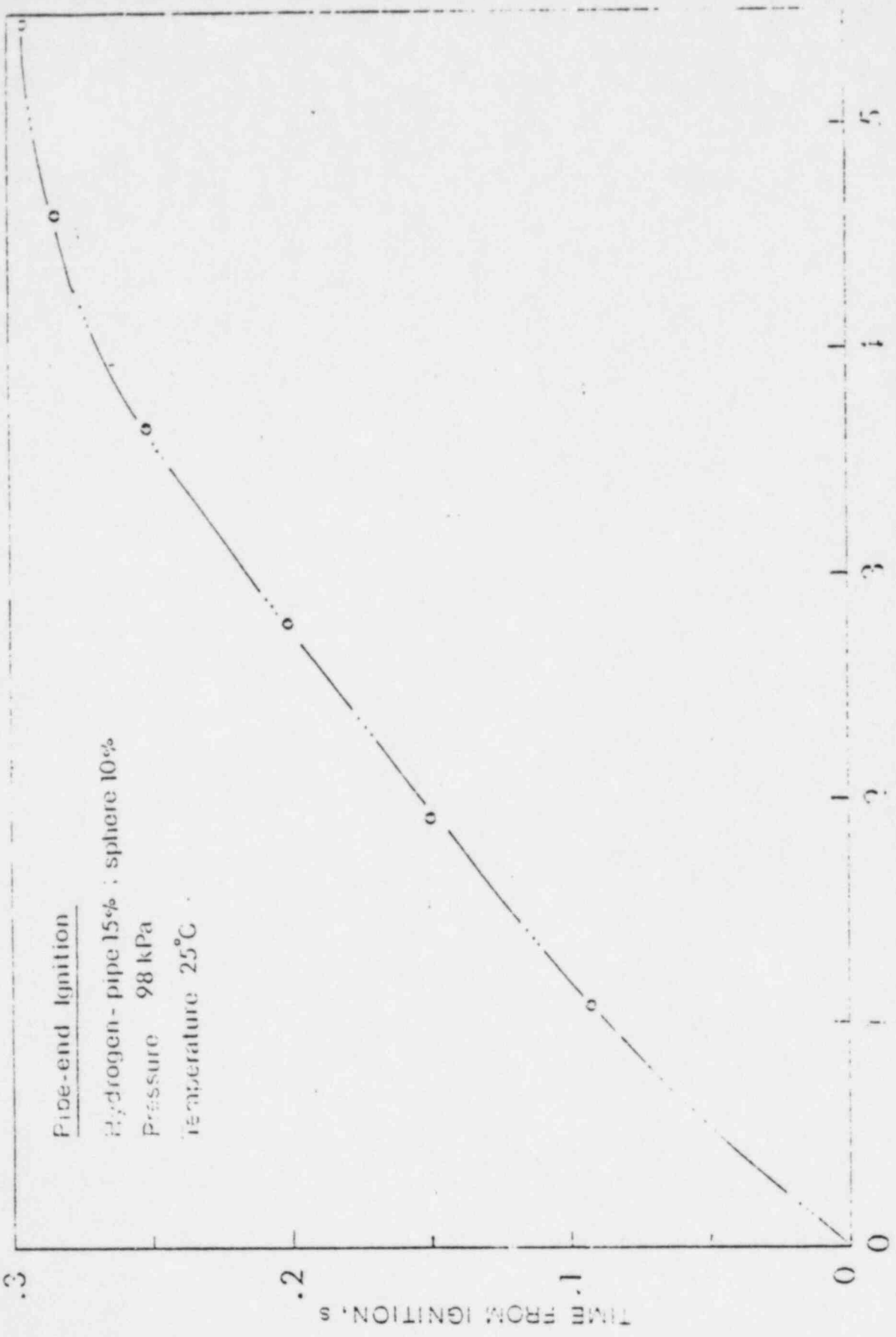


FIGURE 23



DISTANCE FROM IGNITER, m

FIGURE 24

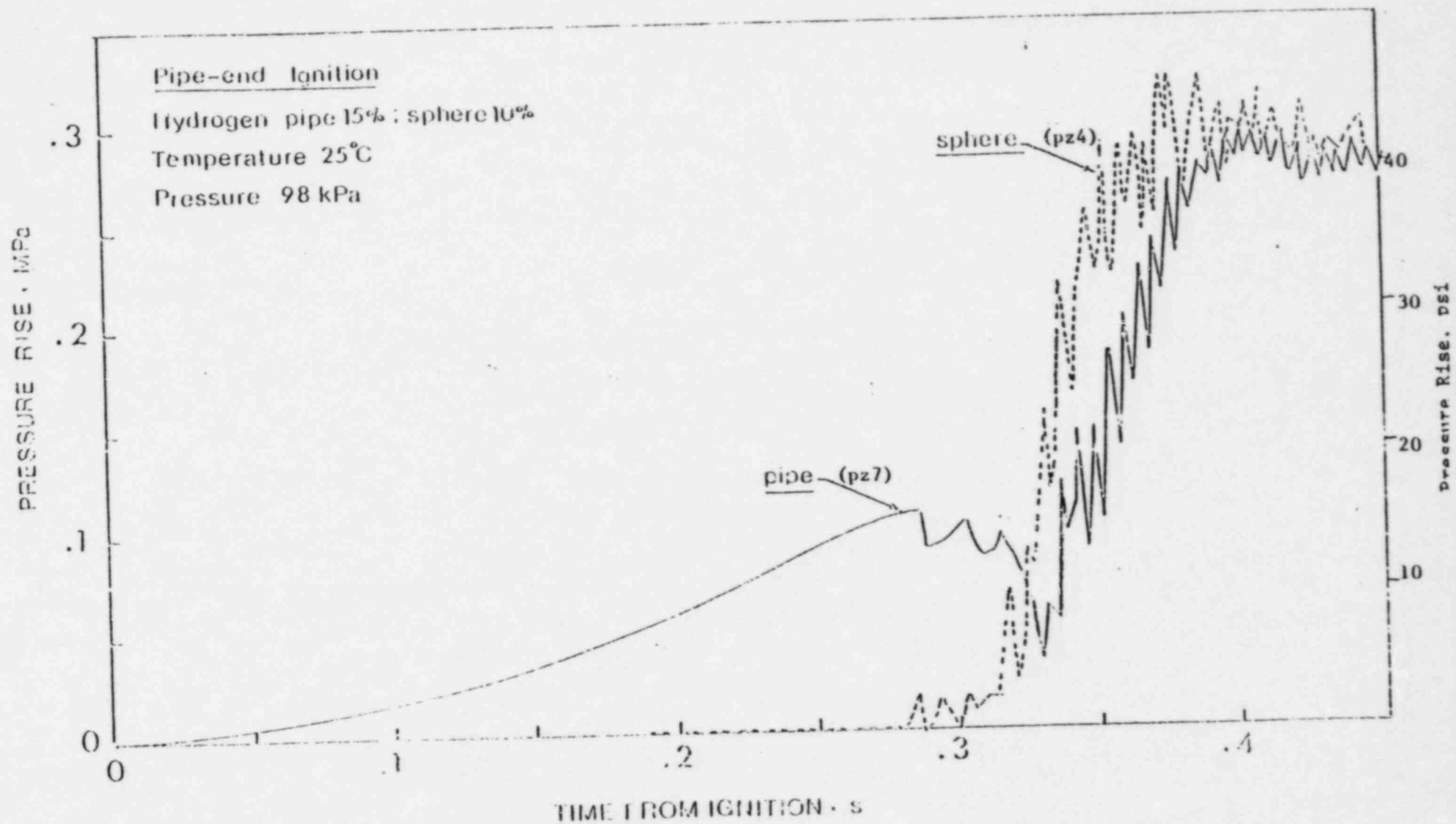


FIGURE 25

Pipe-end Ignition

Hydrogen pipe 15% , sphere 20%

Pressure 98 kPa

Temperature 25°C

Pressure Rise, MPa

Time After Ignition, s

pipe (pz7)

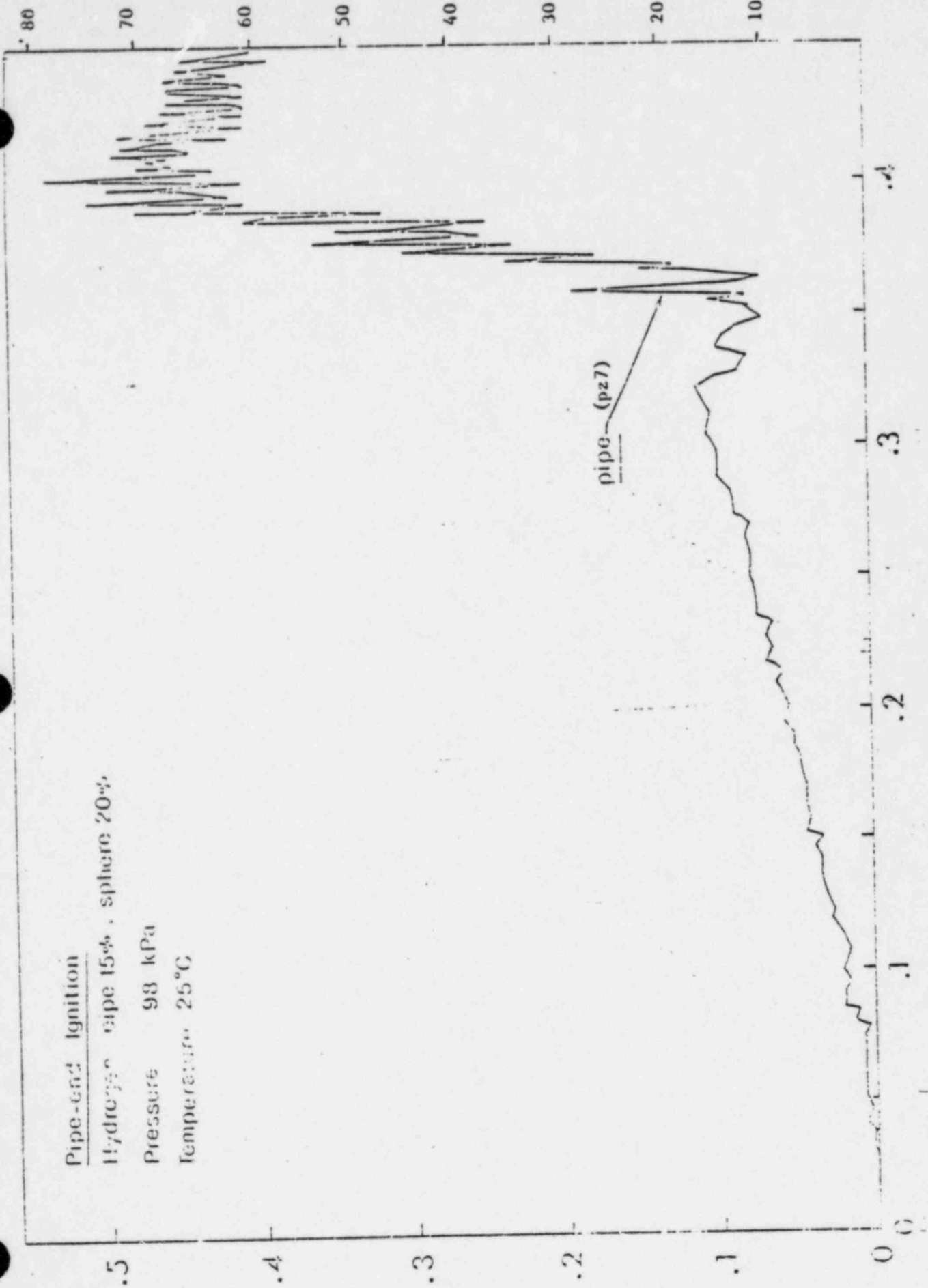


FIGURE 26

Table 4.3-7
McGujre CLASIX Input

Ice Bed Parameters

| <u>Parameter</u> | <u>Value</u> | |
|--------------------------------|------------------------------------|---|
| Initial Ice Mass | 2.46×10^6 lbm | |
| Initial Ice Heat Transfer Area | 2.96×10^5 ft ² | |
| Heat of Fusion of Ice | 150 Btu/lbm | 5 |
| Flow Loss Coefficient | 0.0 | |
| Initial Net Free Gas Volume | 86300 ft ³ | |

6.2 SUMMARY

The accident at Three Mile Island Unit 2 prompted a reevaluation of hydrogen control measures at light water cooled nuclear power plants. Duke Power Company began this reevaluation in January, 1980 by establishing a task force to examine hydrogen control measures at the McGuire Nuclear Station. Work was performed specifically related to McGuire as well as reviewing Tennessee Valley Authority (TVA) actions regarding its Sequoyah Nuclear Plant and monitoring NRC/industry activities related to hydrogen control. In June 1980, Duke, TVA, and the American Electric Power Service Corporation (AEP) consolidated efforts to evaluate hydrogen control measures in nuclear power plants with ice condenser containments. The major emphasis of this joint effort was to: 1) fund initial research and/or studies on prospective hydrogen control concepts and 2) fund development of a containment response code that would adequately model hydrogen combustion within an ice condenser containment. In January, 1981, the Electric Power Research Institute (EPRI), joined the ice condenser owners in evaluating hydrogen combustion. The result of this effort was a research program designed to investigate in more detail phenomena associated with the controlled combustion of hydrogen. Analyses performed by Duke Power Company, as well as the joint research programs, have been completed. The results of these efforts were twofold: 1) a distributed ignition system was selected as an adequate method of hydrogen control during degraded core accidents. 2) The ability of the distributed ignition system to perform its intended function was demonstrated by research and analysis.

The McGuire Hydrogen Mitigation System consists of 33 pairs of GM AC-7G glow plugs located throughout containment. All compartments within containment contain at least one pair of ignitors. This distribution of ignitors assures that hydrogen combustion will occur wherever flammable concentrations first appear. The Hydrogen Mitigation System can be manually loaded onto the emergency diesel generators. Ignitor redundancy is preserved through its power sources. This system is relatively easy to install and maintain. Its simplicity creates a situation of high reliability, while its predictable and repeatable, principle of operation provides a high degree of confidence that the system will perform its intended function. Additionally, there are no adverse consequences that result from an inadvertent or unnecessary actuation of the system. A detailed discussion of the system design is provided in Section 3.0.

Calculations of the containment's response to hydrogen combustion have been performed using the CLASIX computer code developed by Westinghouse Offshore Power Systems and funded, in part, by the ice condenser owners. The CLASIX code has been shown to compare favorably with industry accepted containment codes and conservatively predict the response from several hydrogen combustion tests. Several sensitivity studies were performed to assure that the Hydrogen Mitigation System would perform its intended function under a variety of diverse conditions. These sensitivity studies included: 1) operation of only one instead of two trains of containment safeguards, 2) increased hydrogen release rate to a peak of 260 lbm/min, 3) depletion of ice prior to release of hydrogen into containment, 4) inerting selected compartments within containment, and 5) varying the assumed flame speed. The calculated peak pressure for the

base case, i.e., all containment safeguards operating as intended, was 12.6 psig. Note that the McGuire containment's design pressure is 15 psig. The calculated peak pressure from the sensitivity studies, 20 psig, was only slightly above the containment's design pressure, but well below the ultimate capacity of 67.5 psig. Detonation was not evaluated since it was not considered to be a credible phenomena inside containment. This conclusion was based on two factors. 1) Both analysis and research have shown that due to the mixing characteristics of an ice condenser containment and operation of the Hydrogen Mitigation System, hydrogen concentrations will remain well below the classical limits of hydrogen detonation, 2) There are no areas inside containment with sufficient confinement to promote the flame acceleration necessary for a transition from deflagration to detonation. Although there is some experimental evidence of detonation outside of the classical detonability limits, large amounts of explosive were required to initiate detonation. This is a situation that is not applicable to an ice condenser containment. A detailed discussion of the containment response analyses is provided in Section 4.0.

In order for the Hydrogen Mitigation System to adequately perform its intended function, certain essential components located within containment must function during operation of the system. Additionally, operation of the Hydrogen Mitigation System must not degrade the remaining components in containment to the point where the severity of the accident is increased. Therefore, analyses were performed using conservative assumptions concerning geometry and heat transfer coefficients, as well as considering all relevant forms of heat transfer in multidimensional configurations, to evaluate the effect of hydrogen combustion on components located within containment. These analyses demon-

strated that: 1) All essential equipment would survive and continue to operate following hydrogen combustion, and 2) the effect of hydrogen combustion on non-essential equipment would not increase the severity of the accident. Additional confidence in the survivability of equipment to hydrogen combustion was obtained by observing the fact that all equipment and instrumentation used in the numerous hydrogen combustion tests was off the shelf equipment and functioned properly throughout the various research programs. A detailed discussion of the equipment survivability analyses is provided in Section 5.0.

An extensive research program was conducted to evaluate alternative hydrogen control concepts and, eventually, to confirm the initial conclusions concerning the ability of distributed ignition system to adequately mitigate the effects of hydrogen generated during degraded core accidents. Research on hydrogen control concepts was funded by the ice condenser owners. Tests conducted by Fenwal Inc. demonstrated that glow plugs utilized as ignitors consistently and effectively initiate hydrogen combustion under a variety of diverse environmental conditions. A feasibility study conducted by Atlantic Research Corp. concluded that Halon 1301 would be an effective containment atmosphere post-inertent. However, testing performed by TVA's Singleton Laboratories demonstrated that the water chemistry resulting from post-accident Halon injection resulted in a very corrosive environment. For this reason, further study of Halon as a hydrogen mitigation concept was not conducted. Keiser Engineering evaluated the effects of electromagnetic emission from spark ignitors on sensitive instrumentation. It was shown that at distances greater than 2 feet the radiated emissions did not produce a significant effect. However, due to the demonstrated effectiveness of the glow plug as a

hydrogen ignitor, further study of spark ignitors and electromagnetic emissions was precluded. Tests performed by Acurex Corporation proved that catalytic combustors are an effective hydrogen removal concept. However, the tests also indicated that environmental effects, i.e., temperature and catalyst poisoning, on the combustor would require significant support systems to assure adequate performance of a catalytic combustor system in containment. It was concluded that pursuing the catalytic combustor concept would not be cost-effective. Confirmatory research in support of the distributed ignition system was funded by the ice condenser owners and EPRI. Scoping tests performed by Factory Mutual Research Corporation provided data on the effect of various water micro-fog parameters on hydrogen combustion. From this data two micro-fog conditions were selected for larger scale testing to evaluate the pressure suppressant effects of a water micro-fog during hydrogen combustion. Intermediate scale tests performed by Acurex Corporation investigated the effects of ignitor location within the test vessel and the pressure suppressant effects of a water micro-fog. The ignitor location test indicated that the location of the ignitor relative to the hydrogen source location does affect the resulting peak pressure. However, this effect was minimized by the presence of turbulence. The introduction of a water micro-fog into the test vessel had no significant effect on the peak pressures attained. Tests conducted by AECL-Whiteshell demonstrated that the glow plug is an effective hydrogen ignition source at steam concentrations in excess of 50%. Additional tests confirmed our understanding of the effects of steam and turbulence on the combustion of lean and rich hydrogen air mixtures. A simulation of the mixing characteristics of an ice condenser lower compartment was performed by HEDL. This

simulation clearly demonstrated that the lower compartment is very well mixed, and thus pocketing is precluded. More detailed discussions of these research projects are presented in Section 2.0.

Duke Power Company has selected the distributed ignition concept for post-accident hydrogen control at its McGuire Nuclear Station. This system is redundant, capable of functioning in a post-accident environment, seismically mounted, and capable of being powered by the diesel generators. Analyses have been conducted to investigate the effects of system operation on the containment and essential components located within containment. These analyses have shown that essential equipment is not adversely effected and that peak calculated containment pressures are over a factor of two below the containment ultimate strength. In addition, an extensive research program has been conducted to confirm our understanding of hydrogen combustion and mixing, as well as to investigate other hydrogen control concepts. Based on nearly three calender years of analysis, design, and research, Duke Power Company concludes that: 1) The Hydrogen Mitigation System installed at the McGuire Nuclear Station will perform its intended function, if called upon to do so. 2) All relevant issues regarding the design and operation of the Hydrogen Mitigation System have been resolved in a manner consistent with good engineering practices. 3) The additional analysis and/or research will only serve to further confirm the adequacy of the system design.

Response to Request for Information on CLASIX Code
Transmitted by Mr. Thomas M. Novak's Letter of August 9, 1982

- 1) Provide additional details regarding the ice bed nodalization scheme used in CLASIX, specifically:
 - a) It is not clear whether all or just part of the volume initially occupied by ice is added to the lower plenum volume as the ice melts. Clarify how the free volume and ice volume in the ice bed are handled in CLASIX, both initially and as the ice melts; and
 - b) It is our understanding that the present version of CLASIX, unlike earlier versions, does not treat the ice bed as a separate volume. As a result combustion in the ice bed cannot be modelled. Combustion in this region can potentially be more severe than in the plenums due to the larger ice bed volume. Discuss the consequences of modelling the ice bed as a flow path rather than as an individual volume, and demonstrate that the CLASIX approach yields more conservative results than if combustion in the ice bed were permitted.

Response:

Early versions of CLASIX treated the upper plenum, lower plenum, and ice bed as a single volume. The entrance to this volume was the lower inlet doors; the exit was the top deck doors. When it was discovered that the phenomenon of hydrogen burning in the upper plenum was very important in the overall effect of hydrogen burning on containment, the ice condenser was split into two volumes. These have been called the upper plenum and lower plenum, but at all times the total volume of the ice condenser, including that of the ice bed, is accounted for. When the ice condenser is full of ice, the free volume in the ice bed is evenly distributed between the upper and lower plenum. As ice begins to melt, all of the additional free volume created by melting ice is added to the lower plenum. In addition, since the ice melts from the bottom, a larger proportion of the original free volume is added to the lower plenum and subtracted from the upper plenum. When the total ice mass has melted, the upper plenum volume consists only of the volume above the intermediate deck doors. All of the volume initially occupied by ice, and all of the initial free volume in the ice bed, has been added to the lower plenum. The following equations describe this process:

V3 - volume of upper plenum (function of time)
V31 - initial volume of upper plenum
V2 - volume of lower plenum (function of time)
V21 - initial volume of lower plenum
VICE1 - initial free volume of ice condenser
VICE - free volume of ice condenser (function of time)
MICE1 - initial mass of ice
MICE - mass of ice (function of time)
RICE - ice density

equations:

$$V3 = V31 + \frac{1}{2} \left(\frac{V1CE1 \times M1CE}{M1CE1} \right)$$

$$V2 = V21 + V1CE1 \left(1 - \frac{1}{2} \frac{M1CE}{M1CE1} \right) + \frac{M1CE1 - M1CE}{R1CE}$$

thus, before ice begins to melt

$$V3 = V31 + \frac{1}{2} V1CE1$$

$$V2 = V21 + \frac{1}{2} V1CE1$$

when the ice is half melted ($M1CE = \frac{1}{2} M1CE1$)

$$V3 = V31 + \frac{1}{4} V1CE1$$

$$V2 = V21 + \frac{3}{4} V1CE1 + \frac{1}{2} \frac{M1CE1}{R1CE}$$

and when all of the ice has melted

$$V3 = V31$$

$$V2 = V21 + V1CE1 + \frac{M1CE1}{R1CE}$$

We conclude that this is a realistic method of accounting for the volume associated with the upper plenum, the free space in the ice bed, the additional free space created by melting ice, and the lower plenum. Combustion is allowed to occur in both plenum volumes, therefore the code does not preclude burning in the free volume of the ice bed. When we say that the ice bed is modeled as a flow path, we mean that the total pressure drop associated with the ice condenser is localized to the junction between the lower and upper plenum volumes, volumes 2 and 3 in the program. The practice of placing the distributed pressure drop of a volume at the junction is a common practice in thermal hydraulic codes and is also done in RELAP and RETRAN.

- 2) With regard to the CLASIX flow equations (A-4, A-8) provide the following information:
 - a) Equation (A-4) is used until a Mach number of one is reached without adjusting the loss coefficient for the variation of compressibility over this range of Mach number. Please justify the assumption of a constant loss coefficient.
 - b) The use of steady-flow equations assumes that the effects of transient phenomena, such as inertia, are not important. However, inertia would increase the pressure rise associated with a burn because pressure relief by outflow is reduced. Please describe the junction flow transients and transitions to sonic flow which occur at each of the flow junctions during blowdown and hydrogen burns, and justify that the steady-flow equations are valid for hydrogen burn transients.

- c) The flow equations require a density and velocity. These should be the density and the velocity at the vena contracta (minimum flow area). However, the density defined by Equation (A-7) provides a density that is the average of the source and the sink volumes, which will not be the vena contracta density. In addition, the velocity used in Equation (A-4) is not defined. Please explain and justify the bases for the density and velocity used in the flow equations.
- d) Two-phase flow conditions might result from 1) the breakflow or 2) a condensation fog from the ice condenser. As a result, the effects of mechanical (slip), thermal, and chemical (vapor diffusion) non-equilibria may become important. Justify the use of Equations (A-4) and (A-8) to estimate the transient flow of a two-phase fluid.

Response:

The thermodynamic conditions associated with breakflow release are generally very slowly varying functions of time. For all practical purposes, except during the times that hydrogen is being burned, the containment volumes are in a quasisteady state condition, and the steady flow equations are an excellent choice for a model. During times that hydrogen burning is occurring in one or more containment volumes, thermodynamic conditions change more rapidly and more specific criteria must be examined in regard to the applicability of steady flow models. In response to the specific questions:

- a) The results of the CLASIX analysis were reviewed and it is noted that all pressure ratios are well below critical; therefore, flow velocities did not approach $M = 1$. It is concluded that compressibility effects are not important, and incompressible flow equations apply. Accordingly, the loss coefficients may be considered constant.
- b) No transitions to sonic flow occur in any of the junctions in CLASIX analysis for McGuire. It is also noted that for inertia to be an important effect, the parameter L/A must be significant, where L is the length of a volume and A is the associated junction area. For the McGuire containment, typical values of L/A are 0.05 (lower compartment), 0.03 (ice bed), 0.001 (upper plenum). These values are not considered significant enough to require that inertia be considered in the CLASIX analysis of containment. Inertia tends to become significant in pipe flow problems where the values of L/A are an order of magnitude higher than for typical containment analysis.
- c) Provided no significant pressure drops exist in a flow path, the error introduced by using average density and a velocity based on the mass flow rate is acceptably small. Guidance given in the Crane handbook (Crane technical paper 410) is that for pressure drops less than 40% of the inlet pressure, one need not consider any adjustment for compressibility. The CLASIX analysis for McGuire was reviewed and no instances where pressure drops approach 40% of the inlet pressure in any flow path were found. It is concluded that no adjustment for compressibility is required for typical CLASIX analysis.

- d) Containment analysis traditionally does not consider non-equilibrium effects. There are no provisions in widely accepted containment analysis codes such as CONTEMPT to account for the analysis of transient two phase flow. Accordingly, there is little justification for such considerations in CLASIX.
- 3) Justify the CLASIX assumption that the breakflow can be assumed to separate immediately into a liquid portion that falls to the containment floor and a vapor that is added to the inventory of the containment atmosphere.

Response:

The assumption that the breakflow separates immediately into a liquid portion that falls to the containment floor and a vapor portion that is added to atmosphere is a conservative assumption to maximize the containment temperature and pressure response. This is the standard method used in all containment analysis as described in SRP 6.2.1.3. No additional justification is required.

The breakflow into a compartment (or volume) of lower thermodynamic state will seek thermodynamic equilibrium. The process of equilibration depends upon the relative thermodynamic states of the breakflow and the receiving volume. Breakflow with a thermodynamic state greater than the volume can produce saturated vapor produced by assuming that all excess heat is utilized to produce saturated vapor. This process combined with the removal of the saturated liquid from the atmosphere to the sumps yields a higher specific energy for the volume atmosphere and results in higher compartment temperatures and pressures. This also yields a more conservative estimate of compartment conditions after hydrogen combustions because of lowered atmospheric heat capacity. Studies employing strict thermodynamic accounting have shown the conservatism inherent in the CLASIX procedure.

- 4) Provide the following information regarding the CLASIX hydrogen burn model:
- a) The burn time values used in CLASIX analyses submitted for two similar plants differ by as much as a factor of three for the same compartment and flame speed, thus suggesting an inconsistency in computing burn length. To clarify this point, describe the methodology for evaluating the burn length as it applies to containment analyses.

Response:

Burn time in a compartment is a function of burning velocity, ignitor location, and ignitor spacing. It is computed by considering the distance between ignitors or the distance from the ignitors to the farthest point of the compartment (whichever is greater) and dividing by the flame speed. Uncertainty in the analysis is handled by using several burn times for each compartment in sensitivity studies. Because ignitor location, spacing, and assumed burning velocity vary among the three utilities, differences in burn times assumed for the base case are not unusual.

- b) Discuss the rationale for precluding flame propagation in fan flow paths.

Response:

Laminar burning flames at low hydrogen concentration could not be sustained in the highly turbulent high velocity flow present in the fan flow paths. However, since ignition does not occur in the upper containment for any reasonable combination of assumptions, the fact that the code precludes burning in the fan flow paths is of no consequence to the analysis.

- c) Describe how CLASIX might be applied to model containments with multiple ignition points within containments.

Response:

CLASIX can be used to model any number of ignition sites in a containment volume. This is taken into account in the calculation of the burn time. See response to question 4a above.

- d) Equation (D-3) appears to be a calorimeter equation where the preburn mixture is at 70°F and the products of combustion are cooled to the same temperature. Equation (D-4) appears to represent the net energy addition rate due to hydrogen burning. Clarify these equations, and explain how they are applied. Specifically:
- i) Provide a more detailed description of the heat rate parameters, HR_F and HR in Equation (D-3), and discuss the significance of the specific heat terms used to "correct" the heat rate of combustion. Include approximate parameter values used in CLASIX analyses.
 - ii) Discuss the relevance of Equation (D-3) for the typical CLASIX analysis in which the containment temperatures before and after a burn are very different; i.e., the products of combustion are not cooled to the initial temperature.
 - iii) Provide a more detailed discussion and development of Equation (D-4). Describe the significance of the specific heat terms, and how Equation (D-4) is ultimately applied.
 - iv) Explain why in Equation (D-4) the effective heat rate is reduced due to the removal of hydrogen and oxygen but is not increased due to the formation of water vapor.

Response:

For a chemically reactive system, the conservation of energy principle for a steady flow process can be written as

$$q = \sum_{\text{prod}} (N_i h_i) - \sum_{\text{reac}} (N_i h_i)$$

where h_i is the molar enthalpy of any product or reactant at the temperature and pressure of the reaction and N_i is the number of moles of any product or reactant. Because combustion processes are assumed to occur at a reference temperature of 530°R , and heats of formation are given at this temperature, combustion would be written as

$$q = \Delta h_R + \sum_{\text{prod}} N_i (h_t - h_{530})_i - \sum_{\text{reac}} N_i (h_t - h_{530})_i$$

where Δh_R is the molar heat of combustion for the process at the reference state (530°R , 1 atm), h_t is the molar enthalpy at temperature, and h_{530} is the molar enthalpy at 530°R , 1 atm.

For combustion of hydrogen, this equation may be written (converting molar to specific enthalpies):

$$q = \Delta h_R + 9(h_t - h_{530})_{\text{H}_2\text{O}} - (h_t - h_{530})_{\text{H}_2} - 8(h_t - h_{530})_{\text{O}_2}$$

Within the program, various reference states are used - water at 32°F , and gasses at 0°F . To account for this, each enthalpy term must be adjusted by the equation

$$h_t = h_{\text{ref}} + \int_{T_{\text{ref}}}^t C_p dT$$

Therefore

$$q = \Delta h_R - 9(C_p)_{\text{H}_2\text{O}}(70-32) + 70[8(C_p)_{\text{O}_2} + (C_p)_{\text{H}_2}] - T[8(C_p)_{\text{O}_2} + (C_p)_{\text{H}_2}]$$

if we define an equivalent heat of combustion

$$HR_E = \Delta h_R - 9(C_p)_{\text{H}_2\text{O}}(70-32) + 70[8(C_p)_{\text{O}_2} + (C_p)_{\text{H}_2}]$$

we get equation D-3 in the report. Note that the sign is reversed; this is a consequence of our classical development in which the heat of combustion of a process is negative. The author of CLASIX chose to use the opposite sign.

Substituting in the energy balance equation, and using equation D-2

$$Q = \dot{m}_R \cdot q = \dot{m}_R \{ HR_E - [8(C_p)_{\text{O}_2} + (C_p)_{\text{H}_2}]T \}$$

This is equation D-4. Note that adjustment is not made for the enthalpy of water produced by the reaction because Δh_R is the high heat of combustion. Implicit in the use of the high heat of combustion is that the products appear at their reference temperature, the point at which their enthalpy is zero. Hence, the water produced from hydrogen combustion is added to the volume as liquid at 32°F . When an energy balance is then performed on the volume, the water will appear with the

proper final temperature. Because combustion is only one of many competing processes which affect the final temperature of a volume, one cannot predict from the combustion equation what the final temperature of the combustion products will be.

- e) Describe where in the CLASIX calculations the mass inventory of oxygen and steam is adjusted due to combustion, and when in the calculations the energy released from a hydrogen burn is added.

Response:

During each time step, the mass and energy contained in each volume is computed by applying appropriate balance equations of the form

$$\left(\begin{matrix} \text{mass} \\ \text{energy} \end{matrix}\right)_{N+1} = \left(\begin{matrix} \text{mass} \\ \text{energy} \end{matrix}\right)_N - \text{net outflow of } \left(\begin{matrix} \text{mass} \\ \text{energy} \end{matrix}\right)$$

Net outflow of mass is found by considering additions from flow, addition tables such as breakflow, and changes in the constituents of a volume by phase change or chemical reactions. Separate balances are performed on hydrogen, nitrogen, oxygen, water vapor, and liquid water. Similar balancing is performed for energy, which includes the energy removed by heat sinks and the energy added by combustion. These new mass and energy components in a volume are used to calculate a new equilibrium thermodynamic state. This is a classical method of containment analysis, having been used in CONTEMPT and CONTEMPT4.

- f) It is our understanding that the hydrogen burn rate, \dot{M}_B , is determined upon ignition by Equation (D-2) and held constant for the duration of each burn, while the mass of hydrogen to be burned is updated each interval by Equation (G-20). Intuitively the burn rate should also be updated to reflect the mass of hydrogen present, which may be greater or lesser than that at the onset of burning depending on the hydrogen injection rate. Please justify the use of a constant burn rate in view of the changing hydrogen concentration during a burn.

Response:

Whereas the hydrogen burning rate could be adjusted during the burn, it is not believed that the use of a constant burn rate significantly affects the results of the analysis for the following reason. Typical burn times for our best estimate analysis are 27 seconds for the lower compartment and 15 seconds for the upper plenum. At a hydrogen addition rate of 1.07 lbm/sec, the maximum amount of hydrogen which could be added to a compartment during a burn is about 29 lbm (lower compartment) and 16 lbm (upper plenum). At 8.5% hydrogen by volume in the lower compartment, the hydrogen mass at the start of ignition is about 100 lbm, so consideration of hydrogen addition would lower the burn time by a factor of 1.27. But raising the flame speed to six feet/second, which was done in many sensitivity studies, lowers the burn time by a factor of three. Accordingly, it is concluded that any effect of increasing the burn rate during a hydrogen burn due to addition is well bounded by the variety of burn times and flame speeds considered in the sensitivity studies.

- 5) Provide the following information regarding the calculation of heat and mass transfer to passive heat sinks:
- a) Equation (B-1) provides for the use of either the Tagami or Uchida correlation to determine the heat and mass transfer to passive heat sinks. The Tagami correlation is for conditions very different from those expected for the application of CLASIX, that is, small-break containment analyses. The Uchida correlation is for natural convection heat transfer, including condensation, in the presence of a noncondensable gas. Clarify how Equation (B-1) is used and justify the use of the Tagami correlation.

Response:

The "Tagami correlation" should not be confused with the work done by Tagami on heat transfer during the initial stages of blowdown from a large LOCA. The Tagami correlation consists of two parts - one part is applicable to the blowdown period prior to the peak pressure occurrence in the containment; the second part applies to the period following the peak pressure and is a modified Uchida correlation. These two parts of the Tagami correlation are shown in equation B-1 in OPS-07A35. This modified Uchida correlation is also applicable to the whole period of a small break LOCA. In the user input to CLASIX, one is able to turn off the first part of the Tagami correlation by setting $t_p = 0$. This is what was done by Duke Power in analysis of containment response for McGuire. Accordingly, CLASIX analysis was performed using a correct heat transfer correlation.

- b) The natural convection heat transfer correlation for $Gr < 10^9$ that is used in the Tagami/Natural convection heat transfer correlation Equation (B-6), yields heat transfer rates lower than other text book correlations by a factor of three. Please discuss this discrepancy.

Response:

Equation B-6 is incorrect. It should be written

$$Nu = 0.508 Pr^{1/4} Gr^{1/4} / (0.952 + Pr)^{0.25}$$

For $Pr \ll 1$, the error in the use of this equation is conservative and on the order of a factor of 2.

- c) Describe and justify the passive-heat-sink heat-transfer assumptions regarding (i) the temperature difference used with the film coefficients; (ii) the model used to account for the removal of mass that is condensed on the heat-sink surfaces; and (iii) the energy removal associated with the condensed mass.

Response:

The use of the difference between the wall and bulk temperatures in conjunction with film heat transfer coefficients at the wall is a standard method used in CONTEMPT and CONTEMPT4. It should be noted that

film transfer coefficients are normally measured or derived from experiments based on the temperature difference between the bulk fluid and the wall. CLASIX accounts neither for the mass of fluid condensed on the walls or any energy removal attributable to such condensation. This is a conservative assumption because it underpredicts the ability of the walls to remove energy from the containment.

6) Concerning the radiation transfer model used in CLASIX:

- a) If the wall surfaces are assumed to be "black," the radiant heat transfer equation, (B-8), does not reduce to a classical expression of the form $Q_R = \sigma A (\sum_v T_v^4 - \alpha_w T_w^4)$ as it should.

Provide the development of Equation (B-8), and justify the use of the vapor and wall emissivities as multipliers on the T^4 terms.

Response:

CLASIX subroutine HRADTN computes the radiant heat transfer rate between hot gases in a compartment and the enclosing walls (heat sinks). It is assumed that all of the walls comprising the enclosure are at the same temperature so that no net radiant energy exchange occurs between the walls. Furthermore, it is assumed that the view factor between the walls and hot gases is unity.

With these assumptions CLASIX computes the net radiant heat exchange as given by:

$$Q_R = A_W (W_g - W_w) \left(\frac{1 - \epsilon_w}{\epsilon_w} + \frac{1}{\epsilon_g} \right)^{-1} \quad \text{(Egn. B-8 in OPS-07A35)}$$

where: Q_R = net radiant heat transfer rate (Btu/hr)

A_W = wall surface area (ft²)

$W_g = \epsilon_g \sigma T_g^4$ = emissive power of gas (Btu/hr-ft²)

$W_w = \epsilon_w \sigma T_w^4$ = emissive power of wall (Btu/hr-ft²)

ϵ_g = emissivity of gas

ϵ_w = emissivity of wall

σ = Stefan-Boltzmann constant (Btu/hr-ft²-°R⁴)

T_g = gas temperature (°R)

T_w = wall temperature (°R)

The use of gas and wall emissivities as multipliers on the temperature terms W_g and W_w appears to be an error in modeling. The use of emissivities in these terms does, however, result in an underestimation of radiant heat flux to the walls and thus to conservative gas temperature predictions, as described below.

Section 13.10 of Reference (6a) presents the case of a gray gas in an enclosure comprised of a gray surface and a refractory (no net flux) surface. Assuming the analysis holds true in the limit, the solution for no refractory surface reduces to:

$$Q_R = \sigma A_W F_{gw} (T_g^4 - T_w^4) \quad (6-1)$$

$$\text{or: } Q_R = \sigma A_W (T_g^4 - T_w^4) \frac{1 - \epsilon_w}{\epsilon_w} + \frac{1}{\epsilon_{gw}}^{-1} \quad (6-2)$$

where: F_{gw} = radiant interchange factor

ϵ_{gw} = effective emissivity for gray gas radiating to walls

For the case of steam, ϵ_{gw} and ϵ_g are approximately equal, and equation (6-2) may therefore be written as:

$$\text{or: } Q_R = \sigma A_W (T_g^4 - T_w^4) \frac{1 - \epsilon_w}{\epsilon_w} + \frac{1}{\epsilon_g}^{-1} \quad (6-3)$$

It should be noted that equation (6-3) is also the classical radiant heat transfer equation for two infinite parallel plates with emissivities ϵ_g and ϵ_w . An underlying assumption in the parallel plates case is that the surface of emissivity ϵ_g is opaque to radiant heat. The gas in a compartment, however, is not opaque and thus gas radiation reflected from a wall may have further opportunity for absorption at another wall. For this reason equation (6-3) may be considered a suitably conservative estimate for radiant heat transfer.

The absolute emissive powers of the walls and the gas are implicit in the development of the radiant interchange factor, F_{gw} . Therefore, further multiplication of the temperature terms in equation (6-3) by the gas and wall emissivities results in conservative CLASIX predictions (i.e., low radiant heat transfer rate to walls and associated prolonged high gas temperatures).

References (6a) and (6b) also describe the classical approximate solution to this problem, which is given by:

$$Q_R = \sigma A_W (\epsilon_g T_g^4 - \alpha_{gw} T_w^4) \left(\frac{\epsilon_w + 1}{2} \right) \quad (6-4)$$

where: α_{gw} = effective absorptivity of gas to wall radiant emissions

In the limit of a "black" enclosure filled with a gray gas, $\epsilon_w = 1$ and:

$$Q_R = \sigma A_W (\epsilon_g T_g^4 - \alpha_{gw} T_w^4) \quad (6-5)$$

- b) It is conceivable that the breakflow or fog at the ice condenser exit might be introduced as a dispersion of fine drops that would be transported throughout the containment. The small drops might reduce the radiation from the water vapor to the heat sinks by affecting the beam length for radiation. Discuss the impact of this mechanism on the radiant heat transfer calculation.

Response:

The energy interchange phenomena involving fog and/or breakflow droplets dispersed throughout a containment compartment require careful discussion. In addition to affecting radiant energy removal from hot compartment gases (heated by hydrogen deflagration), the cooler droplets also remove heat from surrounding gases by conduction and convection. To obtain a full picture of droplet effects on energy removal from a compartment, it is necessary to consider the heat removal mechanisms of conduction and convection in addition to that of radiation. The overall effect of including all three heat transfer mechanisms is that the droplets will act as a heat sink for the high temperature compartment gases.

A few details regarding fog parameters are first required. We consider droplet sizes of about 10 microns. This is slightly larger than the mean sizes estimated by Gido and Koestel^(6c) for droplets leaving the fragmentation/evaporation zone of a blowdown jet. This allows for droplet agglomeration effects on the breakflow droplets. Ten microns is also commensurate with the mean droplet size found by Neiburger and Chien^(6d) in their study of the growth of clouds of droplets formed by condensation.

Droplet concentrations can be estimated on the basis of work done by Tsai and Liparulo^(6e). They estimate that a fog concentration of 1.61×10^{-4} ft³ H₂O/ft³ mix would inert a compartment with 7.9v/oH₂. A fog concentration of 1.0×10^{-4} ft³ H₂O/ft³ mix will be used here.

The heat sink effect of the droplets can be estimated using the considerations of Tsai and Liparulo. They note that a 4 micron (or smaller) droplet will be completely vaporized inside a thin (1 mm) flame front moving at 2 meters/sec (close to the 6 ft/sec assumed in D. C. Cook plant base case) within the 0.5×10^{-3} droplet residence time within the flame front.

Applying the conservation of energy equation to a small droplet at saturation (with negligible internal temperature gradient and a constant surface heat flux), we find that the time rate of change for the droplet radius is a constant. Information derived from Tsai and Liparulo tells us, therefore, that a spherical shell 2 microns thick will vaporize from the surface of a fog droplet within the flame front. This leads to the conclusion that a thin (1 mm) flame front could easily vaporize 78% of a 10 micron fog droplet.

For the case of the D. C. Cook plant, it is estimated that the resultant total heat removal (i.e., that used to vaporize droplets within the thin flame front) would amount to 1.22×10^6 Btu for the lower compartment, 4.42×10^5 Btu for the upper plenum region, and 3.33×10^6 Btu could be

effectively removed from the upper compartment through droplet vaporization. This amount of heat would be "hidden" from the compartment gases and would not be used in raising their temperature (i.e., compartment temperatures will be lower than for a "no fog" case).

Tsai and Liparulo, however, consider only vaporization of the fog droplets within the flame front because of their interest in flame inerting and quenching effects. It is clear from their work, however, as well as the empirically long heat retention times (greater than 1 second) for a compartment, that complete vaporization of the droplets should occur in a post-reaction period of several milliseconds provided the droplet vaporization removes only a fraction of the total energy released during the burn. Obviously, the small fraction of energy required to raise the droplets to saturation temperature is also included within this time frame.

Once vaporization is complete, the compartment beam length for radiant emissions from steam to the walls returns to its value for the no fog case. However, the fog vaporization energy has lowered the compartment temperature so that there is less radiant heat transfer than for the no fog case.

It is clear that radiation to the walls during the several millisecond vaporization time cannot differ much from a case in which no fog is present. However, because the question indicates an interest in the radiation processes involved, these are now discussed.

Radiation from the hot steam must at some point interact with the fog droplets. The mean free path for such an interaction is estimated to be about 2.6 inches for 10 micron droplets. The interaction involves scattering and may involve absorption.

Three different scattering regimes may be defined, based upon the values of fog droplet diameters and the wavelength of the radiant emissions. For 10 micron droplets, reflection and diffraction will be important for wavelengths less than about 6.3 microns. For wavelengths greater than about 52 microns, Rayleigh scattering is the overriding phenomenon. At 1000°F, Planck's distribution law yields a wavelength at the distribution maximum of 3.6 microns.

Whether there is much absorption in the droplets has not been fully investigated because absorption in a liquid droplet is very different than for absorption in steam. However, Reference (6f) has noted that the results of studies involving a wide range of scattering and absorbing media has led to the conclusion that ". . . the assumption of isotropic scattering is often justified in energy exchange calculations in the enclosures. . .". An assumption of this type would lead to multiple scatters from droplets before finally striking compartment walls. In other words, an effective beam length could be assumed which is longer than the geometric beam length for radiation.

References:

- (6a) W. M. Rohsenow and H. Choi, Heat, Mass, and Momentum Transfer, Prentice-Hall, Inc.: Englewood Cliffs, NJ, (1961).
- (6b) W. H. McAdams, Heat Transmission, McGraw-Hill Book Company, Inc.: New York, NY, (1942).
- (6c) R. G. Gido and A. Koestel, "LOCA-Generated Drop Size Prediction - A Thermal Fragmentation Model", Trans. Am. Nucl. Soc., 30, 371 (1978).
- (6d) M. Neiburger and C. W. Chien, "Computation of the Growth of Cloud Drops by Condensation Using an Electronic Digital Computer", Geophys. Monograph No. 5, pp. 191-209 (1960).
- (6e) S. S. Tsai and N. J. Liparulo, "Fog Inerting Criteria for Hydrogen/Air Mixtures", Paper to be presented at the Second International Workshop on the Impact of Hydrogen on Water Reactor Safety, Albuquerque, NM, October 3-7, 1982.
- (6f) R. Siegel and J. R. Howell, Thermal Radiation Heat Transfer - Vol. III: Radiation Transfer with Absorbing, Emitting, and Scattering Media, NASA SP-164, (1971).
- 7) For the internal heat transfer model, provide additional details with regard to:
- a) The procedure for updating the surface temperature of a wall with two nodes in the surface layer; and
 - b) The evaluation of Q_w in Equation (B-17) with $NN=2$ and $NN>2$. Also, describe the subscript notation for these cases.

Response:

The CLASIX heat transfer model used to compute temperatures in a two node wall layer is a special case of heat sink modeling. Only the first (surface) layer of a passive heat sink exposed to the compartment environment may have two temperature nodes. The two node model is used to approximate a thin layer which impedes heat transfer but has negligible heat capacity, such as a coat of paint. For two node layers, the surface temperature is used in the calculation of radiant heat transfer. The surface temperature of the second (internal) layer is used to calculate convective heat transfer.

Figure #1 presents the basic geometry of this special modeling case. Although a coat of paint could be modeled as a three node surface layer, the time step required to obtain solution stability would be prohibitively short. The two node model is not subject to this problem. The surface temperature of a two node wall surface layer is computed after a heat flux has been determined in a "new" time step:

$$TW_1^{N+1} = TW_3^{N+1} + \frac{QWALL^{N+1}}{AWALL} \cdot \frac{TH}{CO} \cdot \frac{1}{H^{12}} \quad (7-2)$$

where: TW_1^{N+1} = Surface (node 1) temperature of two node layer, computed at "new" time N+1. ($^{\circ}F$)

TW_3^N = Surface (node 3) temperature of next internal wall layer, computed at "old" time N. ($^{\circ}F$)

$QWALL^{N+1}$ = Total heat flux to wall, computed at time N+1. (Btu/hr)

$AWALL$ = Wall surface area. (ft^2)

TH = Thickness of surface layer. (ft)

CO = Thermal conductivity of surface layer. (Btu/hr-ft- $^{\circ}F$)

H_{12} = Interface heat transfer coefficient between surface layer (node 2) and internal layer (node 3). (Btu/hr-ft 2 - $^{\circ}F$)

Furthermore, the temperature of the second node in the two node layer is given as:

$$TW_2^{N-1} = TW_1^{N+1} - \frac{QWALL^{N+1}}{AWALL} \cdot \frac{TH}{CO} \quad (7-2)$$

The two nodes in such a surface layer may thus be considered "floating" nodes, in that they affect other internal wall layer temperatures only by altering the computation of radiant heat transfer in the following time step. Furthermore, the temperature of a surface layer node in any time step does not directly depend upon its temperature in the previous time step.

These two nodes may also be called "imaginary" nodes because they absorb no heat while undergoing a rise in temperature. This effect is due to the assumed negligible heat capacity of the surface layer.

Equation B-17 (OPS-07A35) is used to compute the surface node temperature for the first wall layer comprised of three or more nodes. (In the case of Figure #1, this situation would correspond to node 3.) This equation is also used whenever heat is transferred between wall layers.

In general, Q_c is evaluated as the local heat flux into a wall layer's surface node from a previous wall layer or from the compartment environment (if no two node surface layer is present). Thus, Q_c is given by:

$$Q_c^{N+1} = (H^{N+1})(TA^{N+1} - TN_J^N) \quad (7-3)$$

which is equation B-18 in OPS-07A35.

where: Q_c^{N+1} = heat flux into surface node J. (Btu/hr-ft 2)

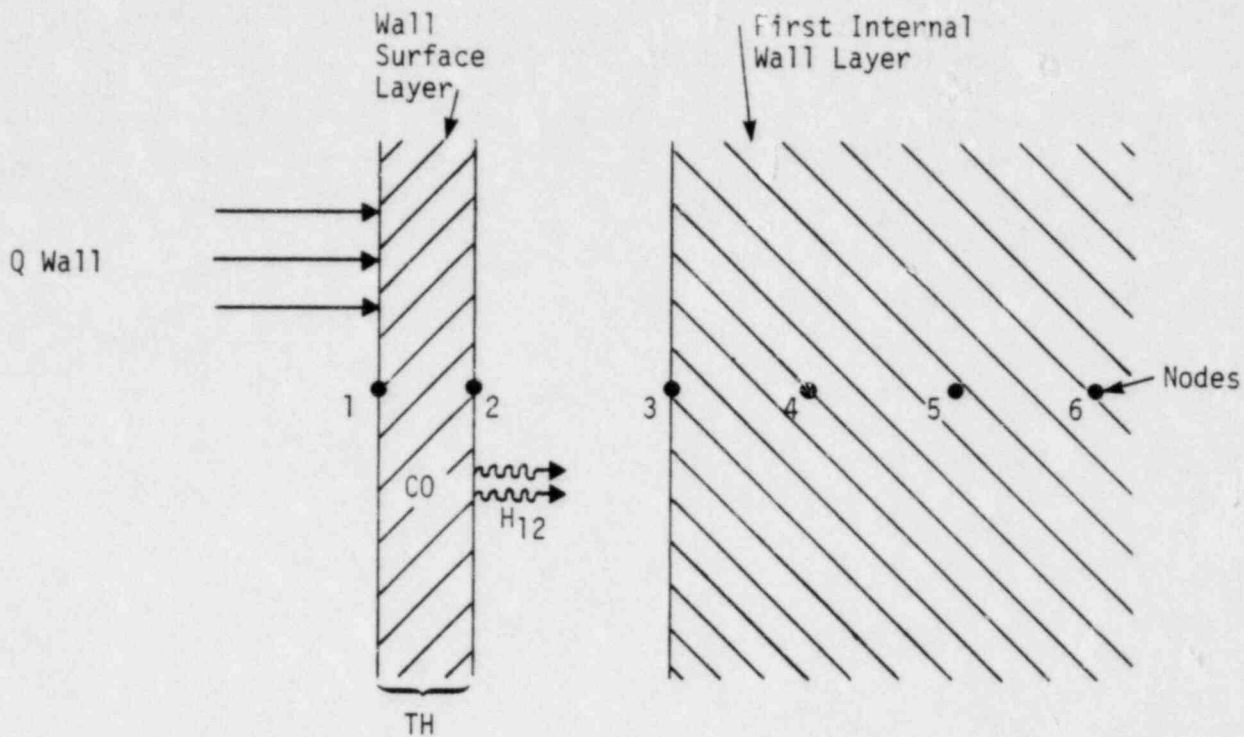


Figure 1

H^{N+1} = heat transfer coefficient into surface node J; equal to either exit heat transfer coefficient of previous wall layer, or to heat transfer coefficient from compartment environment to wall surface. (Btu/hr-ft²-°F)

TA^{N+1} = temperature of last node in previous wall layer, or temperature of compartment environment. (°F)

TN_J^N = temperature of surface node J. (°F)

In the above equation, the superscripts N and N+1 indicate which values are used from consecutive time steps. Thus, the "new" Q_c is calculated using the "old" surface node temperature, TN_J . The values of H and TA used are computed during the "new" timestep before Q_c is evaluated. The subscripts used in Equation B-17 of Report No. OPS-07A35 signify which node temperatures are used in the calculation. TW_J is the temperature at the surface node of the layer of interest, whereas TW_{J+1} applies to the first internal node in that layer.

8) Regarding the analysis of heat transfer in the ice bed:

- a) The assumption that no condensation occurs in the ice bed if the water vapor is superheated, and that condensation only occurs when the vapor is saturated does not seem realistic because (a) both heat and mass transfer can occur simultaneously if there is both a temperature and a concentration gradient; and (b) the vapor concentration gradient can extend into the superheated region. Provide justification for this assumption, perhaps via an analysis of the mass transport occurring in the superheated and in the saturated sections of the ice bed.
- b) The possibility exists to produce a condensate fog in the ice bed capable of being convected along with the flowing gas instead of collecting on the surface of the ice bed. Provide analyses or cite relevant studies which would justify the assumption that no condensate fog leaves the ice condenser.
- c) Provide additional details of the CLASIX ice bed heat transfer solution process, specifically, the procedure by which the ice condenser is subdivided into incremental lengths, and the superheat and saturated heat transfer correlations are applied.
- d) In the condensing region of the ice bed, Equation (C-26) is applied until the flow temperature is equal to the outlet plenum temperature.

Explain why the outlet plenum temperature is used as a cutoff point for the saturated heat transfer correlation rather than some fixed temperature.

- e) The film coefficient correlation for heat transfer to the ice, Equation (C-1), was developed based on ice bed inlet conditions typical of design basis accidents, i.e., relatively low flow v

- f) Specify the parameter dimensions, condensate length, and flow area assumed in Equation (C-1). Also provide some typical calculated values for the film coefficient in the superheated and condensing regions.
- g) Discuss the basic differences between the CLASIX treatment of the ice bed heat transfer and the treatments used in other ice condenser codes such as LOTIC and TMO. Describe the method of handling the heat and mass transport under superheated and saturated conditions in each code.

Response:

Westinghouse has verified that the ice condenser model used in CLASIX is, for all practical purpose, identical to that used in LOTICIII. Because LOTICIII is already accepted by NRC, and because the major purpose of CLASIX is to model hydrogen burning and not ice condenser performance, NRC should refer to WCAP-8282 and reference 6e for additional information.

- 9) Regarding the ice condenser melt water:
 - a) Discuss the heat transfer analyses and assumptions used to determine the melt water temperature on exit from the ice condenser. Provide approximate values of the melt water temperature for CLASIX analyses.
 - b) In the CLASIX description it is not clear whether ice melt water is transferred to the sump or assumed to remain at the ice node. Describe the melt water treatment and sump model used in CLASIX, especially with regard to how the lower compartment volume is adjusted due to the addition of water from melted ice and containment sprays.
 - c) Describe the effect of the reduced lower compartment volume (due to added water) on containment pressure and temperature response.

Response:

The total energy removed by the ice condenser is converted into a mass of ice melted by dividing by the heat of fusion of the ice. This mass of ice melted is then converted into a volume by dividing by the ice or water density depending on whether the volume is that of the lower plenum or that of the lower containment. Appropriate volume is added as free space to the lower plenum of the ice condenser (see the answer to question 1) and is subtracted from the free space available in the lower containment. This models the flow of the water from melted ice out of the ice condenser and into the lower containment. The energy removal in the ice bed is accounted for only in melting ice, therefore the melted ice appears as water at 32°F implicitly. However, no credit is taken for this water in terms of its ability to further remove energy from the containment. This lack of strict accounting for the energy removal capability of the melt water is, of course, conservative in that it underestimates the energy removal capability of the ice condenser process.

In the CLASIX versions used by the three utilities, the sump model was not activated. Therefore the use of a sump to adjust the volume of the lower compartment was not possible. This lack of explicit treatment of the sump was compensated for by assuming that the lower containment was already flooded to the design flood level at the start of the analysis. We note that because any reduction in the volume of the lower containment increases the magnitude of the pressure and temperature response of that containment volume, the handling of the lower compartment in this manner is very conservative. Note also that because the emergency core cooling systems are in a recirculation mode during the hydrogen burn stages of the accident, the spray and break flow do not change the volume of free space available in the lower containment.

10) With regard to the CLASIX spray model:

- a) The mass, momentum, and energy transfer accounting seems to be incomplete. For example, the equations should account for the simultaneous occurrence of either vaporization or condensation with or without a change in the spray-drop temperature. Please verify the CLASIX spray model by comparison with a spray model that includes a more thorough accounting for the mass, energy, and momentum transfers, such as the model developed by G. Minner.
- b) The assumption that spray drops will desuperheat completely from the drop initial temperature to the saturation temperature corresponding to the total pressure results in a certain fraction of the drop mass immediately "flashing" to the atmosphere. It is possible that liquid drops can sustain superheats as much as 8°C, which will reduce the fraction of mass transferred by "flashing". Justify the CLASIX assumption and describe what effect a sustained superheat would have on reported results.

Response:

The spray model developed by G. Minner provides a strict accounting of the mass, energy, and momentum transfer. This is expected since the Minner model is a finite difference approximation of the transient equations which govern this phenomena. The CLASIX spray model explicitly determines the mass and heat transfer by a classical transient technique that freezes compartment conditions during a time step.

Minner performed parametric studies to include the effects of droplet size, initial speed, flow rate, temperature, and fall distance. Minner found that calculations using a large drop size are conservative. The CLASIX S₂D base case and sensitivity studies used a droplet size diameter approximately 2.5 times larger than the manufacturer's published average value. Minner found that any parameter which increased the residence time in the compartment increased the rate of effect on the atmosphere. The fall time in CLASIX is used to conservatively limit the residence time and thereby, according to Minner's studies, decreases heat transfer. The Minner parametric studies demonstrate that the CLASIX spray model predicts conservatively low heat removal rates.

CLASIX updates the mass and energy transfer to the atmosphere in a similar procedure as that used by the Minner model for each sub-region. The mass and energy of the spray water is correctly removed from the spray compartment. (However, CLASIX does not update the mass and energy transferred to the sump.)

The mechanistic modeling of the effects of containment spray in CLASIX is an attempt to improve on the models used in standard containment analysis codes such as CONTEMPT and CONTEMPT4 in which the user specifies a "spray efficiency". This parameter then determines the energy transfer to the spray droplets as they fall through the containment atmosphere. The CLASIX model is considered superior to CONTEMPT in this regard. Sensitivity studies in which the spray flow is cut in half (the minimum safeguards case as described in our earlier submittals) have demonstrated that containment response during hydrogen burning is not strongly affected by containment spray. Accordingly, additional work on the CLASIX spray model is not justified.

The spray droplet temperature assumed in CLASIX analyses is 125°F, which is well below the saturation temperature at a total pressure of one atmosphere. Therefore, even though the computer code has the capability of modeling spray droplet desuperheating, it is not utilized and has no impact upon reported analyses.

- c) Heat and mass transfer during droplet fall is characterized as occurring in two regimes - sensible heating at constant drop volume, and vaporization at constant drop temperature (with excess heat removal). Describe how the times at which each of these mechanisms occur, t_1 and t_2 respectively, are defined in the computations.

Response:

Equation (E-16) of Report No. OPS-07A35 may be used to compute spray droplet heat transfer in either direction provided that there is no vaporization during its period of application. Substitution of equation (E-11) into equation (E-16) and rearrangement of the result yields:

$$\frac{T - T_{sp}}{T - T_1} = \exp\left(\frac{-HA}{W_{sp}c_p}t - t_1\right) \quad (10-1)$$

where: T = compartment ambient temperature (°F)

T_{sp} = spray temperature at nozzle (°F)

H = spray heat transfer coefficient (Btu/sec-ft²-°F)

A = total spray heat transfer area (ft²)

W_{sp} = spray flow rate (lbm/sec)

c_p = droplet specific heat (Btu/lbm-°F)

t = time (sec)

l = subscript used to denote conditions at some statepoint l

Equation (10-1) is applied when conditions may be frozen in time, such that W_{sp} becomes a mass parameter with dimension "lbm", and both sides of the equation become dimensionless. In such a form, equation (10-1) is merely the classical transient temperature equation for bodies with negligible temperature gradients.

In the case when compartment temperature is greater than both spray temperature and saturation temperature, CLASIX utilizes equation (10-1) to compute the time required to heat the sprays to saturation. In such a case, equation (10-1) is written:

$$\Delta t = t - t_{sat} = \frac{-W_{sp} c_p}{HA} \ln((T - T_{sp}) / (T - T_{sat})) \quad (10-2)$$

where: Δt = time required to heat sprays T_{sat} (sec)

T_{sat} = saturation temperature corresponding to compartment pressure (°F)

If Δt is greater than the input spray fall time, or T_{sat} is greater than the compartment ambient temperature, the characteristic time frame is taken as the input fall time, t_{fall} . In these cases, equation (10-1) is used in the following form:

$$TD = T - (T - T_{sp}) \exp\left(\frac{-HA}{W_{sp} c_p} (t_{fall})\right) \quad (10-3)$$

where: TD = droplet temperature at end of fall (°F)

In the case of spray droplet vaporization, such as that occurring when a droplet reaches saturation before completing its fall, a characteristic time interval, $\Delta t = t - t_2$, is assigned to the calculation as per equation (E-21). In this specific case, Δt would be equal to the remaining spray fall time interval (i.e., $\Delta t = t_{fall}$ - time at which saturation was reached).

- d) Please indicate whether the droplet velocity used in CLASIX is user-specified or calculated internally based on the input droplet diameter. Specify the velocity values used/calculated in the spray verification runs. Also, specify the input values for the spray film coefficient.

Response:

Spray droplet velocity calculations are important in many cases, such as in rigid droplet modeling, where heat and mass transfer rates are computed as a function of Reynold's number. The CLASIX code does not, however, use any velocity values (either input or calculated) as the heat transfer model utilized does not rely upon droplet velocity. Rather, an input fall time is used to set the limit on heat transfer, where the droplets are modeled as bodies with negligible temperature gradients (see answer to question 10(c), above).

The spray droplet surface heat transfer coefficient assumed in CLASIX analyses is 20 Btu/hr-ft²-°F. This value is within the range of experimental and theoretical values for single droplets.

- 11) In the evaluation of the effect of a separate spray time domain, it is stated that: 1) the CLASIX spray model always predicts conservatively high containment pressure and temperature responses; and 2) the difference in the heat removal calculated using the CLASIX spray subroutine and the finite difference subroutine approaches zero as the transient progresses. In light of this,
- a) Discuss why the CLASIX spray model underpredicts heat removal as the first statement implies. Holding compartment ambient conditions constant on an increasing temperature ramp would seem to support this. However, if ambient temperature would expose droplets to higher temperatures on the average, resulting in greater CLASIX spray heat removal. Provide additional comparisons of the rates of heat removal for the two models assuming increasing containment ambient conditions, decreasing ambient conditions, and postulated hydrogen burn conditions; i.e., a rapid ambient temperature increase followed by a gradual temperature decrease.
 - b) With regard to the second statement, describe the effect that non-linearities in heat transfer/thermodynamic processes have on the agreement between the two models.

Response:

Because the CLASIX model holds compartment conditions frozen in time while the heat transfer to the spray is calculated, the temperature used for the calculation tends to lag behind the actual response. This lag also has the effect of smoothing out rapid transients, such as those associated with hydrogen burns. The result is that, on the average, spray droplets in CLASIX are exposed to temperatures equal to or lower than those of the upper compartment during all conditions, except those associated with a decreasing ramp followed by an increasing ramp. The analysis that was done previously was reviewed and it was noted that the small errors introduced by the spray model during such ramps was more than offset by the smoothing out of the much greater temperature differences which occurred during hydrogen burning. This lack of sensitivity to the spray model conditions is further supported by the minimal increases in containment response noted when an analysis was performed with spray flow cut in half (the minimum safeguards case). It is concluded that the CLASIX spray model does not make an important contribution to the uncertainty in analysis performed by CLASIX.

The only significant non-linearity in the spray flow model occurs at the point where the compartment conditions become saturated and spray heat removal occurs due both to sensible heating of the droplet and vaporization. If the point at which saturation conditions are attained in a compartment differs between two spray models, this non-linearity will add to that difference.

- 12) Regarding the temperature and pressure responses (Figures D-1 and D-2) presented in the spray comparison, discuss the reason for the sudden change in slope between 120 and 125 seconds.

Response:

This change in slope is due to attainment of saturation conditions in the compartment, and a corresponding change in heat transfer regime.

- 13) In the CLASIX-TMD comparison presented in Appendix A, the response of an ice condenser plant is modeled using both TMD and CLASIX. However, the input parameters for TMD (Tables A-1 and A-2) and CLASIX (Tables A-3 and A-4) do not seem analogous in several respects, and do not accurately represent Westinghouse ice condenser design. Specifically:

- a) The upper compartment volumes used in the two analyses are not in agreement, presumably due to a typographical error in the CLASIX value (Table A03). Even so, the value of 698,000 ft³ used in the analyses actually represent the sum of the upper compartment (651,000 ft³) and upper plenum (47,000 ft³) volumes. The upper compartment volume should not include a contribution from the upper plenum since the latter is represented as a separate mode in both analyses.
- b) In TMD the ice is distributed in the three ice bed compartments and the upper plenum (total volume = 88,499 ft³), while in CLASIX all the ice is assigned to the single ice bed node (volume = 36,830 ft³) and no ice is present in the upper plenum.
- c) The lower plenum volume in TMD is 22,100 ft³ versus 36,830 ft³ in CLASIX. Equivalent volumes would seem to be more appropriate.
- d) In TMD a loss coefficient of 0.5 is specified for each of the ice bed and plenum flow paths (paths 1 through 5 in Figure A2). To be consistent with the CLASIX analysis, TMD loss coefficients should be approximately 0.1 for paths 2 through 5 and 2.0 for path 6.

Discuss the aforementioned differences in the TMD and CLASIX input parameters, and verify the TMD-CLASIX comparison via revised analyses as appropriate.

Response:

The input to CLASIX and TMD was set up only for comparison of the two codes and not to make any prediction concerning performance of any specific ice condenser plant. To that extent, the inputs to TMD and CLASIX are identical when the differences in ice condenser nodalization are taken into account. Looking at the volumes of the various regions at the start of the transient:

| | CLASIX | TMD |
|-------------------|--------|--------|
| lower compartment | 289000 | 289000 |

| | | |
|--|---------------------------------------|--------|
| ice condenser (includes plenums and ice bed free space) | 110490 | 110500 |
| upper compartment | 698000 (typo in original document) | 698000 |
| dead ended compartment | 94000 | 94000 |

NRC correctly notes that the upper compartment volume is slightly larger than that of the typical ice condenser containment. This does not affect the comparison between the two code predictions because the same upper compartment volume is used for both codes. The manner in which the ice bed free space is allocated between the lower and upper plenums (volumes 2 and 3) in CLASIX was discussed in the answer to question 1; all of the free ice bed space is properly accounted for throughout the transient, in both codes. The total ice mass and total ice heat transfer areas used in the two codes are identical. The distribution of ice mass and ice heat transfer area in TMD is a consequence of the manner in which the ice condenser is nodalized. It is concluded that the handling of the ice mass and heat transfer area is analogous between the codes in this comparison, being soundly based on the differences between TMD and CLASIX in the manner of ice condenser nodalization.

In regard to the flow loss coefficients used for the comparison, it should be noted that all of the ice bed pressure drop is assumed to occur at a single node in CLASIX, and that in TMD, pressure losses are distributed over the several nodes which occur within the ice bed. We agree with the NRC comment that a more appropriate distribution of flow loss coefficients could have been made. However, it should be noted that the total pressure drop through the ice condenser is smaller in the CLASIX model than in the TMD model. Therefore, the flow through the ice condenser and the total heat removal by the ice will be greater for the CLASIX model than for the TMD model. This explains the lower temperature predicted by CLASIX for the upper compartment; however, the pressure in the upper compartment as predicted by CLASIX is conservative when compared to TMD. Accordingly, it is concluded that the greater ice condenser mass flow rate has not effect on the conclusion reached in OPS-07A35 that CLASIX results are favorably comparable to the predictions of TMD for the same model.

14) For the CLASIX-COCOCLASS9 comparison:

- a) Explain why a transient hydrogen burn case wasn't considered in addition to the single burn case analyzed.
- b) Specify the surface film coefficient assumed in cases 2 and 5 of this comparison, and discuss whether or not this value would account for pre-burn pressures and temperature in cases 2 and 5 being less than in cases 3 and 6, respectively.

Response:

The purpose of the comparisons of CLASIX with other similar analytical tools is to verify that the models in CLASIX reasonably predict the

proper response of the containment. Because CLASIX is the only code designed to model containments with deliberate ignition systems, the mechanism for initiation of hydrogen burns is unique. The manner in which hydrogen burning was initiated in the comparison between CLASIX and COCOCLASS9 was based on the limitation of COCOCLASS9 in the manner of burn initiation, in order to force the burns to be initiated at the same time and proceed at the same rate. We conclude that the situation analyzed is adequate for the purpose of the comparison. The constant heat transfer coefficient used in cases 2 and 5 is 5.0 Btu/hr-ft²-°F. This is higher than the Tagami coefficient used in cases 3 and 6 and therefore explains the difference in preburn conditions.

- 15) With regard to the comparison of CLASIX results with test measured results (Appendix C):
- a) Complex burn-control parameter adjustment were required to predict conservatively the peak pressure for tests that had (1) a single non-uniform burn (CLASIX Case 10), and (2) multiple burns (Fenwal Case 2-2-2 Transient).
 - (i) Describe the burn-control parameter adjustments made for these cases;
 - (ii) Discuss the corresponding parameter adjustment procedure that would be used to perform an analysis for a nuclear power plant containment that has non-uniform or multiple burns; and
 - (iii) Provide results of CLASIX predictions for these two cases under a best-estimates single set of burn parameters applied over the entire burn event. Compare the pressure trace to that obtained from (1) the "revised" CLASIX model; and (2) the actual test results.

Response:

The CLASIX code is set up to model only uniform hydrogen burning. This implies that the characteristics of the burn are established by user input and the containment conditions at burn initiation, and are held constant for the duration of the burn. Because burning is assumed to initiate at conservatively high hydrogen concentrations and proceed at conservatively high burn rates, the total energy deposited in a volume by a hydrogen burn and the rate at which this energy is deposited are overpredicted by CLASIX when compared to the real world. This results in conservatively high pressure and temperature response for containment. In the Fenwal case and CLASIX analysis cited, burning was not uniform in the test vessel but occurred in three distinct regions at three different rates. Though the underlying assumptions in CLASIX are not applicable to this case, an attempt was made to model non-uniform burning by using the restart capability in CLASIX. The problem was stopped and restarted three times. At each stop, the burn parameters were readjusted to reproduce the pressure ramps seen in the test. At the end of the analysis, the total volume percent of hydrogen predicted to remain in the vessel was compared to that measured at the end of the test. It took several tries before a good match of analysis and measured response could be achieved.

There is no need to repeat similar analyses for an actual containment because all reasonable cases of multiple burns are bounded by the uniform burn cases already analyzed. The use of a single uniform burn to model a non-uniform burn in a test vessel would have very little value.

- b) Sensitivity studies with CLASIX are cited in Appendix C but few test results are provided. Please provide more details, specifically, the ranges over which the parameters were varied, and the results for the bounding cases.

Response:

The following are typical values of parameter variation and the associated results. Refer to the TVA response for a more complete list of parameter variation.

1. Specific heats were varied from those of 176°F to those of 2280°F. Pressure response was lowered by 16 psi when the specific heats were selected based on higher temperatures.
 2. Heat transfer coefficients were varied from 0 to 43 Btu/hr-ft²-°F at the walls. Use of higher heat transfer coefficients lowered pressure response by 11.5 psi over the adiabatic case.
 3. Variations in beam length (2.11 to 6.34 ft.), emissivity (0 to 0.9), and the heat transfer coefficients associated with wall conductivity had negligible effects on pressure response.
- 16) Justify that mass and energy are conserved by CLASIX for a large problem time and for the problem time steps used. Describe quantitatively the time steps and their variation during a typical problem.

Response:

Because mass can leave the analysis by falling into the sump, and energy can leave the analysis by conductivity out through containment shell, over a long problem time mass and energy cannot be said to be "conserved". At each time step, a mass and energy balance is performed on each constituent in order to calculate the thermodynamic conditions at the start of the next time step. These conservation equations have been verified to hand calculation and found to be correct. For all of the CLASIX work done for McGuire, a time step of 0.01 seconds was used. This time step size was kept constant for the duration of the transient.

Response to Request For Information On Hydrogen Control
Transmitted By Mr. T. M. Novak's Letter Of September 17, 1982

1. A substantial number of laboratory tests were conducted as part of the ICOG/EPRI R & D Program for hydrogen control and combustion. Test results were transmitted from the utilities to NRC as they became available; however, for several of the research programs, only selected test results were not provided. This information is required to confirm the adequacy of the test program and assumptions made in the containment analyses. In this regard provide the following:

a) ACUREX

- i) A table of droplet size and droplet density estimates for each of the fog/spray tests;
- ii) A table of estimated flame speed for each test (flame speed should be calculable from thermocouple locations and ignition time data);
- iii) Pressure and temperature traces similar to those depicted in Figures 4-2 of the December 1981 ACUREX Project Report, but for tests 2.10, 2.11, and 2.12;

b) FACTORY MUTUAL

Results of ignition tests in which a glow plug was used in place of the ignition electrodes;

c) WHITESHELL

Tables summarizing pre- and post- burn conditions, igniter locations, maximum measured pressure rise, adiabatic pressure rise, completeness of burn, and estimated flame speed. These tables should be keyed to and cover all of the tests committed to in the test in matrix (tables 1 - 4 Appendix A.1 of the fourth quarterly report on the TVA research program, June 16, 1981) plus any additional AECL tests conducted under this program. Of particular interest to the staff are the results of the 8.5% H₂ test with 30% H₂O and top ignition. Discuss your plans for conducting tests at steam concentrations above 30%, as committed to in previous quarterly reports;

d) HEDL

Figures depicting concentration gradients for each of the tests. Figures provided should permit better resolution than those included in the previous submittal.

Response:

- 1.a.i) The Acurex test vessel was not instrumented to obtain data on either the characteristic droplet size of a fog/spray or the resulting densities. Therefore, in order to obtain estimates for these

parameters, data obtained by Factory Mutual Research Corporation must be used. (See "Water Fog Inerting of Hydrogen-Air Mixtures", Zalash and Bajpai, September, 1981.) Measurements taken by Factory Mutual on the Spraco 2163-7604 nozzle provided the following information:

| <u>Parameter</u> | <u>Pressure Drop Across Nozzle</u> | |
|--------------------------------|------------------------------------|--------------------|
| | <u>20 psid</u> | <u>30 psid</u> |
| Droplet diameter (number mean) | 11 μ | 9 μ |
| Droplet diameter (volume mean) | 35 μ | 21 μ |
| Approximate volume fraction | 2×10^{-4} | 8×10^{-5} |

The flowrates for one nozzle were .12 and .16 gpm at nozzle ΔP 's of 20 and 30 psid, respectively. The Spraco 1713 nozzle used to supply the water spray was very similar to the nozzles used in containment spray systems. Spray characteristics at a nozzle ΔP of 40 psid have been shown to be approximately 15 gpm flowrate and 200 μ number mean droplet diameter. It should be pointed out that in tests where sprays were present, a single Spraco 1713 nozzle was used, whereas nine Spraco 2163-7604 nozzles were used in tests where fogs were present. Therefore, the 1713 spray parameter quoted above are probably a fairly good estimate of the spray conditions inside the test vessel. However, with nine 2163-7604 nozzles present in the test vessel, the fog parameters quoted above obviously do not account for the impingement of the spray cones upon each other and therefore do not provide nearly as good an estimate of fog conditions inside the test vessel. This data uncertainty was known to be present at the onset of the test program. If the test results had shown fogs to be extremely desirable as a hydrogen mitigation concept, then further testing would have been required to further define fog characteristics needed for preliminary system design. See Section 2.6 for more discussion on the test facility design and test program objectives.

- ii) The Acurex test vessel was not instrumented to obtain data on localized flame speeds. However, by knowing the ignitor location and using the resulting pressure traces, "average" flame speeds were calculated. These flame speeds were determined by assuming that the flame front propagated through the test vessel as a disc. The base of a pressure spike represented ignition and the peak represented quenching of the flame. This approach was valid only for tests where discrete burns were observed and propagated throughout the entire vessel. Propagation distances were obtained from Figure 1 and propagation times were obtained from Appendix 2H. The quotient of these two values yielded the average flame speed. Although localized flame speeds were expected to be higher, for the purposes of comparing observed speeds to the average speeds used in containment analyses, this computational approach was believed to be adequate. The calculated average flame speeds were:

| <u>Test #</u> | <u>Ignitor Location</u> | <u>Flame Speed</u> |
|---------------|-------------------------|--------------------|
| 1.2 | top | 1.7 fps |
| 1.5 | bottom | 2.1 |
| 1.6 | bottom | 0.8 |
| 1.7 | bottom | 4.0 |
| 2.1 | bottom | 3.5 |
| 2.2 | bottom | 6.3 |
| 2.3 | bottom | 8.2 |

Two conclusions appear evident: 1) Average flame speeds in lean mixtures appear to be a function of hydrogen concentration. 2) Average flame speeds in dynamic tests appear to be consistently lower than those obtained in quiescent tests.

- iii) The requested temperature and pressure curves are provided in Figures 2-7.
- b) Tables 1 through 3 provide results of the Factory Mutual fog inerting test with the ignition source, i.e., electrode or glow plug, indicated.
- c) Summary tables of the AECL-Whiteshell combustion phenomena tests are provided in Tables 4 through 6. Failure to perform the test with a top ignition location at vessel condition of 8.5% H₂ and 30% steam was unintentional. This test will be performed at the earliest opportunity. AECL-Whiteshell indicates that they should be able to perform this test in November. The scheduling of this test is contingent upon the completion of a series of studies currently being performed within the AECL-Whiteshell test facility.

With regard to testing at elevated steam concentrations, Section 2.8.2 states that steam concentrations for the AECL-Whiteshell combustion phenomena tests would vary from 0-30%. Although Table 5, one of the attached summary tables, shows that several tests were conducted at elevated steam concentration, extensive testing on the effect of elevated steam concentration were conducted as part AECL-Whiteshell ignitor performance testing. Results presented in Appendix 2I show that tests were conducted at steam concentration in excess of 50%.

- d) Concentration traces from the HEDL distribution tests on a scale greater than presented in Appendix 2K are not currently available. However, to assist in analyzing the data presented, refer to Figures 8 and 9. These figures present traces of the maximum gas concentration difference. With the exception of a

spike in tests HM-1A and HM-2, the maximum measured difference is less than 3%. The spikes observed in the referenced tests occurred shortly after the source jet was terminated. Since these tests were run without fans, steam condensation in the lower compartment resulted in a partial vacuum. This partial vacuum resulted in a transfer of mass from the upper to lower compartments. Since the lower and intermediate doors of the ice condenser would act as a check valve and prevent such a flow reversal from occurring within containment, the referenced spikes were considered to be an anomaly due to the test vessel design and not an anticipated characteristic of mixing within containment during degraded core accidents.

Figure 1

Igniter Locations within the Acurex Test Vessel

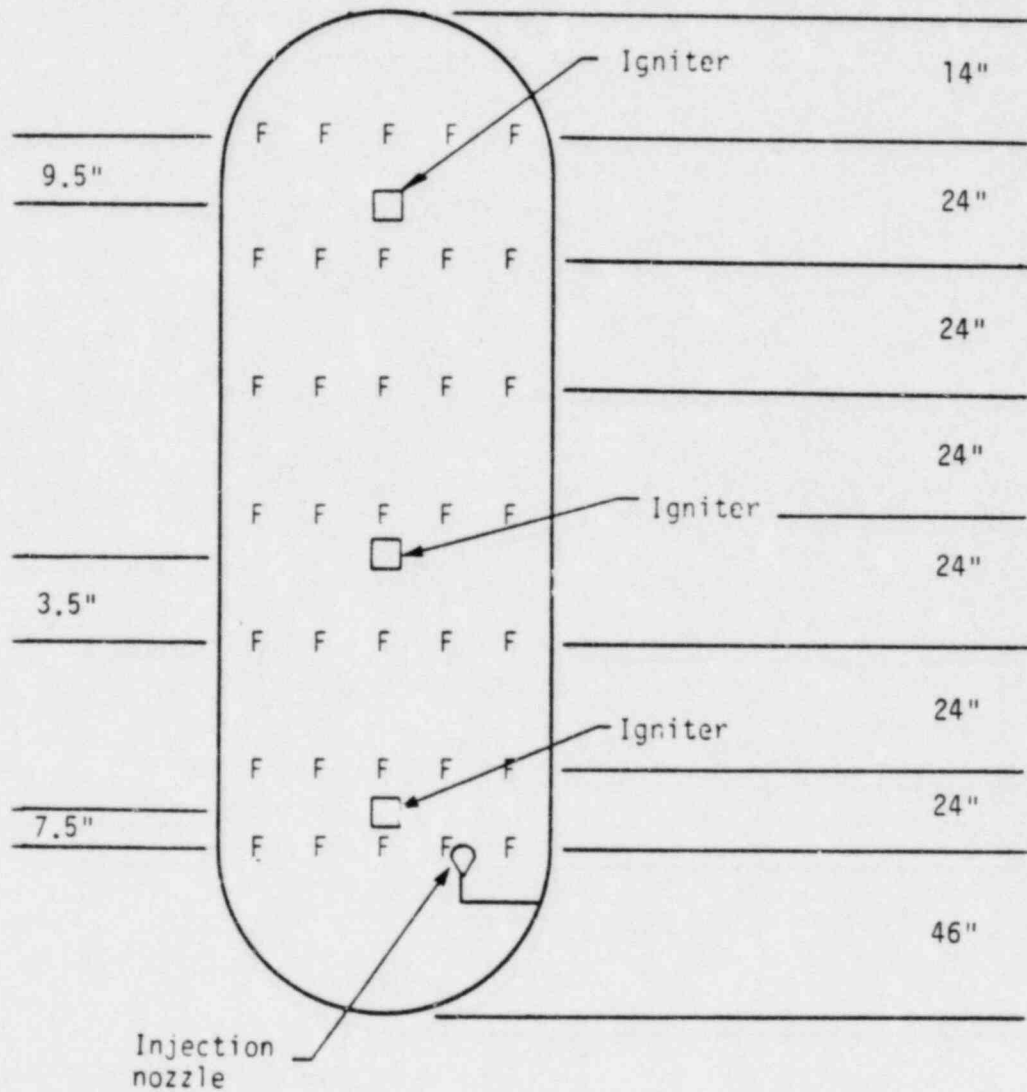


Figure 2

Test 2.10
Centerline Temperature T2

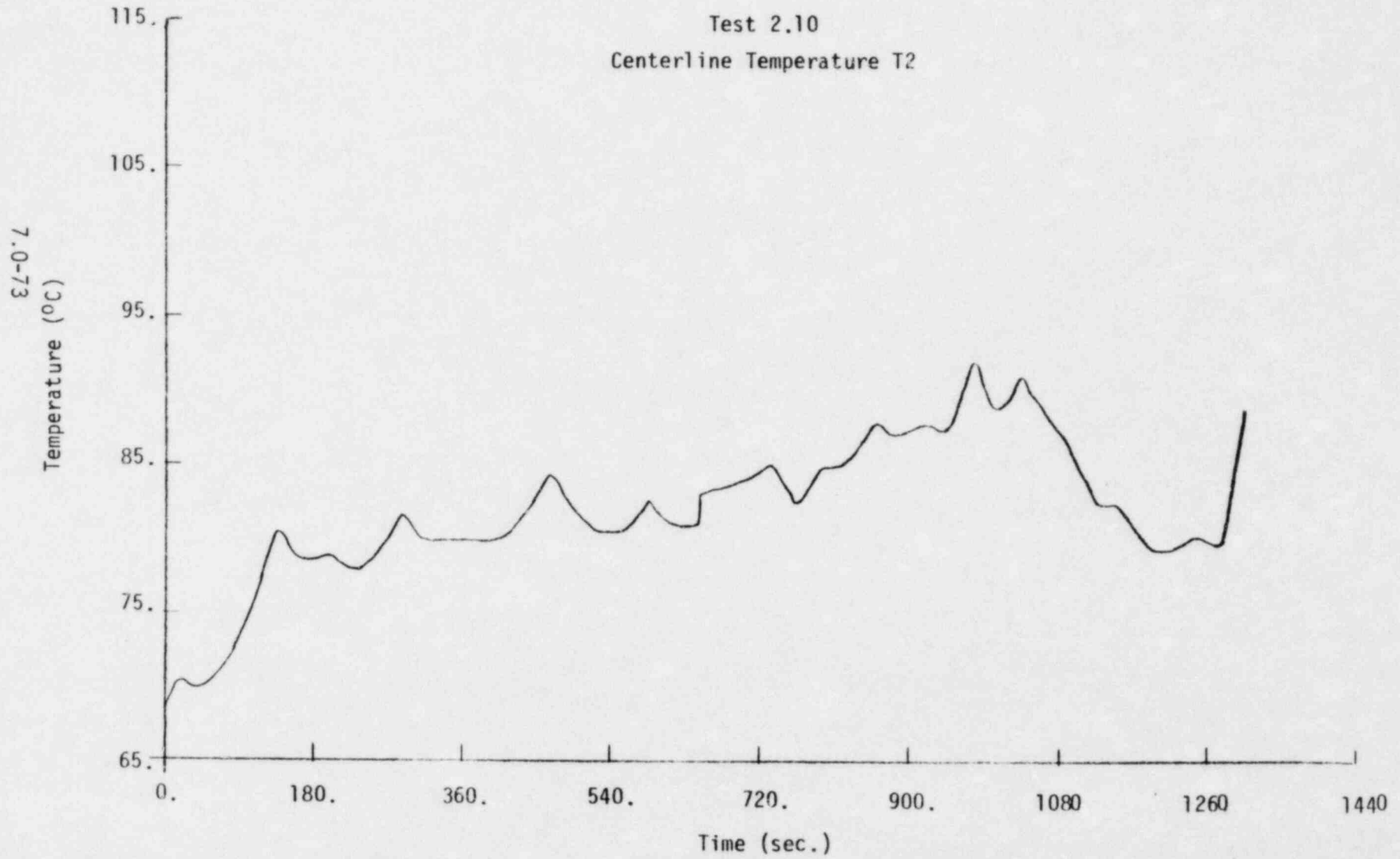


Figure 3

Test 2.10
Vessel Pressure P2

7.0-74

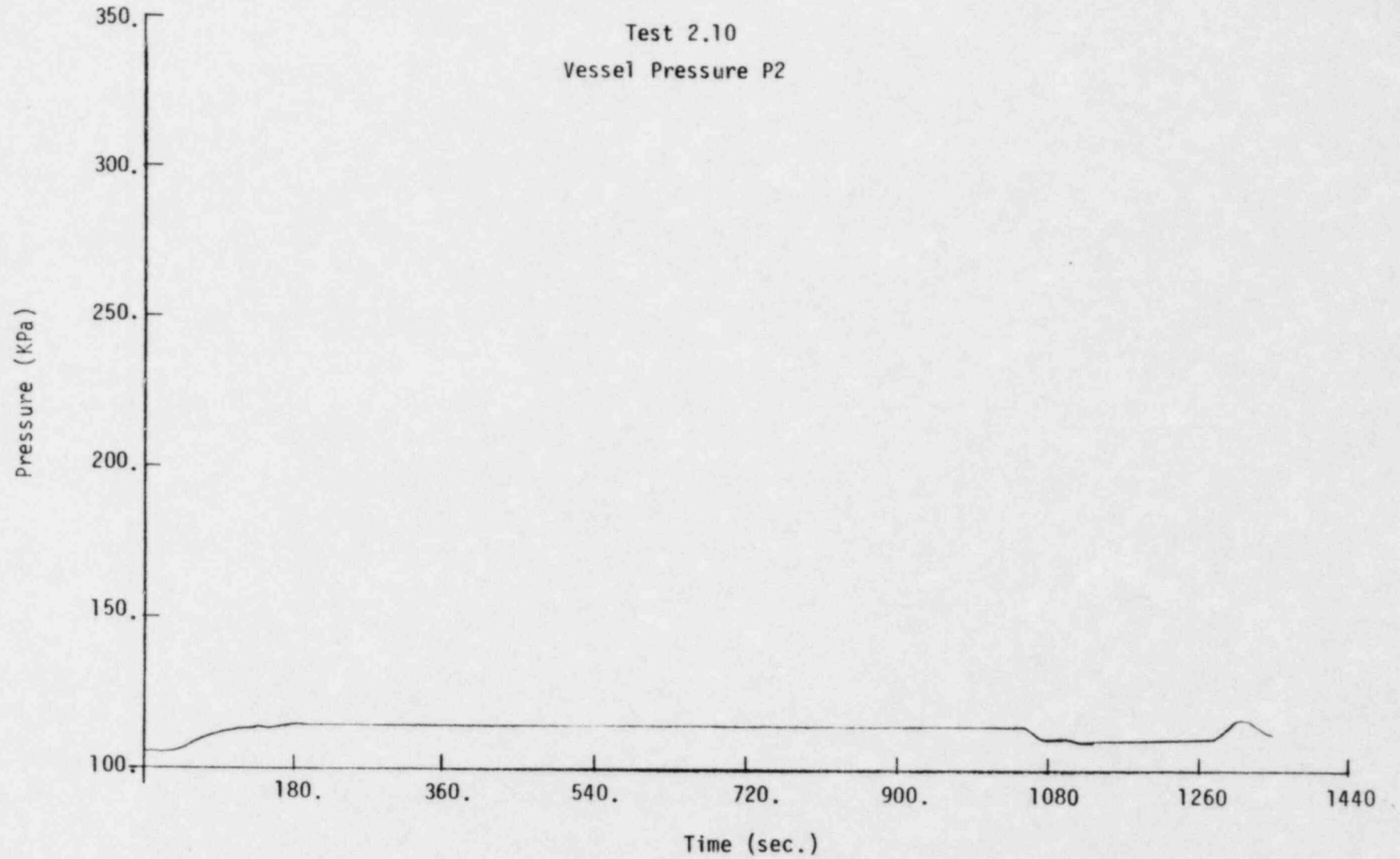


Figure 4

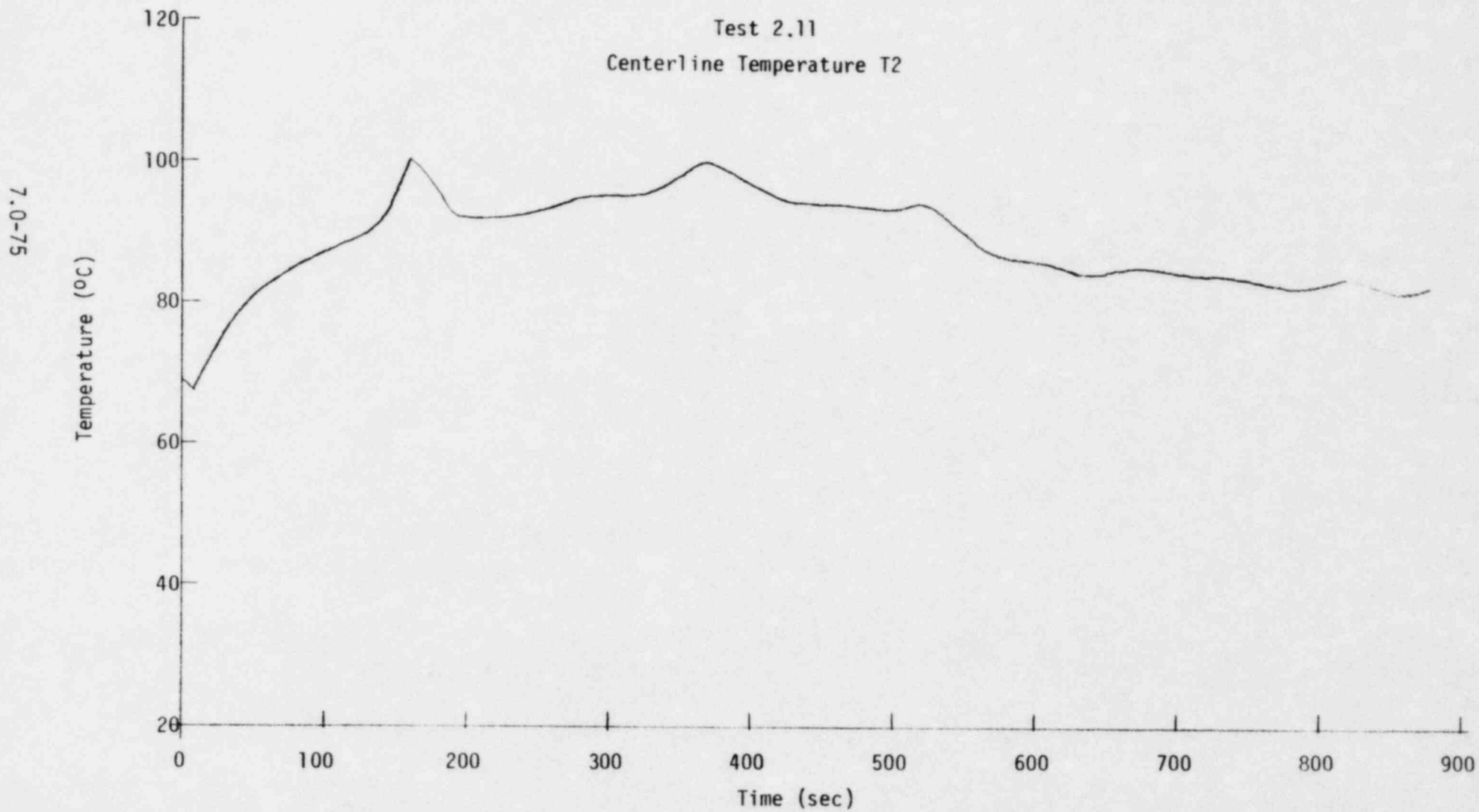


Figure 5

Test 2.11
Vessel Pressure P2

7.0-76

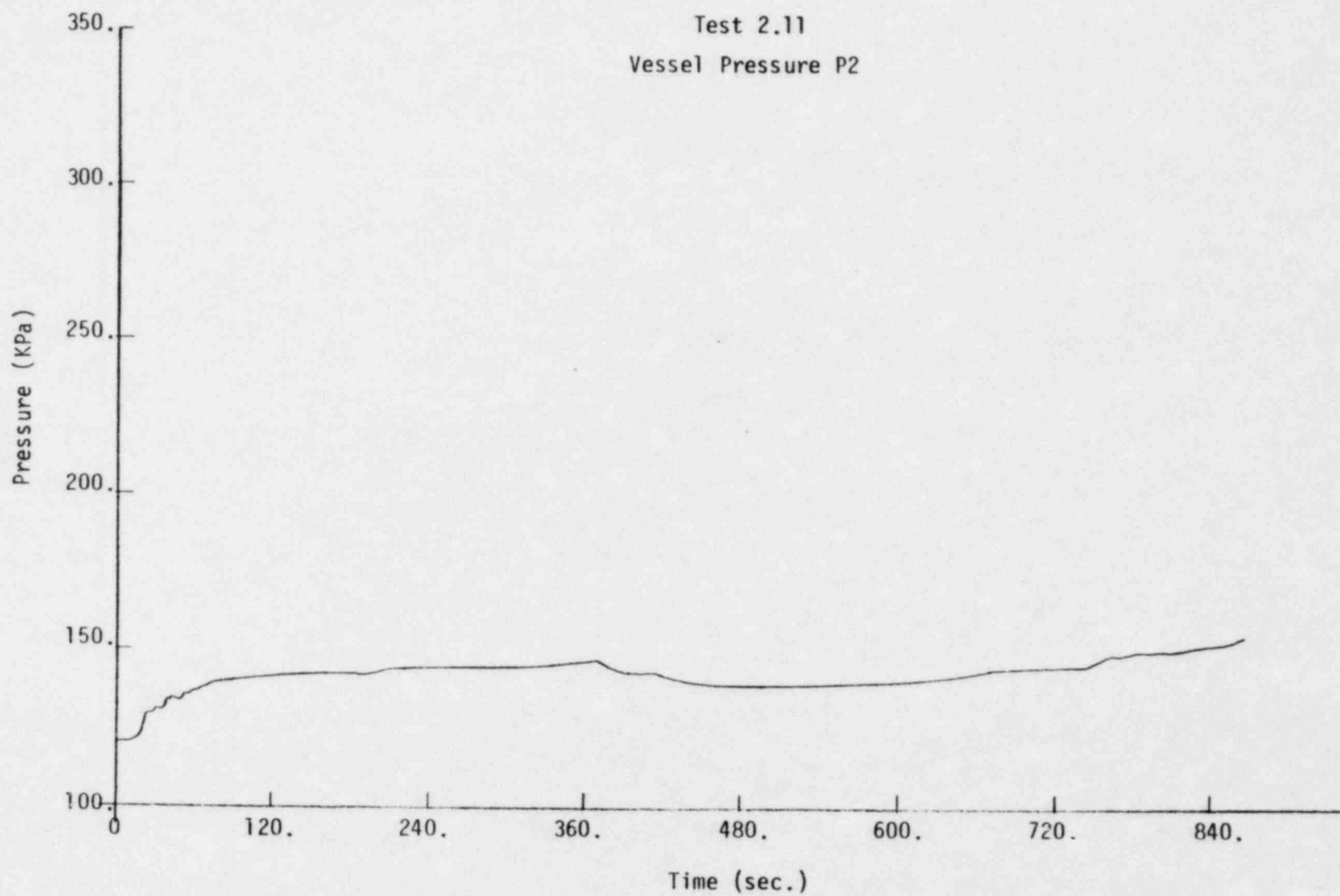


Figure 6

7.0-77

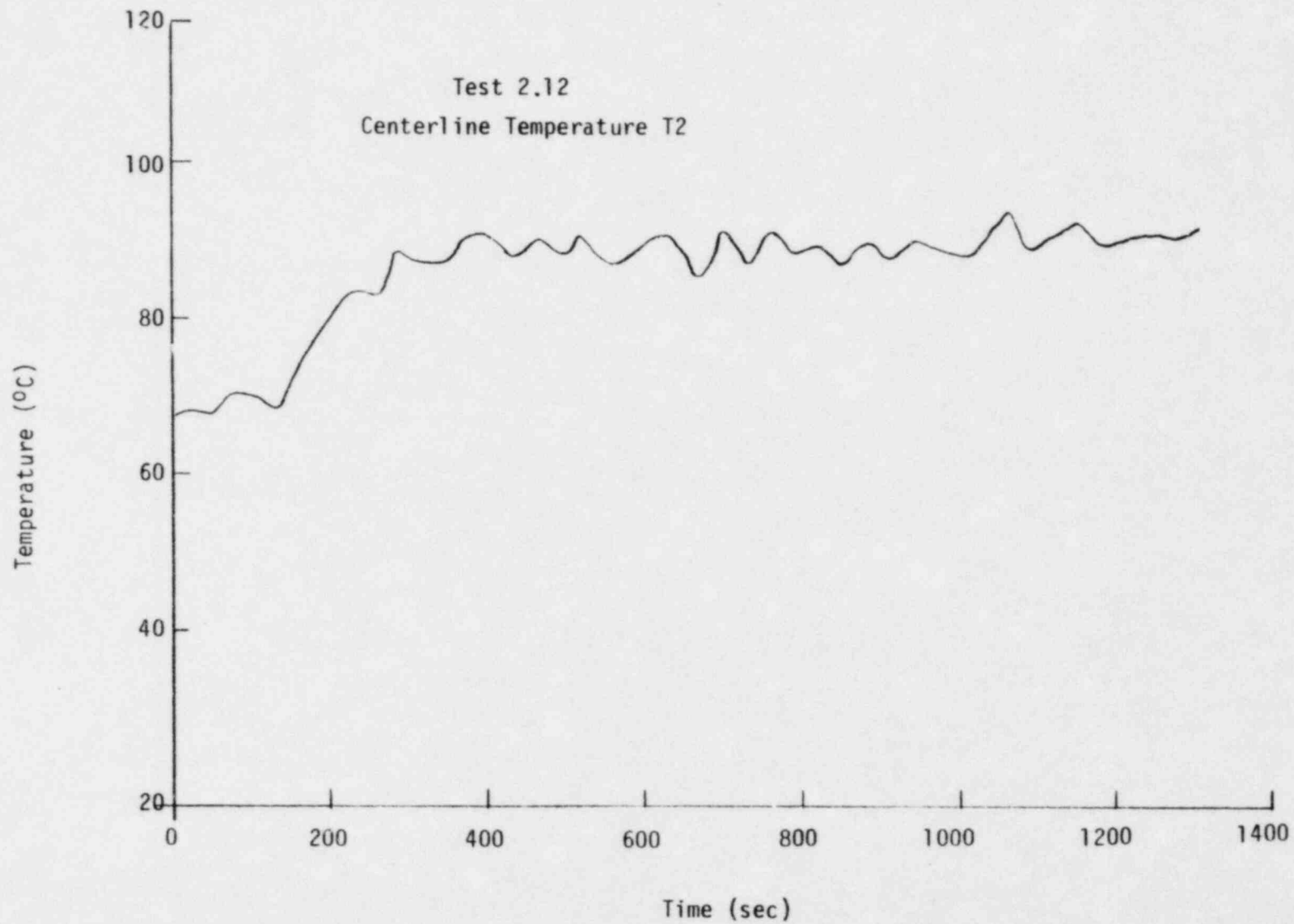
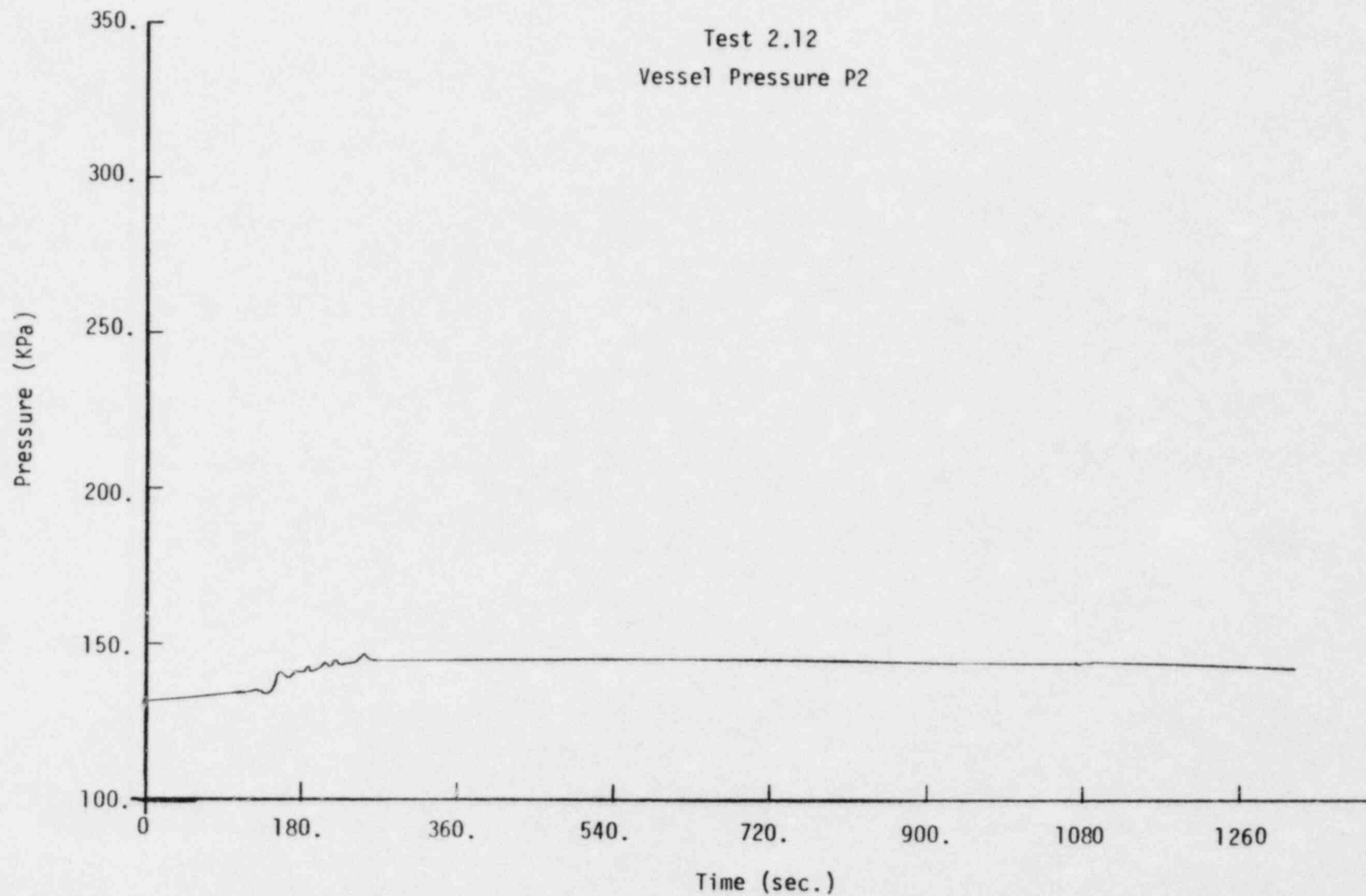


Figure 7

Test 2.12
Vessel Pressure P2

7.0-78



MAXIMUM GAS CONCENTRATION DIFFERENCE
FOR TEST HM-1A, HM-2, HM-4C, AND HM-6

7.0-79

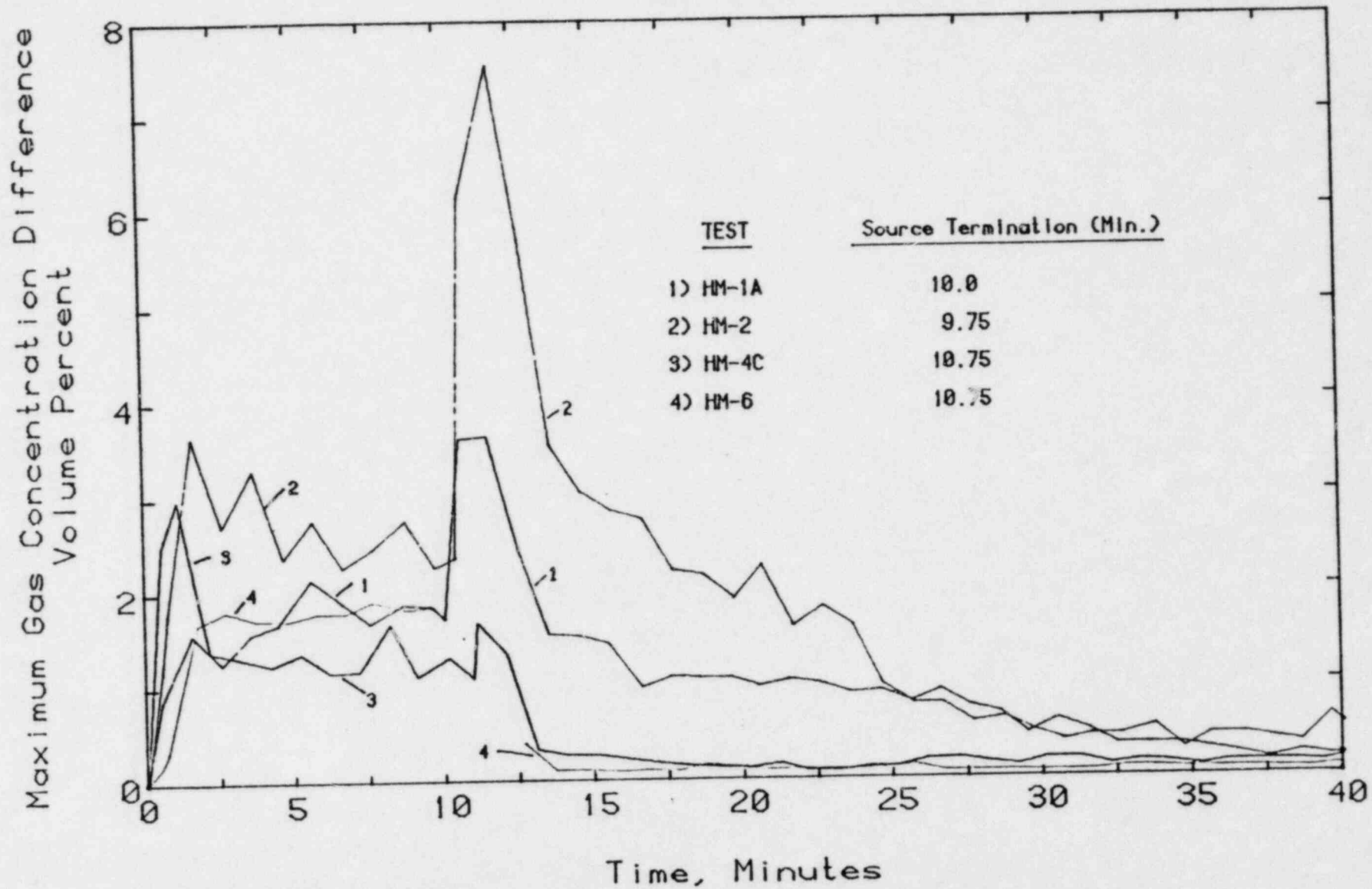


Figure 8

7.0-80

MAXIMUM GAS CONCENTRATION DIFFERENCE FOR TEST HM-3A, HM-5A, AND HM-7

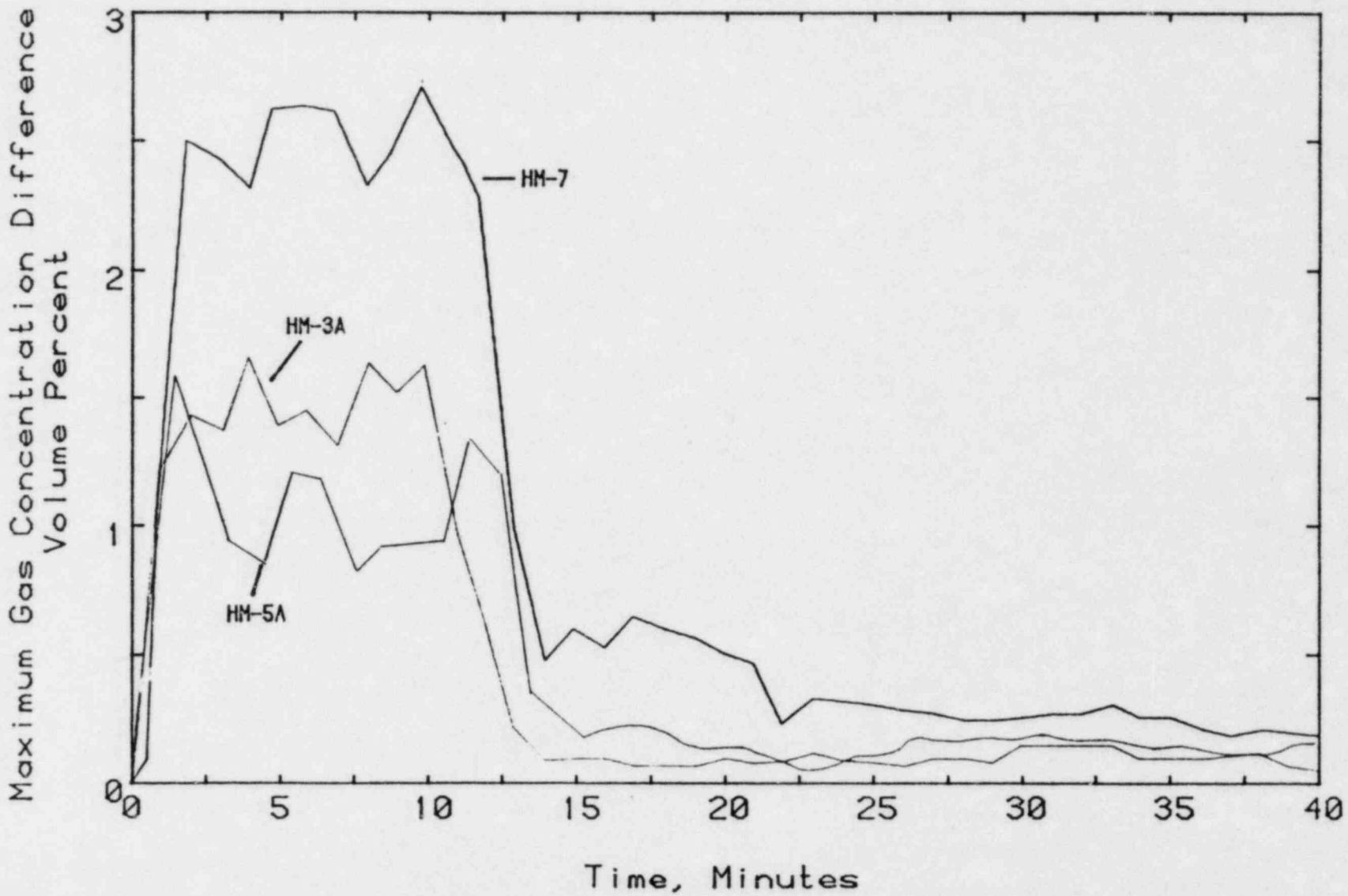


Figure 9

Table 1

HYDROGEN-WATER FOG INERTING DATA AT 20°C

| Nozzle | Pressure (psig) | Spray Angle (Full) | Drop Size | | Conc. $\frac{\text{cm}^3 \text{H}_2\text{O}}{\text{cm}^3 \text{Mix}}$ | Igniter | Hydrogen LFL (vol %) |
|-----------|--------------------|--------------------------|--------------------------|---------------------------|---|-----------|-------------------------|
| | | | Vol. Mean (Micron) | No. Median (Micron) | | | |
| Spraco | 10 | | 111 | 9.8 ₊ | 8.1×10^{-4} | Spark | 4.42 \pm 0.11 |
| 2163-7604 | 20 | $\approx 60^\circ$ | 54.5 | 4.7 ₊ | 3.8×10^{-4} | Spark | 4.76 \pm 0.31 |
| | 25 | $\sim 60^\circ$ | 44.1 | 3.8 ₊ | 2.7×10^{-4} | Spark | 4.76 \pm 0.31 |
| | 30 | $\sim 60^\circ$ | 20.6 | 1.5 ₊ | 2.8×10^{-4} | Spark | 4.72 \pm 0.28 |
| | 30 | $\sim 60^\circ$ | 20.6 | 1.5 ₊ | 2.8×10^{-4} | Glow Plug | 5.0 \pm 0.24 |
| Spraco | 10 | 61° | 139 | 13 ₊ | 3.6×10^{-3} | Spark | 4.64 \pm 0.12 |
| 2020-1704 | 20 | | 86.2 | 6.8 ₊ | 8.5×10^{-4} | Spark | 4.76 \pm 0.31 |
| | 25 | | 58.4 | 4.8 ₊ | 2.9×10^{-4} | Spark | 4.76 \pm 0.31 |
| | 30 | 80° | 35.7 | 5.6 ₊ | 1.5×10^{-4} | Spark | 5.26 \pm 0.19 |
| Spraco | 10 | | 136 | 13 ₊ | 9.4×10^{-5} | Spark | 4.40 \pm 0.10 |
| 1806-1605 | 20 | | 59.3 | 5 ₊ | 6.0×10^{-5} | Spark | 4.76 \pm 0.31 |
| | 25 | | 66 | 4 ₊ | 5.7×10^{-4} | Spark | 4.76 \pm 0.31 |
| | 30 | $\sim 40^\circ$ | 47.8 | 6.4 ₊ | 3.2×10^{-4} | Spark | 4.65 \pm 0.34 |
| Spraco | 10 | | 136 | 14 ₊ | 4.5×10^{-3} | Spark | 4.64 \pm 0.12 |
| 1405-0604 | 20 | | 110 | 10 ₊ | 2.2×10^{-2} | Spark | 4.76 \pm 0.31 |
| (20-30°) | 25 | | 114 | 11 ₊ | 2.7×10^{-2} | Spark | 4.76 \pm 0.31 |
| | 30 | 20° | 115 | 14 ₊ | 3.3×10^{-2} | Spark | 5.26 \pm 0.19 |
| Sonicore | 20 | | - | 5 | 1.1×10^{-3} | Spark | 7.2 \pm 0.22 |

03514

Table 2

HYDROGEN-WATER FOG INERTING DATA AT 50°C

| Nozzle | Pressure (psi) | Drop Size | | Conc. $\frac{\text{cm}^3 \text{H}_2\text{O}}{\text{cm}^3 \text{Mix}}$ | Igniter | Hydrogen LFL (vol %) |
|-----------|-------------------|--------------------------|---------------------------|---|-----------|-------------------------|
| | | Vol. Mean (Micron) | No. Median (Micron) | | | |
| Spraco | 40 | 33.1 | 5.2 ₊ | 1.4×10^{-4} | Spark | 7.19 ₊ 0.22 |
| 2163-7604 | 30 | 21.4 | 4.2 ₊ | 8.1×10^{-5} | Spark | 5.55 ₊ 0.11 |
| | 20 | 34.5 | 4.5 ₊ | 1.9×10^{-4} | Spark | 5.55 ₊ 0.11 |
| Spraco | 40 | 24.5 | 3.8 ₊ | 9.3×10^{-5} | Spark | 7.19 ₊ 0.22 |
| 2020-1704 | 30 | 27.1 | 4.2 ₊ | 1.1×10^{-4} | Spark | 7.19 ₊ 0.22 |
| | 20 | 50.3 | 6.2 ₊ | 4.0×10^{-4} | Spark | 6.32 ₊ 0.22 |
| Spraco | 10 | - | - | - | Glow Plug | 4.98 ₊ 0.22 |
| 1806-1605 | 20 | 43.2 | - | 9.7×10^{-5} | Glow Plug | 5.22 ₊ 0.42 |
| | 30 | 15.2 | - | 1.6×10^{-5} | Glow Plug | 5.44 ₊ 0.22 |
| | 40 | 11.2 | 3 ₊ | 1.9×10^{-5} | Glow Plug | 5.18 ₊ 0.42 |
| | 40 | 11.2 | 3 ₊ | 1.9×10^{-5} | Spark | 5.35 ₊ 0.42 |
| Spraco | 40 | 87.8 | 9.6 ₊ | 3.2×10^{-2} | Spark | 5.55 ₊ 0.11 |
| 1405-0604 | 30 | 91.8 | 11.5 ₊ | 2.0×10^{-2} | Spark | 5.55 ₊ 0.11 |
| | 25 | 115 | 14 ₊ | 1.7×10^{-2} | Spark | 5.55 ₊ 0.11 |
| Sonicore | 25 | 24 | 2.4 ₊ | 1.1×10^{-3} | Spark | 7.93 ₊ 0.23 |
| 035H | 20 | 24.4 | 2.8 ₊ | 1.1×10^{-3} | Spark | 7.19 ₊ 0.22 |

Table 3

HYDROGEN-WATER FOG INERTING DATA AT $\sim 70^{\circ}\text{C}$

| Nozzle | Press. (psi) | Igniter | Hydrogen LFL (vol %) |
|---------------------|-----------------|-----------|-------------------------|
| Spraco 2163-7604 | 10 | Glow Plug | 6.76 \pm 0.22 |
| | 20 | Glow Plug | 7.18 \pm 0.22 |
| | 30 | Glow Plug | 7.62 \pm 0.22 |
| | 40 | Glow Plug | 8.46 \pm 0.22 |
| Spraco 1405-0604 | 10 | Glow Plug | 5.88 \pm 0.21 |
| | 20 | Glow Plug | 6.32 \pm 0.21 |
| | 30 | Glow Plug | 7.62 \pm 0.21 |
| | 40 | Glow Plug | 7.62 \pm 0.21 |

Table 4 (1 of 2)

CTF EXPERIMENTAL SERIES I

| Exp. No. CTF- | Hydrogen (%) | Steam (%) | Air (%) | Fan | ΔP_m kPa | t_{max} sec | Burn (%) |
|------------------|-----------------|--------------|------------|-----|---------------------|------------------|-------------|
| 101 | 5 | 0 | 95 | off | 13 | 9.5 | ~ 20 |
| 102 | 5.5 | 0 | 94.5 | off | 24 | 6 | ~ 26 |
| 110 | 5 | 15 | 80 | off | 10 | 6.5 | ~ 20 |
| 111 | 5 | 15 | 80 | off | 8 | 7.0 | ~ 20 |
| 124 R | 5 | 30 | 65 | off | ~ 7 | 7.0 | ~ 20 |
| 123 | 6.2 | 0 | 93.8 | off | ~ 47 | 6.0 | 30 |
| 105 | 5.5 | 0 | 94.5 | on | 105 | 1.5 | ~ 83 |
| 106 | 7 | 0 | 93 | off | 125 | 7.0 | ~ 100 |
| 107 | 7 | 0 | 93 | on | 161 | 1.2 | 100 |
| 125 | 6 | 15 | 79 | on | 87 | 1.5 | 60 |
| 126 | 6 | 30 | 64 | on | 65 | 1.6 | 50 |
| 108 | 8 | 0 | 92 | off | 146 | 4.2 | 100 |
| 113 | 8 | 15 | 77 | off | 126 | 4.9 | 100 |
| 116 | 8 | 30 | 62 | off | 38 | 5.0 | 38 |
| 109 | 8 | 0 | 92 | on | 187 | 0.8 | 100 |
| 117 (CI) | 7 | 0 | 93 | off | 110 | 11.4 | 100 |
| 118 (CI) | 7 | 15 | 78 | off | 45 | 4.5 | ~ 0 |
| 118A (CI) | 7 | 15 | 78 | on | 142 | 1.0 | 100 |
| 119 (CI) | 10 | 0 | 90 | on | 215 | 0.53 | 100 |
| 120 (CI) | 14 | 0 | 86 | on | 290(?) | 0.4 | 100 |
| CT 704 (TI) | 11 | 0 | 89 | on | 225 | 0.6 | 100 |
| CT 701 (TI) | 8 | 0 | 92 | on | 180 | 0.9 | 100 |
| CT 702 (TI) | 8.5 | 0 | 91.5 | off | 157 | 3.2 | 100 |
| CT 700 (TI) | 7 | 0 | 93 | on | 145 | 1.1 | 100 |
| CT 703 (TI) | 5.7 | 0 | 94.3 | on | 75 | 1.9 | ~ 72 |
| *CT 502 | 8.4 | 0 | 91.6 | off | 175 | --- | ~ 100 |
| *CT 501 | 10 | 0 | 90 | off | 260 | --- | ~ 100 |
| *CT 504 | 5 | 0 | 95 | off | 10 | 5.5 | ---- |
| *TST 10 | 6 | 0 | 94 | off | 175 | --- | ---- |
| *TST 16 | 8.5 | 0 | 91.5 | off | 232 | --- | ---- |
| 103 | 6 | 0 | 84 | off | 27 | 5 | ~ 23 |

Table 4 (2 of 2)

| | | | | | | | |
|---------|-----|---|------|-----|----|-----|------|
| *TST 15 | 7.5 | 0 | 92.5 | off | 20 | --- | ---- |
| *TST 11 | 5.5 | 0 | 94.5 | off | 19 | --- | ---- |

NOTE: All experiments at 100°C

- Conducted at 28 ± 2°C

Initial pressure 98 kPa

Unless stated, all experiments are with bottom ignition

CI = central ignition

TI = top ignition

Table 5 (1 of 3)

CTF EXPERIMENTAL SERIES 2 & 3

| Exp.No. CTF- | Hydrogen (%) | Steam (%) | Air (%) | Final H ₂ (%) | ΔP_m kPa | t_{max} sec | Burn (%) |
|-----------------|-----------------|--------------|------------|-----------------------------|---------------------|------------------|-------------|
| 204 | 41.5 | 0.0 | 58.3 | 20.0* | 403 | 0.07 | 56 |
| 230 | 41.6 | 0.0 | 58.4 | 19.7* | 424 | 0.06 | 59 |
| 203 | 32.6 | 0.0 | 67.4 | 6.0* | 452 | 0.06 | 84 |
| 222 | 36.5 | 0.0 | 63.5 | 13.0* | 434 | 0.06 | 70 |
| 203A | 31.0 | 0.0 | 69.0 | 3.4* | 455 | 0.06 | 94 |
| 223 | 27.0 | 0.0 | 73.0 | 0.0 | 441 | 0.07 | 100 |
| 236 | 29.5 | 0.0 | 70.4 | 0.0 | 469 | 0.05 | 100 |
| 217 | 15.0 | 0.0 | 85.0 | 0.0 | 303 | 0.11 | 100 |
| 202C | 20.0 | 0.0 | 80.0 | 0.0 | 390 | ----- | 100 |
| 201R | 10.0 | 0.0 | 90.0 | 0.0 | 215 | 0.87 | 100 |
| 233 | 36.4 | 20.0 | 43.6 | 20.0* | 331 | 0.12 | 50 |
| 232 | 24.6 | 20.0 | 55.4 | 1.5* | 369 | 0.12 | 93 |
| 219 | 25.0 | 20.0 | 55.0 | 2.2* | 359 | 0.18 | 92 |
| 212 | 35.5 | 20.0 | 44.5 | 19.0* | 338 | 0.13 | 52 |
| 231 | 29.5 | 0.0 | 70.5 | 0.0 | 462 | 0.05 | 100 |
| 205 | 11.0 | 10.0 | 79.0 | 0.0 | 216 | 0.72 | 100 |
| 237 | 30.0 | 10.0 | 60.0 | 5.5* | 410 | 0.09 | 84 |
| 209 | 10.0 | 20.0 | 70.0 | 0.0 | 159 | 2.40 | 100 |
| 213B | 10.0 | 30.0 | 60.0 | 0.0 | 148 | 3.20 | 100 |
| 219B | 10.0 | 40.0 | 50.0 | 0.0 | 112 | 6.10 | 100 |
| 210 | 16.0 | 20.0 | 64.0 | 0.0 | 293 | 0.27 | 100 |
| 219C | 10.0 | 50.0 | 40.0 | 10.0 | 0.0 | ---- | 0 |
| 207 | 27.0 | 10.0 | 63.0 | 0.7* | 407 | 0.15 | 98 |
| 211 | 28.0 | 20.0 | 52.0 | 7.0* | 365 | 0.13 | 78 |
| 229 | 21.0 | 30.0 | 49.0 | 0.5* | 321 | 0.22 | 98 |
| 238 | 28.6 | 10.0 | 61.4 | 3.2* | 407 | 0.07 | 90 |
| 220 (Bot Ign) | 27.0 | 0.0 | 73.0 | 0.0 | 434 | 0.09 | 100 |
| 221 | 25.4 | 0.0 | 74.6 | 0.0 | 434 | 0.075 | 100 |
| 215A | 30.4 | 30.4 | 39.6 | 15.0* | 255 | 0.45 | 55 |

Table 5 (2 of 3)

| | | | | | | | |
|----------------|------|------|------|-------|-----|------|-----|
| 214 | 15.6 | 30.0 | 54.4 | 0.0 | 255 | 0.60 | 100 |
| 234 | 29.0 | 30.0 | 41.0 | 13.0* | 283 | 0.24 | 59 |
| 235 | 31.0 | 0.0 | 69.0 | 2.0* | 463 | 0.05 | 94 |
| 218 (Bot Ign) | 20.0 | 0.0 | 80.0 | 0.0 | 386 | 0.14 | 100 |
| 226 | 22.2 | 30.0 | 47.7 | 2.5* | 300 | 0.27 | 90 |
| 224 | 25.0 | 10.0 | 65.0 | 0.0 | 407 | 0.08 | 100 |
| 201R | 10.0 | 0.0 | 90.0 | 0.0 | 210 | 0.80 | 100 |
| 207A (Fan) | 27.0 | 10.0 | 63.0 | 0.5* | 400 | 0.07 | 98 |
| 208 | 40.0 | 10.0 | 50.0 | 21.0* | 345 | 0.11 | 53 |
| 310 | 20.0 | 0.0 | 80.0 | 0.0 | 359 | 0.09 | 100 |
| 308 (Fan) | 7.0 | 0.0 | 93.0 | 0.0 | 145 | 1.50 | 100 |
| 306 | 6.0 | 0.0 | 94.0 | 3.0 | 55 | 5.50 | 51 |
| 309 | 15.0 | 0.0 | 85.0 | 0.0 | 283 | 0.24 | 100 |
| 307B (Bot Ign) | 10.3 | 0.0 | 89.7 | 0.0 | 179 | 1.25 | 100 |
| 307A (Bot Ign) | 11.5 | 0.0 | 87.9 | 0.0 | 186 | 1.00 | 100 |
| 307 (Bot Ign) | 6.71 | 0.0 | 93.3 | 0.25 | 85 | 4.0 | 96 |

* Calculated

Initial temperature: 100°C

Expt. 300 series is with gratings

Unless stated expt. are with central ignition

Initial pressure: 98 kPa

Table 5 (3 of 3)

- NOTE: 1. All experiments at $24 \pm 2^{\circ}\text{C}$, 98 kPa
2. s = sphere; p = pipe
3. EI = pipe end ignition
CI = sphere central ignition
* = assumed

Table 6

CTF EXPERIMENTAL SERIES 4

| CTF | H ₂ (Pipe) (%) | H ₂ (Sphere) (%) | ΔP_m (kPa) | Δt_m (sec). | Burn (%) |
|--------------|------------------------------|--------------------------------|-----------------------|------------------------|-------------|
| 405 (EI) | 10 | 10 | 248 | 6.75 | 100 |
| 402A (EI) | 8 | 8 | 210 | 14.75 | 100 |
| Fan on | | | | | |
| 402A Fan off | 8 | 8 | 10 | 16 | ~ 0 |
| 404 (EI) | 6.5 | 6.5 | 115 | 23 | 70 |
| Fan on | | | | | |
| 404 (EI) | 6.5 | 6.5 | 2 | 24 | ~ 0 |
| Fan off | | | | | |
| 401 (EI) | 20 | 20 | 510 | 0.2 | 100 |
| Fan off | | | | | |
| 407A (CI) | 8.5 | 8.5 | 165 | 14 | 100 |
| Fan off | | | | | |
| 409 (CI) | 10 | 10 | 225 | 1.3 | 100 |
| Fan off | | | | | |
| 408 (CI) | 20 | 20 | 500 | 0.15 | 100 |
| Fan off | | | | | |
| 410 (CI) | 25 | 25 | 1300 | .075 | 100 |
| Fan off | | | | | |
| 411 (EI) | 10 | 10 | 260 | 5.5 | 100 |
| Constriction | | | | | |
| 412 (EI) | 20 | 20 | 525 | 0.2 | 100 |
| Constriction | | | | | |
| 418 (EI) | 12 | 6 | 105p, 135 | 1.1 | ~ 0 |
| Burst Disk | | | | | |
| 419 (EI) | 15 | 6 | 115p, 115s | .35p, .85s | 70 |
| Burst Disk | | | | | |
| 416 (EI) | 15 | 10 | 120p, 325s | 0.28p, .375s | 100* |
| Burst Disk | | | | | |
| 415 (EI) | 15 | 20 | 120p, 525s | 0.32p, .4s | 100* |
| Burst Disk | | | | | |

2. The majority of the ICOG/EPRI tests which serve to demonstrate the validity of the deliberate ignition concept utilized a GMAC glow plug as the ignition source. TVA currently intends to install 120 V TAYCO ignitors in the permanent Hydrogen Mitigation System instead of the glow plugs. Although ignitor durability tests have been completed by Singleton, additional testing of the 120 V ignitor is required to show that it is an acceptable replacement for the GMAC ignitor. Specifically,
 - a) tests should be conducted to ensure that the ignitor will continue to operate as intended in a spray atmosphere typical of that which would be expected in each region of containment where ignitors are to be located;
 - b) endurance tests should be conducted on a suitable sample size to assure adequacy and consistency of ignitor surface temperature and lifetime.

Response:

This question is not applicable to McGuire since TAYCO igniters are not used.

3. For the 120 V ignitor system, describe the following:
 - a) Performance characteristics of the ignitors including surface temperature as a function of voltage and age;
 - b) A comparison of surface area, power density, and other relevant parameters for the original and currently proposed igniters;
 - c) Igniter mounting provisions
 - d) Proposed preoperational and surveillance testing. If surveillance testing will be based on comparisons of measured voltage/current to preoperational values, specify the range for acceptance;
 - e) Power distribution system for the igniters, in particular, the location of the breakers in the system and the number of igniters on a breaker.

Response:

This question is not applicable to McGuire since TAYCO igniters are not used.

4. Provide details regarding the number and location of permanent igniters in containment. Discuss the influence of considerations such as volume served per igniter, and preferred flame direction on the design of the permanent system.

Response:

The number and location of igniters in the McGuire containment are described in Section 3.4. The selection of igniter coverage included the following:

1. All subcompartments in containment have at least one redundant pair of igniters.
2. In order to ensure that each burn consumes all available hydrogen in the vicinity of an igniter (propagation occurs in all directions upon ignition) and that substantial ignition occurs at a predictable hydrogen concentration, all igniters are located at or near the top of the subcompartments they serve.
3. Igniter spacing was selected to ensure rapid combustion of hydrogen once ignition occurs to prevent hydrogen concentrations from reaching levels above 8.5% by volume.
4. Because of the igniter location in McGuire, it can be assumed that flame propagation is in all directions upon ignition. Parameters such as the volume served per igniter or the preferred flame direction are not relevant considerations in this design.
5. Recent tests conducted at McGill indicate that flame accelerations accompanied by large pressure increases, and detonations can occur at hydrogen concentrations as low as 13%. Although remote, the possibility of flame accelerations and local detonations occurring around obstacles and in confined regions of containment cannot be entirely dismissed. Further analysis of the probability and consequences of these events are thus warranted. In this regard:
 - a) Discuss the chain of events and conditions required to cause flame accelerations and detonations in containment, and the probability that such conditions might exist. Identify the locations in containment at which flame acceleration/detonation would most likely occur.
 - b) Provide quantitative estimates of the extent and magnitude of flame acceleration in containment and the resulting pressure increase and loads on structures and equipment.
 - c) Provide the results of a calculation (pressure versus time curve) for the largest conceivable local detonation which could occur in your containment. Demonstrate that the effects of such a detonation could be safely accommodated by structures and essential equipment. Also, provide an estimate of the limiting size of a cloud of detonable gas with regard to the structural capability of the containment shell.

Response:

It is our position that the results of test conducted at McGill do not warrant further work on local detonation in the McGuire containment. The

results of the McGill work are reported in reference 1. The following facts are noted from this report concerning detonations at 13% volume concentration of hydrogen.

1. The critical tube diameter for hydrogen concentrations of 13% is greater than 10 meters.
2. In order to detonate a hydrogen-air mixture at a hydrogen concentration of 13%, approximately 50 kilograms of high explosive are required.

Since the McGuire containment does not contain any high explosive, and all confined areas are much smaller in diameter than 10 meters, we conclude that reference 1 strongly supports our previous position. Accordingly, the issue of detonation in the McGuire containment requires no further clarification or analysis.

6. The analysis provided to date concerning the survivability of air return fans and hydrogen skimmer fans neglects any fan overspeed or motoring which occurs as a result of postulated hydrogen combustion in the upper plenum and upper compartment. Describe how the fans will react to the differential pressure associated with hydrogen combustion, and justify the assumptions concerning fan overspeed. Describe the effects of combustion in the lower compartment e.g., fan stalling.

Response:

Hydrogen burning in the upper compartment or upper plenum produces pressure differentials across the fans which persist for 7-10 seconds and reach peaks between 1 and 2 psid. The rotating moment of inertia of both fans is very large compared to the impulse of angular momentum produced by these small differential pressures of short duration. Our calculations show that the fan speed will not exceed synchronous during the transient. Thus the transient is of no concern in the consideration of fan integrity.

7. With regard to the equipment survivability analysis, the level of conservatism implicit in the temperature forcing functions developed for the lower containment and the upper plenum is not apparent and quantifiable. Additional analyses should be conducted to provide a baseline or "best estimate" of equipment response, and to ensure that temperature curves assumed in the analyses embody all uncertainties in the accident sequence and combustion parameters. Accordingly, provide analyses of equipment temperature response to:
 - 1) The base case transient assumed in the containment analyses,
 - 2) The containment transients resulting from a spectrum of accident scenarios; and
 - 3) The containment transients resulting under different assumed values for flame speed and ignition criteria for the worst case accident sequence. The range of these combustion parameters assumed for the

equipment survivability analyses should include but not necessarily be limited to the values assumed in the containment sensitivity studies, i.e., 1 - 12 ft/sec flame speed and 6 - 10% hydrogen for ignition.

Response:

The base case analysis of equipment survivability is contained in Section 4.0. A large number of conservative assumptions were used in this analysis which permits the calculated temperatures, as presented in Section 5.4.2.4, to be considered as upper bounds. The analysis of an accident spectrum using the MARCH computer code was presented by TVA in their earlier submittals to NRC. These accident analyses, which may be considered generically applicable to McGuire, show that the total hydrogen release during an accident and the rate at which it is released are bounded by the base case analysis (an S₂D transient) for the ice condenser units. Accordingly, for equipment survivability the base case analysis may be considered the worst case analysis. A number of sensitivity studies have been performed by the three utilities for equipment survivability. It is apparent from this work that lower flame speeds increase the radiative contribution to the total temperature rise of the equipment, therefore, analysis performed at flame speeds of 1 ft/sec bound the possible conditions. This work also shows that burning at different hydrogen concentrations has very little effect on the total temperature rise of the equipment. This result is not surprising because total temperature rise is the function of the integrated energy release to containment, not of the instantaneous value of containment temperature. We conclude that our previous work on equipment survivability provides a conservative basis on which to establish that essential equipment in containment will perform its intended function during and after hydrogen burning and no further analysis of equipment survivability is required.

8. For the survivability analysis, it is our understanding that the current thermal model assumes radiation from the flame to the object only during a burn, with convection occurring at all times outside the burn period. In an actual burn, radiation from the cloud of hot gases following the flame front can account for a substantial portion of the total heat transfer to the object. An additional heat flux term or a combined radiation-convection heat transfer coefficient should be used to account for this radiant heat source. In this regard, clarify the treatment of heat transfer following the burn and justify the approach taken.

Response:

As explained in Section 5.4.2.3 heat transfer after passage of the flame is by natural convection and radiation from the hot gasses surrounding the object.

9. HEDL containment mixing tests conducted as part of the ICOG/EPRI R & D program indicate that spatial hydrogen concentration gradients of as much as 2 to 7% can be expected to exist within containment at a given time.

If such a gradient were to exist within the volume of a hydrogen cloud in which combustion has just been initiated, the volume-average hydrogen concentration for the cloud can conceivably be significantly higher than the hydrogen concentration at the point of ignition. In light of this, discuss the influence of hydrogen concentration gradients on the concentration requirement for ignition that is input to CLASIX, and justify the ignition concentration value used in the CLASIX containment analyses.

Response:

In the HEDL mixing test, the realistic cases were those with the air return fans on. In those cases the greatest difference in hydrogen concentration between any two points in containment was less than 3%. The hydrogen concentrations for ignition and the effects of concentration gradients on the results of CLASIX analysis were discussed in our response to question 4f transmitted by Mr. T. M. Novak's letter of August 9, 1982.

10. Describe in detail the fog formation study cited in response to question 9 of the July 21, 1981, Request for Information. Include in this description the analytical development of the models for fog formation and removal, methods for solution, assumptions, and input parameters. Provide plots of fog concentration and size as a function of time assuming various spray removal efficiencies, and mean droplet diameters.

Response:

References 2 and 3 contain the requested information. These reports are based on a program of research into fogging sponsored by the ice condenser utilities. We understand that NRC already has a copy of reference 2. Reference 3 is being transmitted to NRC by TVA.

11. Describe in detail the analyses of fog effects on hydrogen combustion cited in response to question 9 of the July 21, 1981 Request for Information. Include in this description the analytical development of the combustion kinetics and heat transfer models, and quantitative comparisons between the theoretical results and data obtained from the Factory Mutual Tests. Provide plots of fog droplet size and concentrations required to inert at various hydrogen concentrations under typical post-LOCA containment conditions.

Response:

Refer to response to question 10.

12. In the CLASIX spray model it is not clear whether the mass of spray treated in a time increment is assumed to be only that amount of spray mass which is introduced in a single time step, or the mass of droplet accumulated in the atmosphere over the full time period. Clarify the spray mass accounting used in CLASIX and the mass of spray treated in a single time step. Discuss the significance of any errors introduced by the apparent assumption that only one time increment of spray mass is exposed to the containment atmosphere during a single time step.

Response:

Refer to response to questions 10 and 11 which were transmitted by Mr. T. M. Novak's letter of August 9, 1982.

13. CLASIX spray model analyses provided to date have been limited to the comparison of pressure, temperature, and integrated heat removal for the purpose of evaluating the effect of the spray operating in a separate time domain. Additional information is needed, however, to confirm the adequacy of the heat and mass transfer relationships and assumptions implicit in the CLASIX spray model, especially in treating a compartment in which hydrogen combustion is taking place. In this regard:
- a) Provide a quantitative description of the spray heat and mass transfer under containment conditions typical of a hydrogen burn. Include in your response plots of containment temperature, spray heat transfer, spray mass evaporation, and suspended water mass as a function of time for both the CLASIX spray model and a model in which the spray mass is tracked throughout the fall (and allowed to accumulate in the containment atmosphere).
 - b) Provide analyses of spray mass evaporation and pressure suppression effects for an upper compartment burn.
 - c) Justify the drop film coefficient value assumed in the spray model analyses (20 Btu/h ft²F) and discuss the effect of using a constant value throughout a burn transient.

Response:

Refer to response to questions 10 and 11 which were transmitted by Mr. T. M. Novak's letter of August 9, 1982.

14. Concerning the CLASIX containment response analyses:
- a) Justify the burn time and burn propagation delay times used (reported burn times for Sequoyah and McGuire differ by a factor of 2 to 3);

Response:

Refer to response to question 4a which was transmitted by Mr. T. M. Novak's letter of August 9, 1982.

- b) Justify the radiant heat transfer beam lengths used (a beam length of 59 ft. for the lower compartment in Sequoyah seems high - 20 to 30 ft. may be more appropriate);

Response:

The beam length of 59 feet applies to the upper compartment. Beam length used for the lower compartment is 25 feet. This is clearly shown in Table 4.3-11.

- c) The basic case and majority of S₂D sensitivity studies assume that combustion occurs at an 8% hydrogen concentration with an 85% completeness of burn. Available combustion data for hydrogen/dry air mixtures indicate that lean mixtures of approximately 8% H₂ and below are prevented from reacting completely and adiabatically due to buoyancy, diffusion and heat loss effects. Only as hydrogen concentration is increased to about 8.5% will the reaction begin to approach adiabaticity. While arguments for an 8% ignition concentration may be valid, provide the results of additional CLASIX analyses to indicate the effect of an increase in ignition concentration from 8% to 8.5-9%.

Response:

All CLASIX analysis reported for McGuire in reference 1 uses ignition at 8.5% hydrogen by volume. Refer to section 4.0.

- d) Provide the results of CLASIX analyses for flame speeds of 10 and 100 times the present value;

Response:

Previous CLASIX analysis was performed using flame speed assumptions consistent with the best analytical and experimental results (see our response to question 1 above). The flame speed has also been varied in sensitivity studies over about a 10:1 range. We conclude that there is no justification for the request by NRC to perform analysis using unrealistically high flame speeds, as previous analysis bounds all reasonable cases.

- e) To assess the effect of igniter system failure or ineffectiveness, provide the results of sensitivity studies in which the lower and dead-ended compartments are effectively inerted, and the upper plenum igniters burn with low efficiency or not at all. Assume combustion in the upper compartment at 9-10% hydrogen.

Response:

Section 4.0 reports the results of our analysis of containment response in which the upper plenum igniters were assumed to be ineffective in causing ignition. As a result, a large hydrogen burn occurred in the upper compartment at 8.5% hydrogen by volume with a burn completeness of 100%. This analysis is referred to as Case 5 in Section 4.6.7. Another example of analysis in which the effectiveness of the igniter system was impaired is report as Case 4 in Section 4.6.6. We consider these two cases to be realistic bounding cases for containment response when the hydrogen igniter system is only partially effective. We note that the effectiveness of the igniter system has been proven for hydrogen concentrations of 8.5% in the presence of vapor and spray. There is, therefore, no reasonable basis to assume extensive impairment of the igniter system. Accordingly, no further analysis of impaired igniter effectiveness are considered necessary.

References

1. Lee, J., Knystantas, R., Guiras, C., Benedick, W.B., and Shepard, J.E., "Hydrogen-Air Detonations," presented at the Second International Workshop on the Impact of Hydrogen on Water Reactor Safety, Albuquerque, N.M., October 3-7, 1982.
2. Tsai, S.S., and Liparulo, N.J., "Fog Inerting Criteria for Hydrogen/Air Mixtures," presented at the workshop cited in reference 1.
3. Tsai, S.S., "Fog Inerting Analysis for PWR Ice Condenser Plants," dated October, 1982.